CHARACTERIZATION OF SILICON CARBIDE PARTICULATE REINFORCED SQUEEZE CAST ALUMINUM 7075 MATRIX COMPOSITE

A THESIS SUBMITTED TO
THE GRADUATE SCHOOL OF NATURAL AND APPLIED SCIENCES
OF
MIDDLE EAST TECHNICAL UNIVERSITY

BY

HAMDİ SENCER YILMAZ

IN PARTIAL FULFILLMENT OF THE REQUIREMENTS
FOR
THE DEGREE OF MASTER OF SCIENCE
IN
METALLURGICAL AND MATERIALS ENGINEERING

AUGUST 2004

Approval of the Graduate School of Natural and Applied Sciences

Prof. Dr. Canan Özgen
Director

I certify that this thesis satisfies all the requirements as a thesis for the degree of Master of Science

Prof. Dr. Bilgehan Ögel
Head of Department

This is to certify that we have read this thesis and that in our opinion it is fully adequate, in scope and quality, as a thesis for the degree of Master of Science

Prof. Dr. Ali Kalkanlı
Supervisor

Examining Committee Members

Prof. Dr. Ahmet Geveci	(METU,METE)
Prof. Dr. Ali Kalkanlı	(METU,METE)
Prof. Dr. Ekrem Selçuk	(METU,METE)
Prof. Dr. Rıza Gürbüz	(METU,METE)
Assoc. Prof. Baybars Oral	(TEKNOPLAZMA)

I hereby declare that all information in this document has been obtained and presented in accordance with academic rules and ethical conduct. I also declare that, as required by these rules and conduct, I have fully cited and referenced all material and results that are not original to this work.

Name, Last name : Hamdi Sencer Yılmaz
Signature :

ABSTRACT

CHARACTERIZATION OF SILICON CARBIDE PARTICULATE REINFORCED SQUEEZE CAST ALUMINUM 7075 MATRIX COMPOSITE

Yılmaz, Hamdi Sencer
M.S. Department of Metallurgical and Materials Engineering
Supervisor: Prof. Dr. Ali Kalkanlı

August 2004, 99 Pages

The aim of this study is to investigate the mechanical behavior and its relation with processing and microstructure of the silicon carbide particulate (SiC_p) reinforced aluminum matrix composite. Aluminum 7075 alloy is chosen as matrix alloy, in which zinc is the main alloying element. Four different additions of SiC_p were used and the weight fractions were 10%, 15%, 20% and 30%. Composites were processed by with squeeze casting and the applied pressure during casting was 80 MPa. The mould is specially designed to produce both specimens ready for tensile and three point bending tests.

Both as-cast and heat treated aluminum composites were examined and T6 heat treatment was applied. Three point bending tests were performed to reveal the fracture strength of aluminum composites. 10wt% SiC_p aluminum composites showed the maximum flexural strength in both as-cast and heat treated composites. The mechanical test results revealed that precipitated phases in heat treated composites, behaved like fine silicon carbide particulates and they acted as barriers to dislocation motion. Maximum flexural strength increased about 40 MPa (10%) in as-cast and 180 MPa (44%) in heat treated composites. Tensile testing was also conducted to verify the results of the three point bending tests.

Hardness tests were done to find the effect of silicon carbide addition and to find the peak hardness in heat treatment. For as-cast specimens hardness values increased from 133 to 188 Vickers hardness (10 kg.) with increase in SiC_p content from 0 to 30wt% and for heat treatment specimens hardness values increased from 171 to 221 Vickers hardness (10 kg.). The peak hardness values were obtained at 24 hours precipitation heat treatment. SEM studies were carried out to examine the heat treated composites, to take SEM photographs and to obtain a general elemental analysis. Theoretical volume percentage addition of SiC_p was checked with Clemex Image Analyzer program. Distribution of SiC_p was determined by mettalographic examination. Second phases that were formed during heat treatment was searched by x-ray analysis.

Keywords: Metal Matrix Composites, Silicon Carbide Particulates, Squeeze Casting, Al/SiC_p, Heat Treatment

ÖZ

SİLİSYUM KARBÜR PARÇACIK TAKVİYELİ SIKIŞTIRMA DÖKÜM ALUMİNYUM 7075 ALAŞIMIN KARAKTERİZASYONU

Yılmaz, Hamdi Sencer
Yüksek Lisans, Metalurji ve Malzeme Mühendisliği Bölümü
Tez Yöneticisi: Prof. Dr. Ali Kalkanlı

Ağustos 2004, 99 Sayfa

Bu çalışmanın amacı silicon carbür parçacık (SiC_p) takviyeli alüminyum matriks kompozitlerin mekanik davranımını ve bu mekanik davranımın süreç ve içyapı ile bağlantısını incelemektir.. Matriks alaşımı olarak alüminyum 7075 seçilmiştir ve çinko ana alaşım elementidir. Dört farklı SiC_p ağırlık yüzdesi kullanılmıştır, bunlar; 10%, 15%, 20% ve 30%'dur. Kompozitler sıkıştırma döküm yöntemi ile dökülmüştür ve döküm sırasında 80 MPa basınç uygulanmıştır. Kalıp, numunelerin çekme ve üç-nokta bükme testlerine hazır halde üretilmesini sağlayacak şekilde özel olarak dizayn edilmiştir.

Hem döküm sonrası hem de ısıl işlem görmüş alüminyum kompozitler incelenmiştir ve T6 ısıl işlemi uygulanmıştır. Alüminyum kompozitlerin kırılma dayanıklılığını ortaya çıkarmak için üç nokta bükme testleri gerçekleştirilmiştir ve 10% SiC_p alüminyum kompozitleri hem döküm sonrası hem de ısıl işlem görmüş kompozitler içinde en yüksek kırılma dayanımını göstermişlerdir. Mekanik testler ısıl işlem görmüş kompozitlerdeki çökelmiş fazların küçük silicon karbür parçacıkları gibi davrandıklarını ve dislokasyon hareketine engel olduklarını ortaya çıkarmıştır. En yüksek kırılma dayanıklılığı işlem görmemiş kompozitlerde 40 MPa(10%), ısıl işlem görmüş kompozitlerde 180 MPa (44%) artmıştır. Üç nokta bükme testinin sonuçlarını doğrulamak için çekme testleri de yapılmıştır.

Silicon karbür parçacılarının etkisini bulmak ve ısıl işlemde elde edilen en yüksek sertlik değerini bulmak için sertlik testleri yapılmıştır. Sertlik değerleri SiC_p içeriğinin 0 dan 30wt% yükselmesi ile döküm sonrası numunelerde 133 den 188 Vicker sertliğine (10 kg.) yükselmiştir ve ısıl işlem görmüş numunelerde 171 den 221 Vickers sertliğine (10 kg.) ulaşmıştır. En yüksek sertlik değerleri 24 saatlik çökeltme ısıl işleminde elde edilmiştir. Isıl işlem görmüş kompozitleri incelemek, SEM fotoğrafları çekmek ve genel analiz almak için SEM çalışmaları yapılmıştır. Teorik hacimsel SiC_p yüzdeleri “Clemex Image Analyzer” programı ile kontrol edilmiştir. SiC_p dağımı metalografi ile araştırılmıştır. Isıl işlem sırasında oluşan ikinci fazlar x-ışınları analizi ile taranmıştır.

Anahtar Kelimeler: Metal Matriks Kompozit, Silikon Karbür Parçacıkları, Sıkıştırma Döküm, Al/SiC_p, Isıl İşlem

To my family…

ACKNOWLEGEMENTS

I would like to express my sincere thanks to Prof. Dr. Ali Kalkanlı for his helpful guidance, criticism and encouragement throughout the every stage of this study. I am indebted to his tremendous support to my work.

I would also express my sincere thanks to Salih Türe for the help in casting processes and Özdemir Dinç for the help in metallographic examinations.

Finally, I wish to express my special thanks to my family for their patience, moral support and tolerance during this study and during my life.

TABLE OF CONTENTS

CHAPTERS

CHAPTER 1

INTRODUCTION

Composite materials are composed of at least two phases; a matrix phase and a reinforcement phase. Matrix and reinforcement phase work together to produce combination of material properties that cannot be met by the conventional materials [1]. In most of the composites, reinforcement is added to matrix –the bulk material to increase the strength and stiffness of the matrix. The most common composites can be divided into three main groups [2]:

1. Polymer Matrix Composites (PMC's): Polymer matrix composites are also known as FRP - Fibre Reinforced Polymers (or Plastics). These materials use a polymer-based resin as the matrix, and a variety of fibres such as glass, carbon and aramid as the reinforcement.

2. Metal Matrix Composites (MMC's): Metal matrix composites are increasingly found in the aerospace and automotive industry. These materials use a metal such as aluminum as the matrix, and reinforce it with fibres, particulates or whiskers such as silicon carbide.

3. Ceramic Matrix Composites (CMC's): Ceramic matrix composites are used in very high temperature environments. These materials use a ceramic as the matrix and reinforce it with short fibres, or whiskers such as those made from silicon carbide and boron nitride [2].

Reductions in material density or increases in stiffness, yield strength, ultimate tensile strength can be directly translated to reductions in structural weight. This led the aerospace industry to develop and examine new materials with combinations of low density, improved stiffness and high strength as attractive alternatives to existing high-strength aluminum alloys and titanium alloys. These high-strength metal matrix composites combine the high strength and hardness of reinforcing phase with ductility and toughness of light metals [3]. Moreover, the need for improved design procedures has resulted from an attempt to achieve significant improvement in structural efficiency, reliability and overall performance through reductions in either absolute weight or increases in strength-to-weight ratio. Recent research results have made it possible to envision combining these effects through the development of reinforced lightweight alloys [4].

System trade-studies, such as the ones outlined above, have been the primary motivating factor resulting in the resurrection of much interest in developing and using metal-matrix composites. Metal-matrix composites, in general, consist of at least two components, one is the metal matrix and the second component is reinforcement. In all cases the matrix is defined as a metal, but a pure metal is rarely used as the matrix, it is generally an alloy. The distinction of metal-matrix composites from other two- or more, phase alloys come about from the processing of the composite. In the production of the composite, the matrix and the reinforcement, are mixed together. This is to distinguish a composite from a two-, or more, phase alloy, where the second phase forms as a particulate and a phase separation such as a eutectic or a eutectoid reaction occurs [5].

The metal-matrix composites offer a spectrum of advantages that are important for their selection and use as structural materials. A few such advantages include the combination of high strength, high elastic modulus, high toughness and impact resistance, low sensitivity -to changes in temperature or thermal shock, high surface durability, low sensitivity to surface flaws, high electrical and thermal conductivity, minimum exposure to the potential problem of moisture absorption resulting in environmental degradation, and improved fabricability with conventional metal working equipment [5].

Metal-matrix composite reinforcements can be generally divided into five major categories:

a) Continuous fibers
b) Discontinuous fibers
c) Whiskers
d) Wires
e) Particulates

With the exception of wires, which are metals, reinforcements are generally ceramics. Typically these ceramics are oxides, carbides and nitrides, which are used because of their excellent combinations of specific strength and stiffness at both ambient temperature and at elevated temperatures. The typical reinforcements used in metal-matrix composites are listed in Table 1.1. Silicon carbide, boron carbide and aluminum oxide are the key particulate reinforcements and can be obtained in varying levels of purity and size distribution. Silicon carbide particulates are also produced as a by-product of the processes used to make whiskers of these materials [5].

Table 1.1 The typical reinforcements used in metal-matrix composites [5].

Reinforcement	**Matrices**
Boron, fiber (including coated)	Aluminum, titanium
Graphite fiber	Aluminum, magnesium, copper
Alumina fiber	Aluminum, magnesium
Silicon carbide fiber	Aluminum, titanium
Alumina-silica fiber	Aluminum
Silicon carbide whisker	Aluminum, magnesium
Silicon carbide particulate	Aluminum, magnesium
Boron carbide particulate	Aluminum, magnesium

The particulate-reinforced metal-matrix composites have emerged as attractive candidates for use in a spectrum of applications to include industrial, military and space-related. The renewed interest in metal-matrix composites has been aided by the development of reinforcement material, which provides either improved properties or reduced cost when compared with existing monolithic materials [5].

Particulate reinforced metal-matrix composites have attracted considerable attention on account of:

a) Availability of a spectrum of reinforcements at competitive costs,
b) Successful development of manufacturing processes to produce metal-matrix composites with reproducible microstructures and properties
c) Availability of standard and near standard metal working methods, which can be utilized to form these materials.

Furthermore, use of discontinuous reinforcements minimizes problems associated with fabrication of continuously reinforced metal-matrix composites such as fiber damage, micro-structural heterogeneity, and fiber mismatch and inter-facial reactions. For applications subjected to severe loads or extreme thermal fluctuations such as in automotive components, discontinuously-reinforced metal-matrix composites have been shown to offer near isotropic properties with substantial improvements in strength and stiffness, relative to those available with monolithic materials. [6]

Several metallic systems have been considered for use as a matrix material for metal matrix composites Table 1.2.

Table 1.2 Typical matrix alloys [5].

Aluminum
Titanium
Magnesium
Copper
Bronze
Nickel
Lead
Silver
Superalloys (nickel- and iron-based)
Niobium (columbium)
Intermetallics
Nickel aluminides
Titanium aluminides

The most important have been the non-ferrous lightweight materials for structural use such as aluminum, titanium and magnesium because specific properties of these materials can be enhanced to replace heavier monolithic materials. Aluminum is the most attractive non-ferrous matrix material used particularly in the aerospace and transportation industries where weight of structural components is critical [5].

The most common particulate composite system is aluminum reinforced with silicon carbide. So far most of the alloys that have been employed as matrices in aluminum have been focused on the A356, 2xxx and 6xxx series alloys. Although very few studies have been reported on the 7xxx series alloys reinforced with silicon carbide particles, much less attention has been paid to the 7xxx Al alloy matrix composites, which show the highest strength of all commercial Al alloys and widely used for structural applications [7].

Stronger matrix alloys tend to produce stronger composites, but within these composite systems there are many variables such as ageing conditions, weight/volume fraction of particulate, particulate size, which can affect mechanical properties [8].

Therefore the objective of this study is to investigate the fracture behavior of silicon carbide reinforced aluminum matrix composite.

CHAPTER 2

THEORY AND LITERATURE SURVEY

2.1. Processing Techniques of Particulate Reinforced Metal Matrix Composites

Several processing techniques have evolved in an attempt to optimize the microstructures and mechanical properties of particulate reinforced metal matrix composites. The processing methods utilized to manufacture particulate reinforced metal matrix composites can be grouped according to the temperature of the metallic matrix during processing. Accordingly, the processes can be classified into three categories [5]:

1) Liquid-phase processes
2) Solid-phase processes
3) Two-phase (solid/liquid) processes

2.1.1. Liquid-phase processes:

In liquid-phase processes, the ceramic particulates are incorporated into a molten metallic matrix using various proprietary techniques. This is followed by mixing and eventual casting of the resulting composite mixture into either shaped components or billets for further fabrication. The process involves a careful selection of the ceramic reinforcement depending on the matrix alloy. In addition to compatibility with the matrix, the selection criteria for a ceramic reinforcement includes the following factors [9]:

1) Elastic modulus
2) Tensile strength,
3) Density
4) Melting temperature
5) Thermal stability
6) Size and shape of the reinforcing particle
7) Coefficient of thermal expansion
8) Cost.

Most ceramic reinforcement materials are not wetted by the molten alloy. Consequently, introduction and retention of the ceramic particulate necessitates addition of wetting agents to the melt or coating the ceramic particulates prior mixing.

2.1.1.1. Liquid metal/ceramic particulate mixing:

Several approaches have been utilized to introduce ceramic particles into an alloy melt. These include [5]:

a) Injection of powders entrained in an inert carrier gas into the melt using an injection gun;
b) Addition of ceramic particulates into the molten stream as it fills the mould;
c) Addition of particulates into molten metal through a vortex introduced by mechanical agitation;
d) Addition of small briquettes into the melt followed by immediate stirring;
e) Forcing the particulates into the melt through the use of reciprocating rods;
f) Dispersion of the fine particles in the melt by centrifugal action;
g) Injection of particulates into the melt while the melt is continuously irradiated with ultra sound [10]
h) Zero-gravity processing. The zero gravity approach involves utilizing the synergism of ultra-high vacuum and elevated temperatures for prolonged

periods of time.

In all of the above processes, a strong bond between the metal matrix and the reinforcement is achieved by utilizing high processing temperature and alloying the matrix with an element to produce a new phase and thereby, effect “wetting” between the matrix and the ceramic. This reaction must be constrained so as to be adequate enough to wet the reinforcement to promote bonding, without causing reinforcement degradation during composite fabrication and/or utilization [11]. Agitation during processing is essential to disrupt the formation of contamination films and absorbed layers. This facilitates interfacial bonding [12].

2.1.1.2. Melt Infiltration:

In the melt infiltration process, a molten alloy is introduced into a porous ceramic pre-form utilizing either an inert gas or a mechanical device such as pressurizing medium. The pressure required to combine the matrix and reinforcement is a function of friction effects arising from viscosity of the molten metal matrix as it fills the ceramic preform. Wetting of the ceramic preform by the liquid alloy depends on several competing factors such as alloy composition, nature of ceramic preform, ceramic surface treatment, surface geometry, interfacial reactions, surrounding atmosphere, temperature and time[5].

2.1.1.3. Melt Oxidation Process:

In the melt oxidation processing, a ceramic pre-form, formed into the final product shape by a fabricating technique such as pressing, injection moulding or slip casting, is continuously infiltrated by a molten alloy as it undergoes reaction with gas phase [5].

2.1.2. Solid-phase processes:

2.1.2.1.Powder Metallurgy:

Powder metallurgy is a commonly used fabrication method in metal matrix composite fabrication [13]. Solid phase processes involve the blending of rapidly solidified powders with particulates, platelets or whiskers, through a series of steps as summarized in Figure 2.1. The sequence of steps include (i) sieving of the rapidly solidified particles, (ii) blending of the particles with reinforcement phase(s), (iii) compressing the reinforcement and particulate mixture to approximately 75% density, (iv) degassing and final consolidation by extrusion, forging, rolling or any other hot working method.

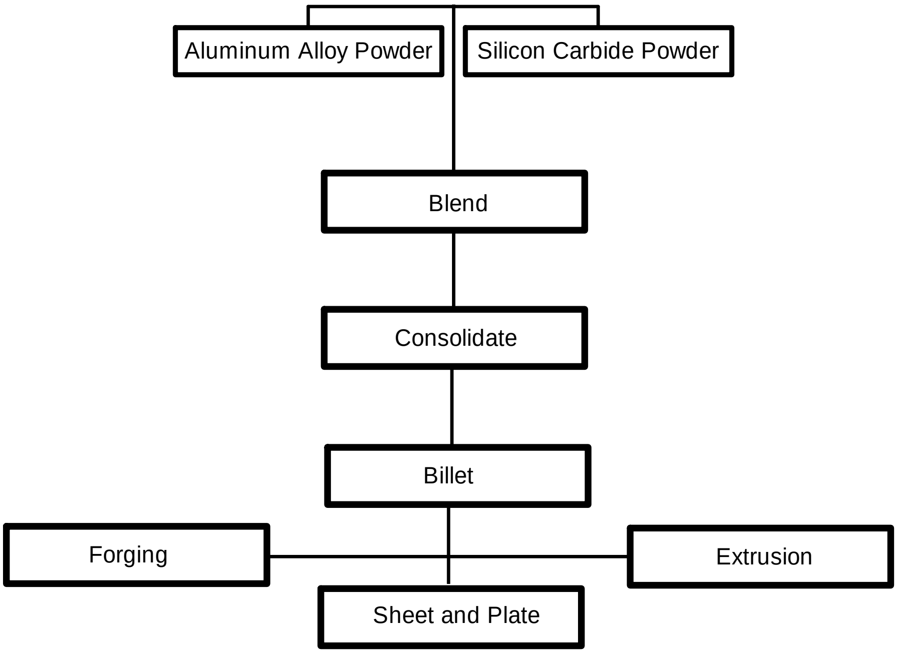

Figure 2.1. Flow chart showing key fabrication steps for a powder metallurgy metal- matrix composite. [5]

2.1.2.2. High energy-rate processes:

In this approach, the consolidation of a metal ceramic mixture is achieved through the application of a high energy in a short period of time. [5]

2.1.3. Two-phase processes:

Two-phase processes involve the mixing of ceramics and matrix in a regime of the phase diagram where the matrix contains both solid and liquid phases.

2.1.3.1.Osprey^{TM} deposition:

In the osprey process, the reinforcement particulates are introduced into a stream of molten alloy, which is subsequently atomized by jets of inert gas. The sprayed mixture is collected on a substrate in the form of reinforced metal matrix billet [5].

2.1.3.2. Rheocasting:

In the rheocasting process, fine ceramic particulates are added to a metallic alloy matrix at a temperature within the solid-liquid range of the alloy. This is followed by agitation of the mixture to form low viscous slurry [5].

2.1.3.3. Variable co-deposition of multiphase materials (VCM):

In the variable co-deposition of multiphase materials process, the matrix material is disintegrated into a fine dispersion of droplets using high-velocity inert gas jets. Simultaneously, one or more jets of strengthening phases are injected into atomized spray at a prescribed spatial location [5].

2.2. Squeeze Casting

Squeeze casting is an important solidification technique in the liquid phase processes. This casting process is a combination of the casting and forging process. Molten metal is poured into a die. As the metal starts solidifying, the die is closed and pressure is applied till the material fully solidifies [14].

Squeeze casting offers high productivity and excellent near-net-shape formability. This process consists of solidifying the alloy under a certain applied pressure that is maintained until the end of solidification. The result is a cast structure that exhibits more isotropic and improved mechanical properties. The potential advantages of the process include elimination of shrinkage and the formation of fine-grained equiaxed structure with small dendrite arm spacing and small constituent particles. The emergence of composite materials with properties that are far superior compared to those of conventional materials that has also caused a growing interest in squeeze casting [15].

The main parameters that effect the cast microstructure and which must be optimized are melt superheat, mould preheating temperature, applied pressure level, time delay between pouring of the metal in the die and application of pressure, pouring temperature and duration of pressure application. The applied pressure during solidification prevents the formation of both shrinkage and gas porosity in the solidifying material. The pressure necessary to eliminate shrinkage defects varies from alloy to alloy. It depends mainly on the freezing range of the alloy, the growth morphology of the material and the flow stress of the casting when the material is nearly solid [15].

The elimination of shrinkage porosity by squeeze casting suggest that it should be possible to produce sound castings with some of the high strength wrought alloys which normally exhibit a certain amount of dispersed shrinkage porosity. This means that castings could be used in such cases, instead of forged components [15].

2.3. Factors That Have Influence on Properties of Silicon Carbide Reinforced Aluminum Matrix Composites

2.3.1. Wetting of Silicon Carbide and Aluminum Alloy / Interface Between Silicon Carbide and Aluminum Alloy

Wetting of silicon carbide (SiC) or wettability of SiC to aluminum and aluminum alloys is an important phenomenon in processing of SiC reinforced aluminum metal matrix composites. Many parameters effect the wettability such as free silicon in silicon carbide, wetting angle and kinetics of SiC. [16-18].

M. Kobashi and T. Choh made a study to find the wettability and the reaction for silicon carbide particle and aluminum alloy system. A total amount of 60 g aluminum or alloy was melted in an MgO crucible in an induction furnace. After the melt been held at 1023 K silicon carbide particles wrapped in an aluminum foil were preheated above the melt for 600s. Then the silicon carbide particles (d_{av}=14μm) were added to the liquid aluminum and melt stirring had been started by an alumina rod.

It is clearly found that silicon carbide particles did not incorporate into the liquid aluminum immediately and an incubation time existed until silicon carbide particles began to be incorporated into the liquid aluminum. This indicates that the silicon carbide particles had been gradually wetted by liquid aluminum. Thus the incorporation time represents duration, which is necessary for full particulate wetting [19].

The effect of magnesium and titanium on the incorporation time of SiC particles into liquid aluminum is measured. The incorporation time is shortened by alloying magnesium and titanium as shown in Figure 2.2.

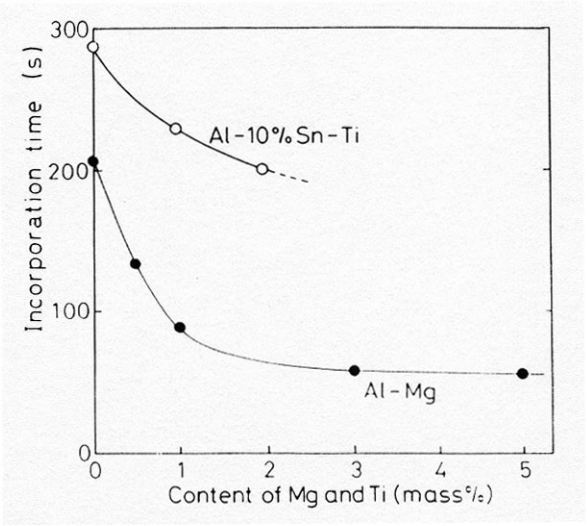

Figure 2.2. Effect of magnesium and titanium on the incorporation time of α-SiC particles and aluminum [19].

In both additions, reaction products are detected in x-ray images and there are silicon and magnesium overlaps in SiC/Al-5,0% Mg composite. This indicates the formation of magnesium silicide in the matrix. Also as observed in SEM titanium-enriched zone was found to be formed around SiC particles. The standard free energies of formation of titanium silicide and titanium carbide are low enough to form TiSi, Ti_2Si, Ti_5Si_3 and TiC, so titanium seems to react with SiC to produce silicade or carbide. In these cases, the dissolution of SiC is considered to be dominant factor of the wetting process.

$SiC \rightarrow (Si) + (C)$……………………………………………….…………………(1)

where (Si) or (C) indicates a dissolved element. Above equation is promoted by the reaction between these elements and an alloying element (Me)

$(Si) + m\mathrm{Me} = \mathrm{Me}_m\mathrm{Si}$………………………………………………...…….(2)

$(C) + n\mathrm{Me} = \mathrm{Me}_n\mathrm{C}$……………………………………………...…(3)

Owing to the reactions given above a new active surface appears on the SiC particles and the wetting ability is improved [19].

T. Choh and T. Oki have analyzed the wetting process of aluminum alloy by SiC by dip coverage method and found that alloying element addition decreased the incubation period. These results are [20]:

1. The incubation period is decreased by about10-20% by alloying silicon, manganese or iron with the aluminum, and this phenomenon results in some improvement in wettability.
2. The incubation period is decreased by 25-40% by adding chromium, molybdenum or tungsten to liquid aluminum and the wetting rate is also increased by the presence of molybdenum and tungsten.
3. Wetting rate increased with the addition of VA group elements such as vanadium, niobium and tantalum.
4. Addition of IVA group elements such as zirconium, hafnium and titanium increased the wetting rate.

Also T. Choh and T. Oki found that the incubation period decreased and the wetting rate increased with increasing temperature (in 1273-1373 K temperature range)

Another approach is made by W. Zhou and Z.M. Xu. They state that when the SiC particles were added into the molten alloys, they were observed to be floating on the surface, though they have a larger specific density than the molten alloys. This was due to high surface tension and poor wetting between the particles and the melt. A mechanical force can usually be applied to overcome surface tension to improve wettability. However, for the composites studied the problem of poor wetting could not be solved by mechanical stirring in a completely liquid state. Mechanical stirring could indeed mix the particles into the melt, but when stirring stopped, the particles tended to return to the surface. Most of these particles still stuck to one another to remain in clusters. It is not surprising for these clusters to resurface because it might be argued that pores could exist in them to make them float. However, the fact that single particles also tended to return to the surface strongly indicates that the particles floated mainly because of the surface gas layers surrounding them. The gas layers might be the main factor for the poor wettability [21].

Firstly, gas layers can cause the buoyant migration of particles, making it difficult to incorporate the particles into melts. Secondly, even the particles can be suspended in the melts by vigorous agitation; it is still difficult for the particles to be wetted by the molten metals because of the gas layers [21].

The above analysis leads to the conclusion that it is necessary to break the gas layers in order to achieve good wettability. Single particles and particle clusters can flow easily in a completely liquid melt; therefore, no large mechanical forces are actually applied to the particles during agitation, making it very difficult to break the gas layers simply by stirring in the conventional way [21].

2.3.2. Effect of Silicon Carbide Particle Size

T.J.A. Doel and P. Bowen made a study about the effect of particulate size on the mechanical properties of silicon carbide reinforced metal matrix composites. As matrix alloy, aluminum 7075 (nominally 5,6wt% Zn – 2,5wt% Mg – 1,6wt%Cu) is chosen. Three grades of silicon carbide are used; F1000 (nominal average particle size d= 5μm), F600 (d=13 μm) and F230 (d=60 μm). The nominal volume fraction of all of the materials used is 15%. Three aging conditions are selected; under-aged, peak-aged and over-aged.

It is generally found that, 0.2% proof stress, tensile strength and ductility tend to improve with decreasing particle size for a given volume fraction of reinforcement.

The effect of particle size can be seen in Table 2.1. There are only small differences in the 0,2% proof stress and tensile strength of the 5 µm and 13 µm silicon carbide reinforced composites but the 60 µm particulate reinforced has a much lower yield stress and a much lower fracture strength. It is important to note that the materials reinforced with 5 µm and 13 µm silicon carbide have greater 0,2% proof stress and tensile strength than the unreinforced material in the same ageing condition. However, in the case of material containing 60 µm silicon carbide the proof stress and the tensile strength are lower than the equivalent unreinforced material [22].

Table 2.1. Room temperature tensile properties of unreinforced 7075 and 7075 reinforced with5, 13 and 60 µm silicon carbide particles in underaged, peak aged and overaged conditions [22].

Particle Size (µm)	Ageing Condition	0,2% Proof Stress (MPa)	Tensile Strength (MPa)	Elongation to Tensile Strength	Reduction in area (%)	Work Hardening Exponent n
	Under aged	470	575	0,085	18,5	0,12
	Peak aged	552	619	0,068	24	0,1
	Averaged	448	519	0,055	32,3	0,11
5	Under aged	499	609	0,204	10,5	0,11
5	Peak aged	570	630	0,066	10	0,08
5	Overaged	510	574	0,063	12,5	0,1
13	Under aged	502	595	0,068	6,3	0,09
13	Peak aged	595	645	0,035	4,8	0,12
13	Overaged	539	596	0,039	5	0,1
60	Under aged	431	453	0,012	1,3	0,13
60	Peak aged	501	504	0,006	1	0,33
60	Overaged	484	493	0,008	2	0,21

2.3.3. Effect of Silicon Carbide Reinforcement and Aluminum Matrix Type

David L McDanels evaluated mechanical properties and stress-strain behavior for several fabricated aluminum matrix composites containing up to 40 vol. % discontinuous silicon carbide whisker, nodule or particulate reinforcement. Four types of aluminum matrices are used: 6061, 2024/2124, 7075 and 5083. Types of silicon carbide reinforcements are: discontinuous whisker, nodule and particulate reinforcement.

The modulus of elasticity increased with increasing reinforcement content. Figure 2.3. shows this phenomenon. The reinforcement content has been the dominant factor in the improvement of modulus of elasticity in these SiC/Al composites. When the factors influencing strength are considered, the effect of the matrix type is found to be the most important. Figure 2.4. summarize this behavior. These curves show that SiC/Al composites with higher strength such as 2024/2124 or 7075 Al, had higher strengths but lower ductilities. Composites with a 6061 Al matrix showed good strength and higher ductility [23].

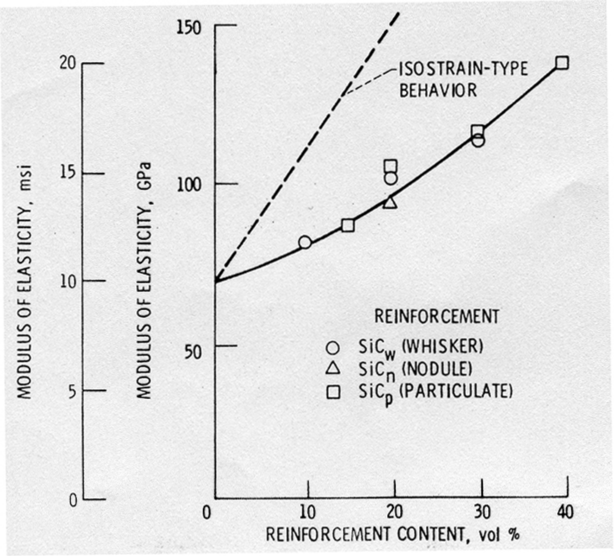

Figure 2.3. Effect of reinforcement content on modulus of elesticity of discontinious SiC/6061 composites [23].

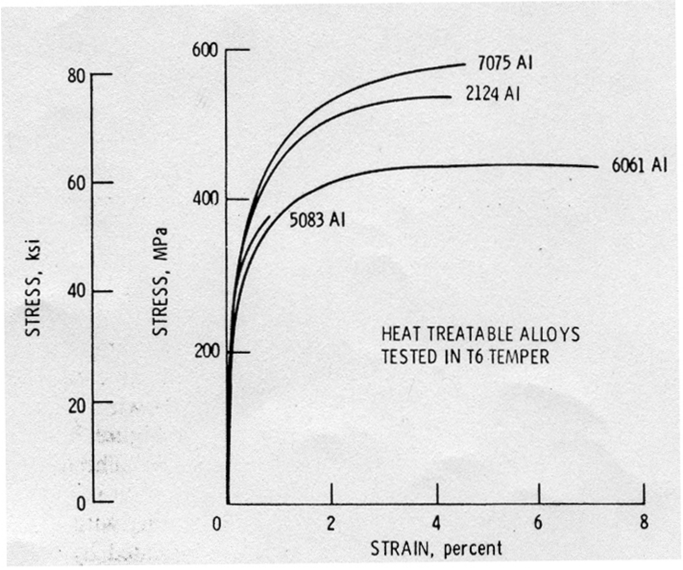

Figure 2.4. Effect of aluminum matrix alloy on stress-strain behavior of composites with 20 vol% SiCw reinforcement (tested in direction parallel to final rolling direction) [23].

Stress-strain curves for 6061 Al matrix composites with 20 vol% of various SiC reinforcements indicated that the yield and ultimate tensile strengths of SiCw and SiCp reinforcements were similar, while composites with SiCn reinforcements were about 10% lower in yield and ultimate tensile strengths. Figure 2.5. The effect of SiC reinforcement type and matrix type on tensile properties of discontinuous SiC/Al composites is summarized on Figures 2.6(a) and 2.6(b).

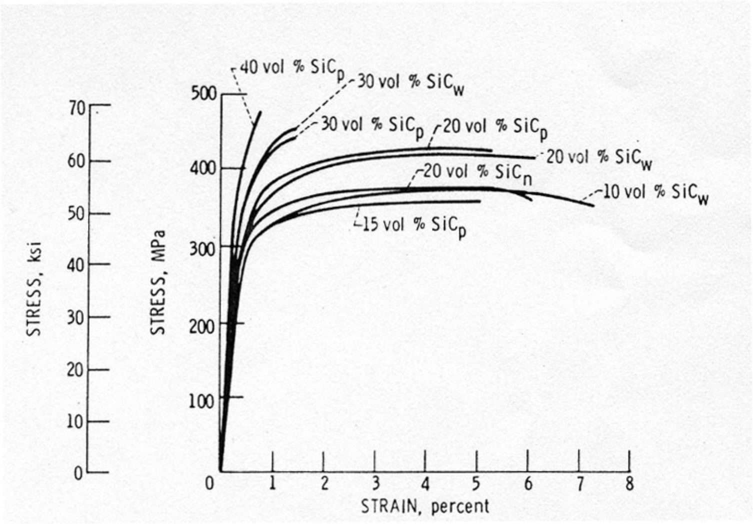

Figure 2.5. Stress-strain curves of SiC/6061 Aluminum composites (T6 temper, tested in longitudinal direction) [23].

Ductility is primarily determined by reinforcement content and matrix alloy. With increasing reinforcement content, the failure strain of composites is reduced, and the stress-strain curves also reflect a change in the fracture mode. Higher strength aluminum composites have lower ductilities [23].

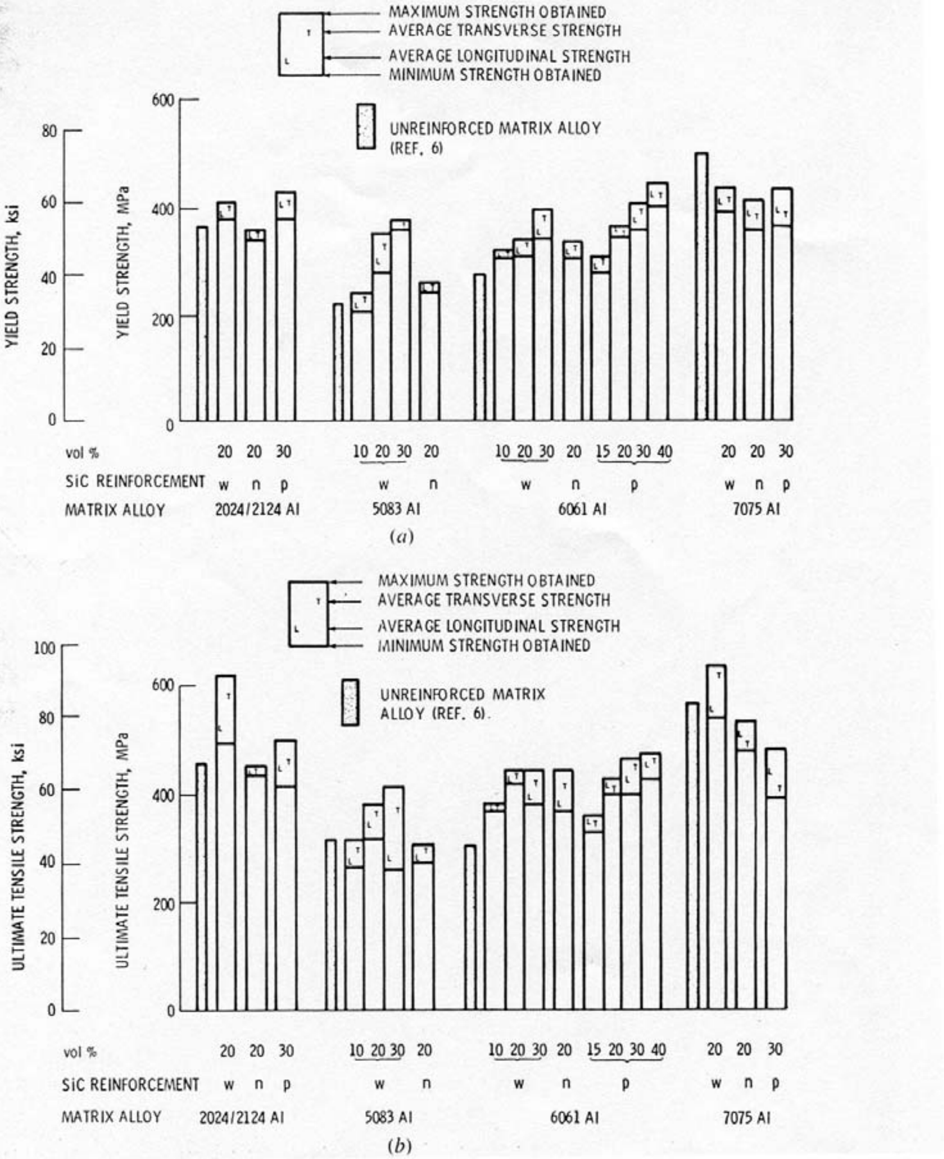

(a)

(b)

Figure 2.6. Effect of SiC reinforcement type and content on tensile properties of discontinious SiC/Al composites. (a) 0,2 % offset yield strength (b) Ultimate tensile strength [23].

2.3.4. Fluidity of Silicon Carbide Reinforced Aluminum Matrix Composites

According to A. Kolsgaard and S. Brusethaug the term fluidity should be separated into two categories: flowability and fillabilty. Flowability is a dynamic criterion, which measures the ability of melts to flow in a large cross-sectional area of the mould. Flowability limits fluidity when heat and mass flow in the system cause premature freezing of the metal. Fillability is a static criterion, which measures the ability of metal to overcome surface tension and fill fine cavities in the mould. Fillability limits fluidity when molten metal reaches fine mould spaces, but does not have enough static pressure to completely fill such a cavity.

In experiments of A. Kolsgaard and S. Brusethaug that are made to find the fluidity parameters, wide solidification range AlSi7Mg alloy is used. Alloys are reinforced with different sized silicon carbide particles. The composites are cast in a spiral mould. The results are based on the casting of 120 spirals [24].

They have concluded that, silicon carbide particles appear to have little influence on the flowability of the material. The difference in flowability between commercially available metal matrix composites and an unreinforced alloy has no influence in practical terms in a foundry. Increasing the volume fraction of SiC particles above 20% reduces the spiral length considerably and the reduction probably largely from an increase in viscosity [24].

The distance of flow of particulate reinforced metal matrix composites in a mould cavity before solidification influences the particle distribution in the solidified composite product. Dendritic aluminum grains grow freely during flow and push the particles at the interface. After 20 cm of flow the microstructure is dominated by larger circular areas without particles and the particle free areas increase with growing flow distance before solidification. The requirement for uniform particle distribution in a particulate metal matrix component will restrict the maximum flow distance in a mould cavity during casting [24].

Al_4C_3 may form if the melt temperature is above 745ºC. This formation of Al_4C_3 drastically increase the viscosity and reduce fillability. Aluminum carbide is formed in the reaction:

$$4Al + 3SiC = Al_4C_3 + 3Si \qquad (4)$$

Increasing the silicon level will shift the equilibrium of the reaction towards lower aluminum carbide levels, thus the higer silicon level of A359 (9%) compared to 356 (7%) should result in better resistance to aluminum carbide formation on silicon carbide particulates. [25]

2.3.5. Effect of Volume Percentage of Silicon Carbide Reinforcement on 7075 Aluminum Matrix Composites:

M.D. Kulkarni, P.S. Robi, R.C. Prasad and P. Ramakkrishnan made a study on the role of percentage volume of SiCp on the tensile properties and fracture behavior of Al 7075 Al alloys at various test temperatures.

The composition of the Al 7075 is given in Table 2.2. β-SiCp particles of average size 42 μm is used as reinforcement. About 10, 20, and 30 vol% SiCp were incorporated in the melt by rheocasting and squeeze-cast at a pressure of 235 MPa to form composite billets. These were hot extruded to 12mm diameter cylindrical rods at an extrusion ratio 17:1 and rectangular bars of cross-section 11 X 22 mm at an extrusion ratio of 7:1 [26].

Table 2.2. Chemical analysis of as-cast 7075 aluminum alloy [26].

%Cu	%Mg	%Si	%Zn	%Fe	%Cr	%Al
1,26	1,94	0,38	5,5	0,35	0,17	Bal.

The found room temperature tensile and fracture toughness properties are reported in Table 2.3. The ultimate tensile stress values for the base alloy exceeded those for the composites. However, the yield strength values for composites were higher than that of the unreinforced alloy. The yield strength increased linearly with increase in SiCp up to 21vol% in the matrix but a further increase in SiCp content resulted in deviation from linearity towards lower yield strength values. Maximum improvement in Y.S. achieved was 41% when the aluminum alloy was reinforced with 21vol% SiCp [26].

Table 2.3. Room Temperature mechanical properties of 7075 Al-SiCp composites [26].

%SiCp in Al	Y.S (MPa)	U.T.S. (MPa)	E (GPa)	K_Q (MPa√m)
0	325	461	64	21,1
13	383	421	84	30,5
21	458	458	94	28,8
32	395	395	114	24,7

2.3.6. Heat Treatment

Heat treating, in its broadest sense, refers to any of the heating and cooling operations that are performed for the purpose of changing the mechanical properties, the metallurgical structure or the residual stress state of a metal product. When the term is applied to aluminum alloys, however, its use frequently is restricted to the specific operations employed to increase strength and hardness of the precipitation-hardenable wrought and cast alloys. These usually are referred to as the “heat treatable” alloys, to distinguish them from those alloys in which no significant strengthening can be achieved by heating and cooling. The latter, generally referred to as “non-heat treatable” alloys, when in wrought form depend primarily on cold work to increase strength [27].

One essential attribute of a precipitation-hardening alloy system is a temperature-dependent equilibrium, solid solubility characterized by increasing solubility with increasing temperature. Although this condition is met by most of the binary aluminum alloy systems, many exhibit very little precipitation hardening, and these alloys ordinarily are not considered heat treatable [27].

The solubility-temperature relationship required for precipitation hardening of aluminum is illustrated by the Al-Zn system in Figure 2.7. The equilibrium solid solubility of zinc in aluminum increases as temperature increases — from about 0% at 300 °C to a maximum of about 45% at 700°C. At temperatures above the lower curve (the curve starting from 0% Zn at 300 °C), the zinc is completely soluble, and when the alloy is held at such temperatures for sufficient time to permit needed diffusion, zinc will be taken completely into solid solution. At temperatures below the solvus, the equilibrium state consists of two solid phases. When such an alloy is converted to all solid solution by holding above the solvus temperature and then the temperature is decreased to below the solvus, the solid solution becomes supersaturated and the alloy seeks the equilibrium two-phase condition; the second phase tends to form by solid-state precipitation [28].

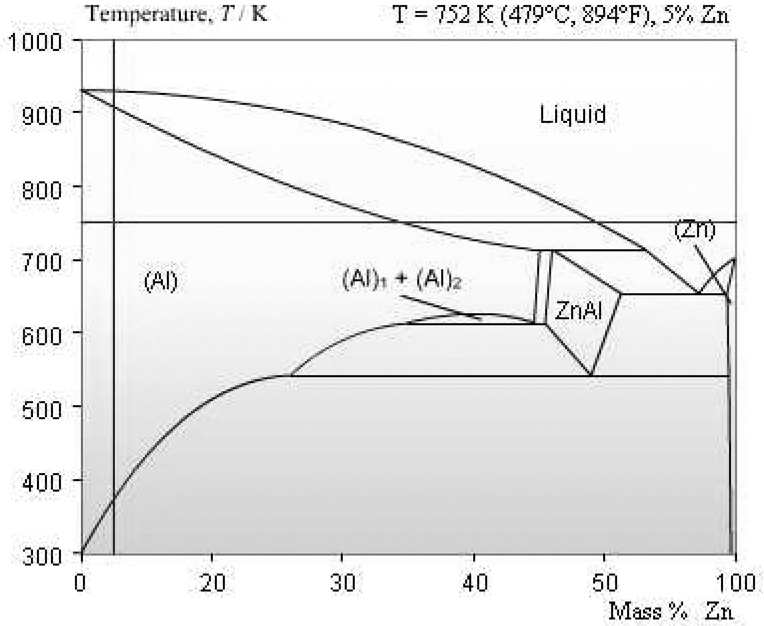

Figure 2.7. Aluminum – Zinc phase diagram [27].

In alloys of the Al-Zn-Mg system, a succession of precipitates is developed from a rapidly cooled supersaturated solid solution (SSS). These precipitates develop sequentially either with increasing temperature or with increasing time at temperatures between room temperature and the solvus. The several stages are listed in Table 2.4 [27].

Table 2.4. Development of precipitates during precipitation heat treatment in Al-Zn-Mg System [27].

Precipitates	**Notes**
No Precipitate	Super Saturated Solid Solution
GP Zones	Spherical GP Zones
η	Hexagonal $MgZn_2$
Γ	Semi Coherent Hexagonal $Mg_{32}(Al,Zn)_{49}$
T	Incoherent Cubic $Mg_{32}(Al,Zn)_{49}$

Commercial alloys whose strength and hardness can be significantly increased by heat treatment include *2xxx, 6xxx* and *7xxx* series wrought alloys (except 7072) and *2xx.O, 3xx.O* and 7*xx.0* series casting alloys. Some of these contain only copper, or copper and silicon, as the primary strengthening alloy addition(s). Most of the heat treatable alloys, however, contain combinations of magnesium with one or more of the elements copper, silicon and zinc. Characteristically, even small amounts of magnesium in concert with these elements accelerate and accentuate the strength changes attributable to precipitation hardening [27].

In the heat treatable wrought alloys, such solute elements are present in amounts that are within the limits of mutual solid solubility at temperatures below the eutectic temperature (lowest melting temperature) [26].

Most of the heat treatable aluminum alloy systems exhibit multistage precipitation and undergo accompanying strength changes analogous to those of the Al-Cu system [27].

Precipitation heat treatments generally are low-temperature, long-term processes. Temperatures range from 115 to 190 °C (240 to 375 °F); times vary from 5 to 48h[27].

Choice of time-temperature cycles for precipitation heat treatment should receive careful consideration. Larger particles of precipitate result from longer times and higher temperatures; however, the larger particles must, of necessity, be fewer in number with greater distances between them. The objective is to select the cycle that produces optimum precipitate size and distribution pattern. Unfortunately, the cycle required to maximize one property, such as tensile strength, is usually different from that required to maximize others, such as yield strength and corrosion resistance. Consequently, the cycles used represent compromises that provide the best combinations of properties [27].

To recap, heat treatment to increase strength of aluminum alloys is a three-step process:

1. Solution heat treatment: dissolution of soluble phases
2. Quenching: development of super saturation
3. Aging: precipitation of solute atoms either at room temperature (natural aging) or elevated temperature (artificial aging or precipitation heat treatment).

2.3.6.1. Solution Heat Treating

To take advantage of the precipitation-hardening reaction, it is necessary first to produce a solid solution. The process by which this is accomplished is called solution heat treating, and its objective is to take into solid solution the maximum practical amounts of the soluble hardening elements in the alloy. The process consists of soaking the alloy at a temperature sufficiently high and for a time long enough to achieve a nearly homogeneous solid solution [27].

Nominal commercial solution heat treating temperature is determined by the composition limits of the alloy and an allowance for unintentional temperature variations [27].

2.3.6.1.1. Solution Treating Time

The time at the nominal solution heat-treating temperature ("soak time") required to effect a satisfactory degree of solution of the undissolved or precipitated soluble phase constituents and to achieve good homogeneity of the solid solution is a function of microstructure before heat treatment. This time requirement can vary from less than a minute for thin sheet to as much as 20 h for large sand or plaster-mold castings [27].

In air furnaces, careful attention should be given to arrangement of the load. Airflow and natural temperature distribution within the furnace should be arranged:

a) To offer minimum resistance to air flow
b) To produce the least disturbance in the natural temperature distribution
c) To afford constant replenishment of the envelope of air around each part.

It is common practice to specify a minimum spacing of 50 mm between parts, but large complex shapes-may require considerably greater spacing.

2.3.6.1.2.High-Temperature Oxidation

There is a condition, commonly but erroneously known as HTO or high-temperature oxidation, which can lead to deterioration of properties in aluminum alloys. Moisture in contact with aluminum at high temperature serve's as a source of nascent hydrogen, which diffuses into the metal. Foreign materials, such as sulfur compounds, function as decomposers of the natural oxide surface film, eliminating it as a barrier either between the moisture and the aluminum or between the nascent hydrogen and the aluminum. The most common manifestation of high-temperature oxidation is surface blistering, but occasionally the only manifestations are internal discontinuities or voids, which can be detected only by careful ultrasonic inspection or by metallographic techniques [27].

Not all alloys and product forms are equally vulnerable to this type of attack. The 7xxx series alloys are most susceptible, followed by the 2xxx alloys [27].

2.3.6.2. Quenching

In most instances, to avoid those types of precipitation that are detrimental to mechanical properties or to corrosion resistance, the solid solution formed during solution heat treatment must be quenched rapidly enough (and without interruption) to produce a supersaturated solution at room temperature - the optimum condition for precipitation hardening. Most frequently, parts are quenched by immersion in cold water [27].

If appreciable precipitation during cooling is to be avoided, two requirements must be satisfied. First, the time required for transfer of the load from the furnace to the quenching medium must be short enough to preclude slow pre-cooling into the temperature range where very rapid precipitation takes place. For alloy 7075, this range was determined to be 400 to 290 °C (750 to 550 °F), and some sources quote this range (or a slightly different range) as the most critical range for quenching of any aluminum alloy [27].

The second requirement for avoidance of appreciable precipitation during quenching is that the volume, heat-absorption capacity and rate of flow of the quenching medium be such that little or no precipitation occurs during cooling. Any interruption of the quench that might allow reheating into a temperature range where rapid precipitation can occur must be prohibited [27].

Table 2.5 shows the typical solution and precipitation heat treatments for aluminum 7075 alloy products.

Table 2.5. Typical solution and precipitation heat treatments for aluminum 7075 alloy products [26].

Alloy	Product Form	Solution Heat Treatment			Precipitation Heat Treatment			
		Metal Temperature		Temper Design.	Metal Temperature		Time (h)	Temper Design.
		C	F		C	F		
7075	Sheet	480	900	W	120	250	24	T6
					120	250	24	T62
	Plate	480	900	W	120	250	24	T62
				W51	120	250	24	T651
	Rolled or cold finished wire, rod and bar	490	915	W	120	250	24	T6
					120	250	24	T62
				W51	120	250	24	T651
	Extruded rod, bar, shapes and tube	465	870		120	250	24	T6
					120	250	24	T62
				W510	120	250	24	T6510
				W511	120	250	24	T6511
	Drawn tube	465	870	W	120	250	24	T6
					120	250	24	T62
	Die Forgings	470	880	W	120	250	24	T6
	Hand Forgings	470	880	W	120	250	24	T6
				W52	120	250	24	T652
	Rolled rings	470	880	W	120	250	24	T6

2.3.6.2.1.Delay in Quenching

Whether the transfer of parts from the furnace to the quench is performed manually or mechanically, for several alloys, maximum thickness that can be quenched in solutions of specific concentrations is difficult while maintaining acceptable property levels [27].

2.3.6.3.Treatments that Precede Precipitation Heat Treating

Immediately after being quenched, most aluminum alloys are nearly as ductile as they are in the annealed condition. Consequently, it is often advantageous to form or straighten parts in this temper. Moreover, at the mill level, controlled mechanical deformation is the most common method of reducing residual quenching stresses [27].

2.3.6.3.1. Natural Aging

The more highly alloyed members of the *6xxx* wrought series, the copper-containing alloys of the 7*xxx* group, and all of the 2xxx alloys are almost always solution heat treated and quenched. For some of these alloys, the precipitation hardening that results from natural ageing alone produces useful tempers (T3 and T4 types) that are characterized by high ratios of tensile to yield strength, high fracture toughness and high resistance to fatigue. For the alloys that are used in these tempers, the relatively high supersaturation of atoms and vacancies retained by rapid quenching causes rapid formation of GP zones and strength increases rapidly, attaining nearly maximum stable values in four or five days. The *6xxx* alloys and to an even greater degree the *7xxx* alloys are considerably less stable at room temperature and continue to exhibit significant changes in mechanical properties for many years [27].

2.3.6.3.2. Precipitation Heat Treatment

In aluminum alloys in the solution heat treated and quenched condition, coloration contrast between grains of differing orientation is relatively high. This contrast is noticeably decreased by precipitation heat treatment. The mechanical properties and other characteristics change continuously with time and temperature; to produce a combination of properties corresponding to specific alloy-temper combination requires one or more rather specific and coordinated combinations of time and temperature [27].

Use of higher temperatures may reduce treatment time; but if the temperature is too high, characteristic features of the precipitation-hardening process reduce the probability of obtaining the required properties [27].

Precipitation heat treatment following solution heat treatment and quenching produces T6 tempers. Alloys in T6-type tempers generally have the highest strengths practically without sacrifice of the other properties and characteristics found by experience to be satisfactory and useful for engineering applications [27]. Temper designations and its explanations given in Table 2.6.

Table 2.6. Temper Designations and their explanations [27].

Temper Designation	Explanation
T1	Cooled from an Elevated-Temperature Shaping Process and Naturally Aged to a Substantially Stable Condition
T2	Cooled from an Elevated-Temperature Shaping Process, Cold-Worked, and Naturally Aged to a Substantially Stable Condition
T3	Solution Heat-Treated, Cold-Worked, and Naturally Aged to Substantially Stable Condition
T4	Solution Heat-Treated and Naturally Aged to a Substantially Stable Condition
T5	Cooled from an Elevated-Temperature -Shaping Process and Artifically Aged
T6	Solution Heat-Treated and Artificially Aged
T7	Solution Heat-Treated and Over-aged or Stabilized
T8	Solution Heat-Treated, Cold-worked and Artificially Aged
T9	Solution Heat-Treated, Artificially Aged and Cold-worked
T10	Cooled from an Elevated-Temperature Shaping Process, Cold-Worked and Artificially Aged

Table 2.7 shows soak times and maximum quench delays for solution treatment of wrought aluminum alloys.

Table 2.7. Soak times and maximum quench delays for solution treatment of wrought aluminum alloys [26].

Thickness, mm	**Soak time, minutes**				**Maximum quench delay, sec.**
	Air Furnace		**Salt bath**		
	min.	**max.**	**min.**	**max.**	
Thru 0,41	20	25	10	15	5
0,51	20	30	10	20	7
0,64	25	35	15	25	7
0,81	25	35	15	25	7
1,02	30	40	20	30	10
1,27	30	40	20	30	10
1,35	30	40	20	30	10
1,8	35	45	25	35	10
2,03	35	45	25	35	10
2,29	35	45	25	35	10
2,54	40	55	30	45	15
3,18	40	55	30	45	15
4,06	50	60	35	45	15
4,57	50	60	35	45	15
6,35	55	65	35	45	15
Over 6,35 thru 12,7	65	75	45	55	15
For each additional 12,7	+30	+30	+20	+20	...
Rivets (all)	60	...	30	...	5

CHAPTER 3

EXPERIMENTAL

3.1. Matrix Material

Al 7075 was used as matrix material. The main alloying element is zinc. The second is magnesium, which is predominantly added to increase the wetting between matrix and reinforcement. Composition of aluminum 7075 was tabulated in Table 3.1.

Table 3.1. Composition (wt%) of Aluminum 7075.

Cu	Mg	Zn	Cr	Si	Ti	Al
1,2 - 2,0	2,1 - 2,9	5,1 - 6,1	0,18 - 0,28	0 -0,40	0 - 0,2	Bal.

Table 3.1 gives ranges of the alloying elements. The actual composition in our casting process is given in Table 3.2. Al-Ti-B (Al-5wt% Ti-1wt%B) was used to refine and decrease grain size of the matrix.

Table 3.2. The actual composition (wt%) of the matrix material.

Alloying Element	**Cu**	**Mg**	**Zn**	**Cr**	**Al-Ti-B**	**Si**	**Al**
Weight (gr)	15,0	28,0	60,0	2,5	4,0	0,0	900,0
Percentage (%)	1,49	2,77	5,94	0,25	0,40	0,00	89,15

3.2. Reinforcement Material

Silicon carbide particulates are used as reinforcement material. The powder was obtained from EGESAN. The type of the silicon carbide is F320. Density of silicon carbide is between 1,29-1,35 g/cm^3 and the mesh size is 29,2 ± 1,5 µm. Surface chemical values are given in Table 3.3.

Table 3.3. Surface chemical values of F 320 silicon carbide.

Product	%SiC	%Free C	%Si	%SiO_2	%Fe_2O_3
F 240 - F 800	99,50	0,10	0,10	0,10	0,05

Silicon carbide powders was supplied from KLA Exalon, Norway. The structure of the silicon carbide is hexagonal 6H with some rhombohedral 15R and sometimes some hexagonal 4H.

3.3. Casting of Silicon Carbide Reinforced Aluminum 7075 Matrix Composite:

The existing vertical filling squeeze casting process was developed at METU. Die assembly made of hot work tool steel, specially machined and heat treated, was used to perform metal matrix composite processing. The three point bending and tensile test specimens were directly and simultaneously. Figure 3.1 shows the squeeze casting machine and Figure 3.2. shows the die. Inducto-therm induction furnace is used to melt the aluminum 7075 alloy.

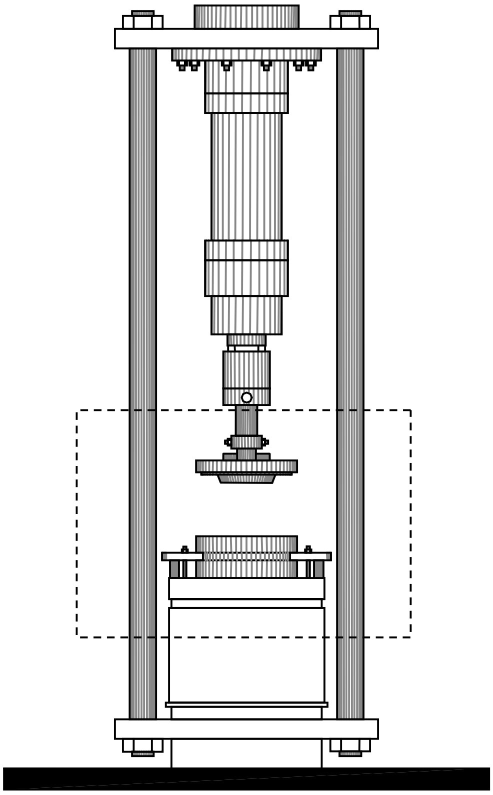

(a)

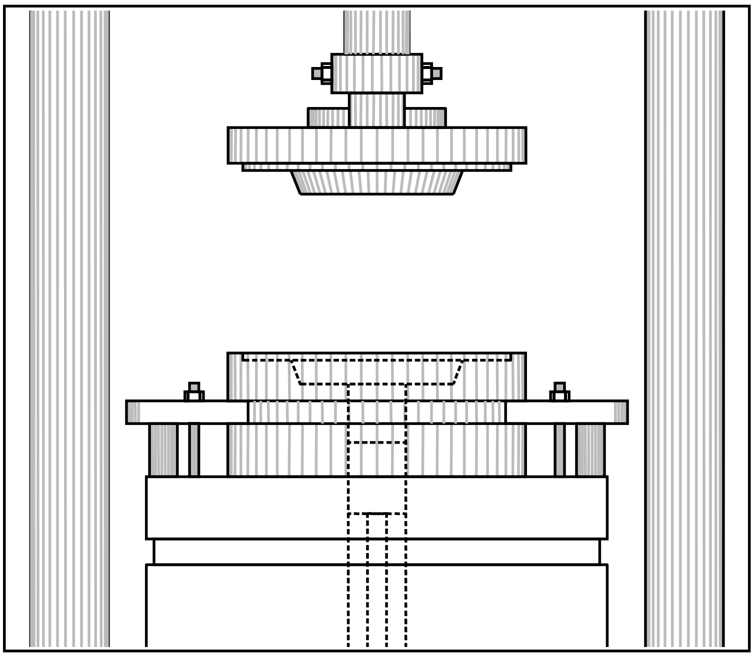

(b)

Figure 3.1. The squeeze casting machine; (a) General view (b) Closer view

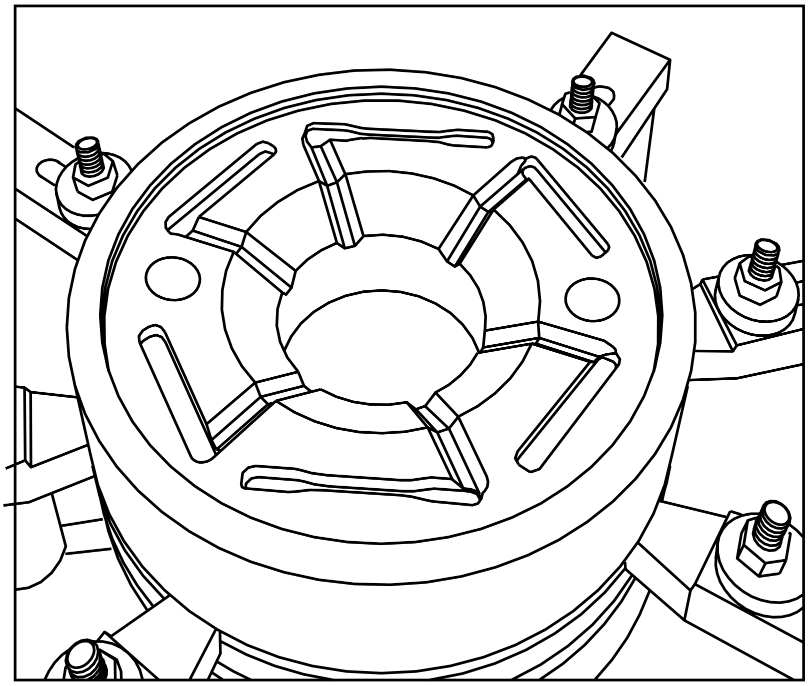

Figure 3.2. Detailed view of the die

Casting process was carried out through the following steps:

1. Chemical composition was adjusted according to the standards.
2. Aluminum alloy’s elements (except magnesium) were added into the induction furnace and temperature of the furnace was adjusted to about 800-900 °C and waited until obtaining a liquid phase. Magnesium was added after the liquid phase is obtained.
3. After obtaining the melt, silicon carbide powder was added into the molten metal.
4. Then furnace was turned off, and mechanical agitation was started.
5. After a certain agitation, furnace was turned on again to melt the alloy. Imaginary magnetic lines helped the mixing of SiC particulates to the molten metal.
6. A homogenous melt was obtained.

7. While making the mechanical agitation, the mould was heated by a torch.
8. Silicon carbide reinforced aluminum 7075 was processed by squeeze casting applying 80 MPa pressure. At each casting operation one to six specimens were obtained. The remaining part was re-melted and recycled.
9. At the end of the casting process several three-point bending test and tensile testing specimens were obtained.

Three Point Bending Test and Tensile Testing Specimens:

Five types (0-10-15-20-30 wt% SiC) of three point bending test and tensile testing specimens were obtained. The specimens were prepared for tensile testing and three point bending tests after casting. Only the burrs were cleaned before starting the tests.

Dimensions and shape of tensile testing specimens are given below:

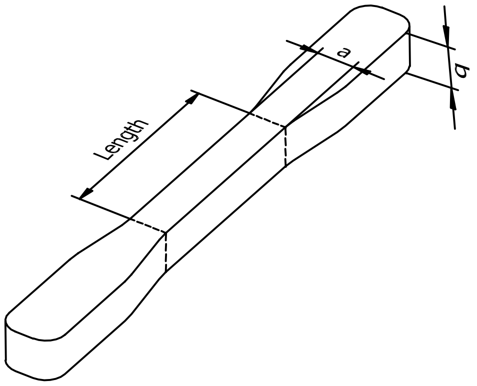

Length = 30 ± 2 mm (length between the necks)

a (width) = 6 ± 0.5 mm

b (thickness) = 5.8 ± 0.4 mm

Figure 3.3. Tensile testing specimen

Dimensions and shape of three point bending test specimens are given below:

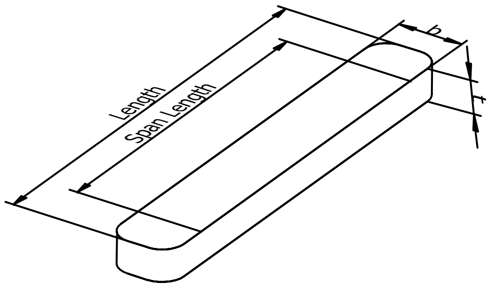

Length = 65 ± 0.3 mm

Span length = 50 mm

b (width) = 10 ± 0.1 mm

t (height) = 5 ± 0.4 mm

Figure 3.4. Three point bending test specimen

3.4. Mechanical Testing and Testing Apparatus

Tensile testing and three point bending tests were done. Seven specimens of three point bending of all compositions, as-cast and heat treated are tested. Also three specimens of tensile testing of all compositions, as cast and heat treated are tested.

Hardness tests data was obtained from Emco Test Automatic hardness test machine. Vickers 10 kg hardness values were acquired. Average values of hardness values were taken. Both sides of the specimens were tested.

3.5. Calculations

Load (P) versus deflection (δ) data were recorded during tensile testing. Also the ultimate tensile strengths was evaluated. Recorded maximum loads are in kilograms and they were converted to maximum stress values (MPa). Cross-sectional areas of tensile testing samples were measured and lengths are compared before and after fracture. All of the burrs were grinded in order to prevent notch effect.

In three-point bending tests, the maximum fracture loads were evaluated. These kilogram values were converted into flexural stress (MPa) values.

The flexural stress formula is given as; $\sigma = My/I$ where σ flexural stress, M the bending moment, y the distance from the natural axis and I the moment of inertia. The maximum flexural surface stress occurs in the mid-point of the specimen. Therefore:

$M = P*L/4$; $y = t/2$; $I = b*t^3/12$
$\sigma_{max} = (3*P*L) / (2*b*t^2)$

P: Load applied by the testing machine,
t: Thickness of the specimen
b: Width of the specimen, and
L: Span length respectively.

3.6. Heat Treatment

All of the specimens were heat treated according to ASM T6 heat treatment procedures. As it is stated in tables 2.4 and 2.5 all of the heat treated samples were solution treated at 480 ºC for 55 to 65 minutes. Then they were quenched into water. Finally precipitation heat treatment was carried out for 24 hours at 120 ºC.

3.7. Metallographic Examination and Image Analyzer Studies:

Microstructures of as-cast and heat treated aluminum composite samples were examined by metallographically. The photographs of samples were taken. Samples were firstly cut and mounted. Then they were grinded, polished and etched with Keller solution which contains 1,5% HCl, 2,5% HNO_3, 1% HF, 95% H_2O. At the end, representative photographs were taken by a digital camera.

In order to have an information about the volume fraction of SiC reinforced aluminum 7075 alloy composites, image analyzer study was performed. With the help of Clemex software, area percentages of SiC and aluminum matrix was calculated and this gives an approximate value about the volume percentages of reinforcement and the matrix.

3.8. X-Ray Study

X-ray studies were made to find out the crystal structure of silicon carbide particulates. The second phases that may form during casting and heat treatment were revealed by x-ray structure analysis. X-ray analysis was made by 100 kV Philips twin tube X-ray diffractometer.

3.9. SEM Study

In order to get detailed and close views of interior structures of aluminum samples SEM studies were done. Especially the precipitates that should form after heat treatment were examined. The percentages of alloying elements were analyzed and their graphs were obtained. SEM studies were done with JSM-6400 Electron Microscope (JEOL), equipped with NORAN System.

CHAPTER 4

RESULTS AND DISCUSSION

Effects of silicon carbide addition on the fracture behavior of aluminum matrix alloy composites was examined in this study. Both as-cast and heat treated matrixes were examined. Hardness tests were also evaluated in order to find out the optimum heat treatment procedure. Five different additions of silicon carbide was carried out and samples were investigated. They are listed in Table 4.1.

Table 4.1. List of silicon carbide (wt%) reinforced aluminum matrix composites.

% SiC Addition	Explanation
Al – 0% SiCp	0 wt% particulate reinforced, squeeze cast aluminum matrix
Al - 10% SiCp	10 wt% particulate reinforced, squeeze cast aluminum matrix
Al - 15% SiCp	15 wt% particulate reinforced, squeeze cast aluminum matrix
Al - 20% SiCp	20 wt% particulate reinforced, squeeze cast aluminum matrix
Al - 30% SiCp	30 wt% particulate reinforced, squeeze cast aluminum matrix

4.1. Hardness Test Results

Hardness tests were carried out to observe the effects of heat treatment and effects of wt% addition of silicon carbide on aluminum alloy matrix since hardness is an indicator of a materials resistance to plastic deformation. Figure 4.1. shows the variation of hardness values with wt% silicon carbide. Hardness test results are listed in Table 4.2.

Table 4.2. Hardness test results of the as-cast specimens measured by Vickers test (10 kg).

Measurement No.	**1**	**2**	**3**	**4**	**5**	**6**	**7**	**Average**
Al - % 0 SiC	131	131	131	136	136	132	135	**133**
Al - %10 SiC	139	138	138	138	136	138	137	**138**
Al - %15 SiC	134	138	153	154	153	154	146	**147**
Al - %20 SiC	155	163	166	155	160	157	160	**159**
Al - %30 SiC	172	205	175	185	182	192	206	**188**

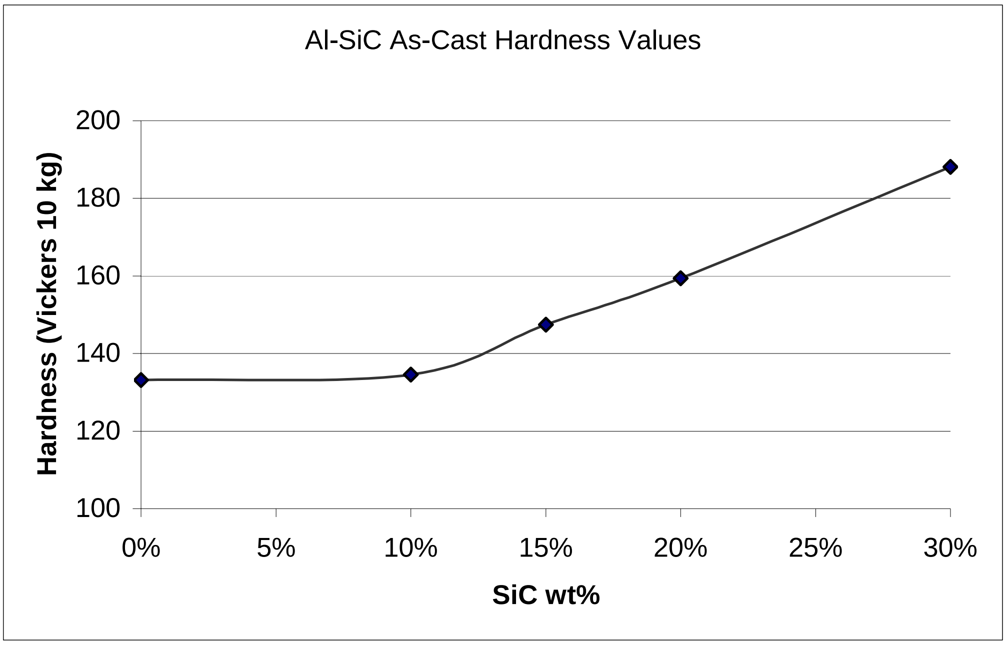

Figure 4.1. Variation of hardness values of as-cast specimens with wt% silicon carbide.

As they are given in Figure 4.1.and Table 4.2, hardness values increase with the addition of silicon carbide. Silicon carbide particulates are ceramic materials that are harder than the aluminum matrix alloy. They pin the dislocation motion and therefore an increase in strain hardening achieved [26].

Heat treatment also has effects on the hardness values of aluminum matrix alloy. By precipitation heat treatment extra hardening was obtained. Precipitates acts like silicon carbide particles and it can be said that they form barricades to dislocation motion. The aluminum matrix composites were solution heat treated at 480ºC for 55-65 minutes and precipitation heat treated at 120ºC for twenty-four hours. Table 4.3. lists the results of hardness tests and Figure 4.2 shows the variation of hardness with wt% addition of silicon carbide particulates.

Table 4.3. Hardness test results of the heat treated specimens measured by Vickers test (10 kg).

Measurement No.	**1**	**2**	**3**	**4**	**5**	**6**	**7**	**Average**
Al - % 0 SiC	173	172	178	171	166	171	168	**171**
Al - %10 SiC	182	180	184	178	183	183	181	**182**
Al - %15 SiC	185	189	186	183	189	184	185	**186**
Al - %20 SiC	201	202	192	199	192	201	200	**198**
Al - %30 SiC	221	222	232	229	218	202	226	**221**

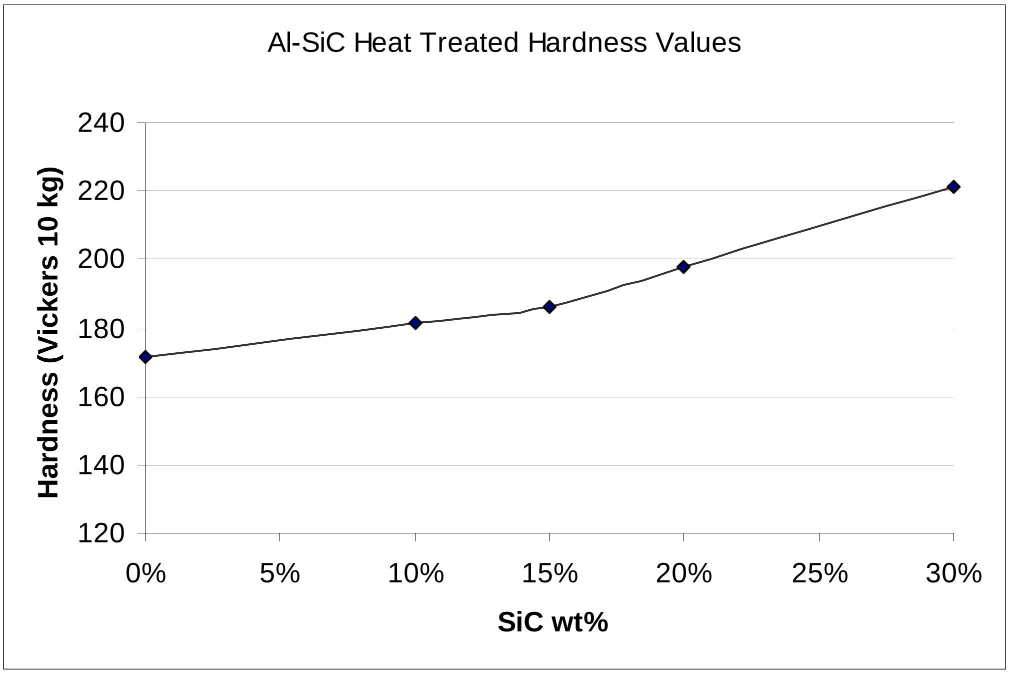

Figure 4.2. Variation of hardness values of heat treated specimens with wt% silicon carbide.

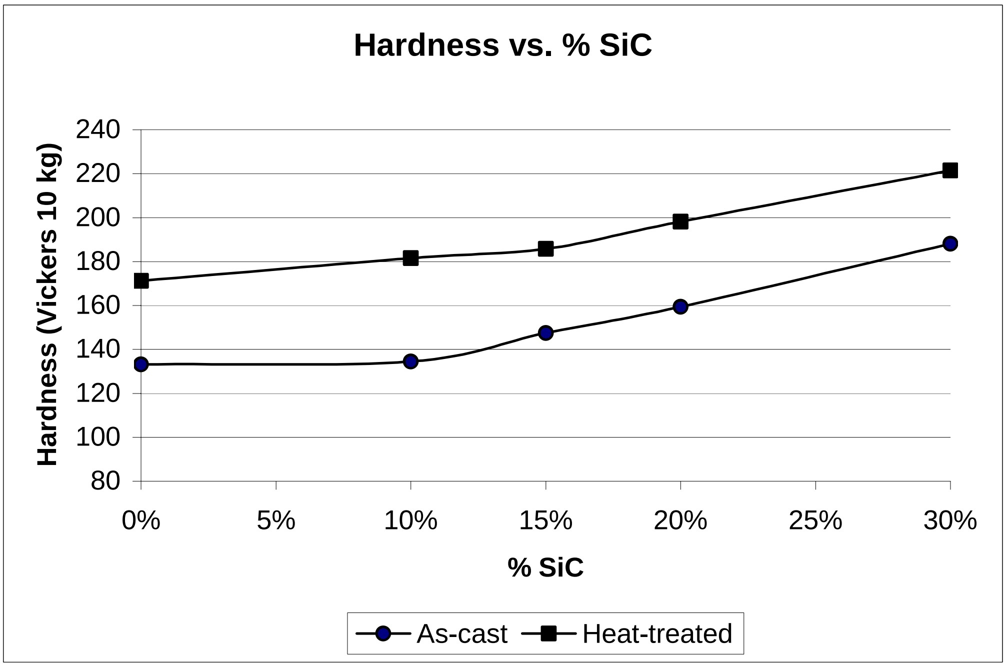

Figure 4.3. Comparison between hardness values of as-cast and heat treated silicon carbide reinforced aluminum matrix composite.

In Figure 4.3. a comparison between hardness values of as-cast and heat treated silicon carbide reinforced aluminum matrix composites was done. It is seen that proper heat treatment increases the hardness values.

Precipitation heat treatments were made according to the publication of ASM Committee on Heat Treating of Aluminum alloys [27]. To find out whether the T6 heat treatment (Table 2.5.) gives the peak hardness, various precipitation heat treatment time periods were applied. Figures 4.4 to 4.8. summarize this process and details of this process are given in Appendix A.

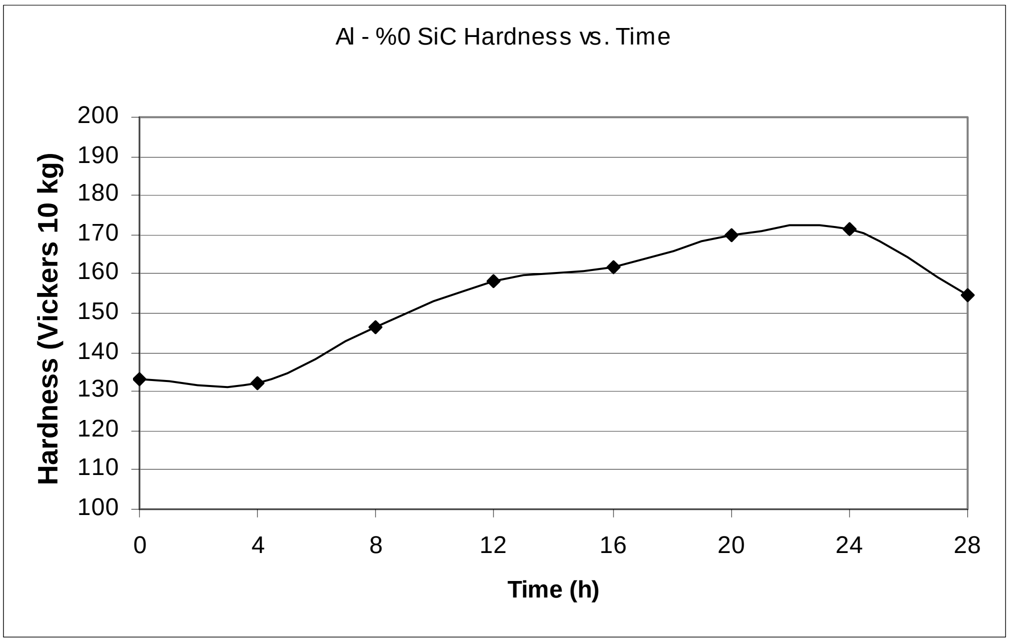

Figure 4.4. Variation of hardness values (Vickers 10kg) with precipitation heat treatment time of Al 7075 alloy.

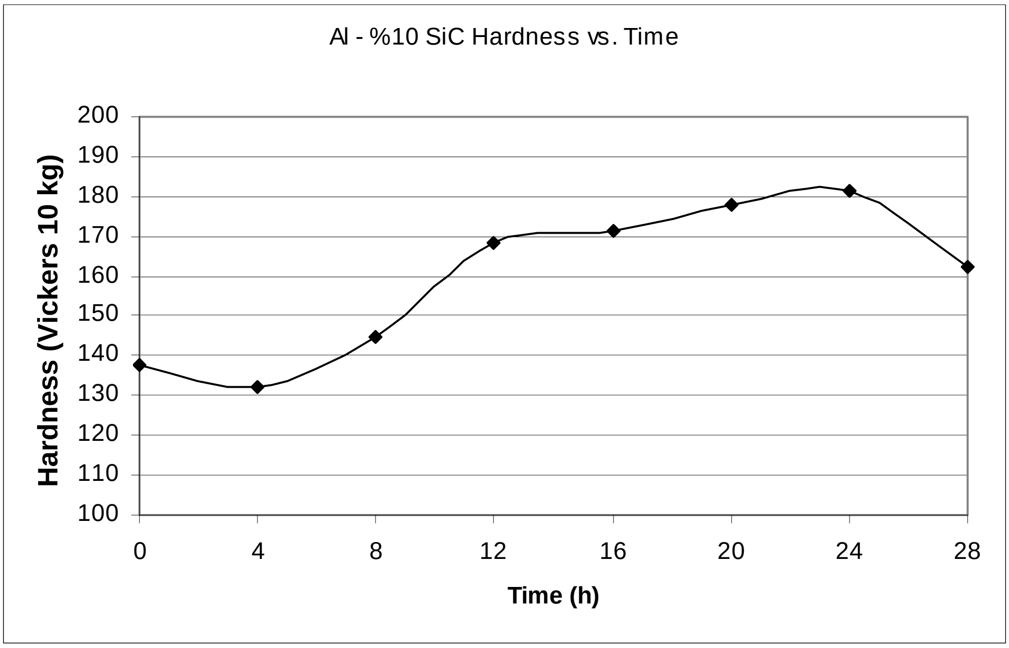

Figure 4.5. Variation of hardness values (Vickers 10kg) with precipitation heat treatment time of Al-10wt% SiC_p composite.

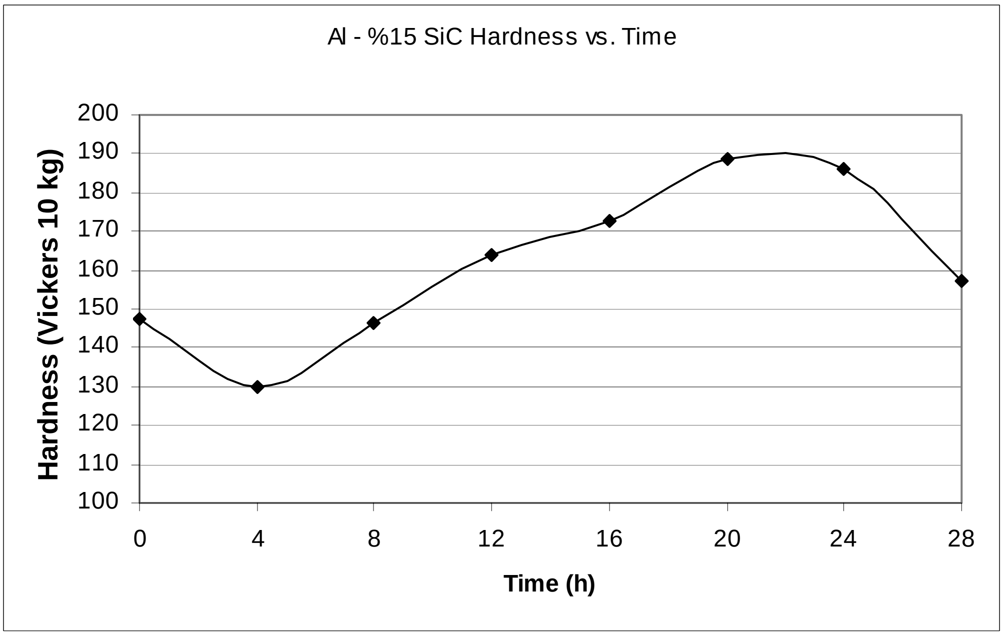

Figure 4.6. Variation of hardness values (Vickers 10kg) with precipitation heat treatment time of Al-15wt% SiC_p composite.

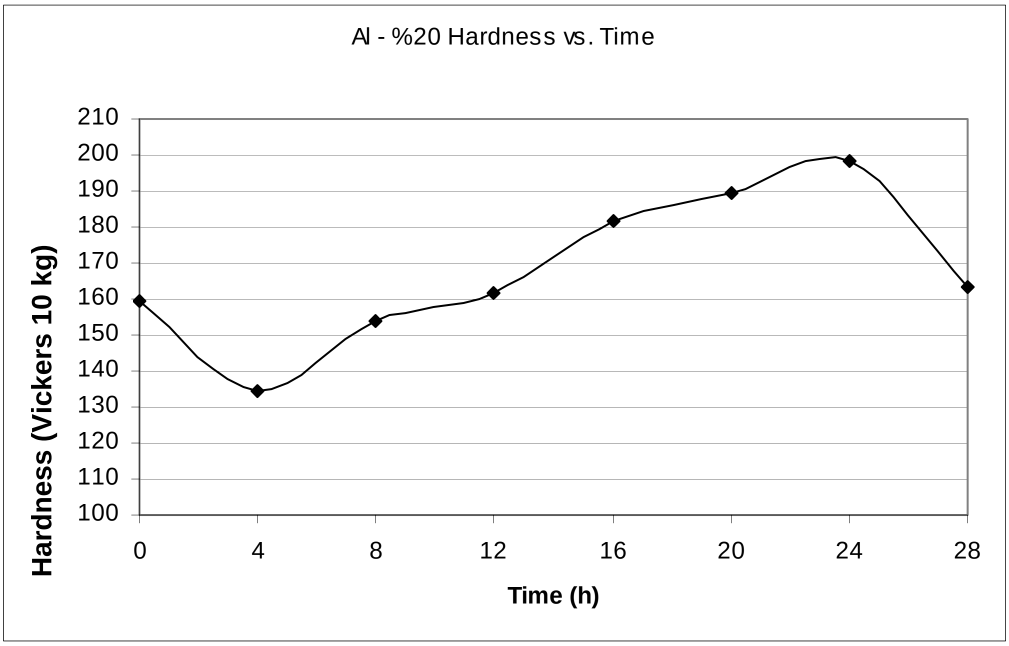

Figure 4.7. Variation of hardness values (Vickers 10kg) with precipitation heat treatment time of Al-20wt% SiC_p composite.

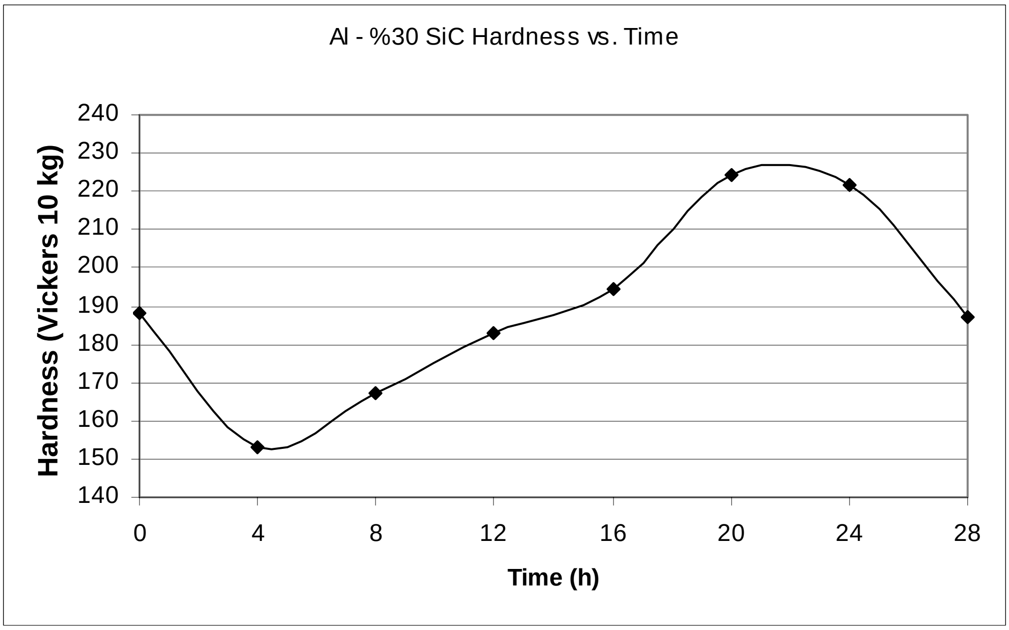

Figure 4.8. Variation of hardness values (Vickers 10kg) with precipitation heat treatment time of Al-30wt% SiC_p composite.

Peak hardness values are obtained after 24 hours precipitation heat treatment at 120 ºC. From 4 hours to 24 hours usually hardness values increased gradually. Only in 15 wt% and 30 wt% SiC composite, a small decrease in hardness observed from 20 hours to 24 hours treatment. This decrease arises from the variation of hardness values in different regions of specimens. If the values were taken from the region where silicon carbide particles existed intensively, hardness values were measured higher than original values. Figure 4.9 shows and compares hardness variation with time for all compositions.

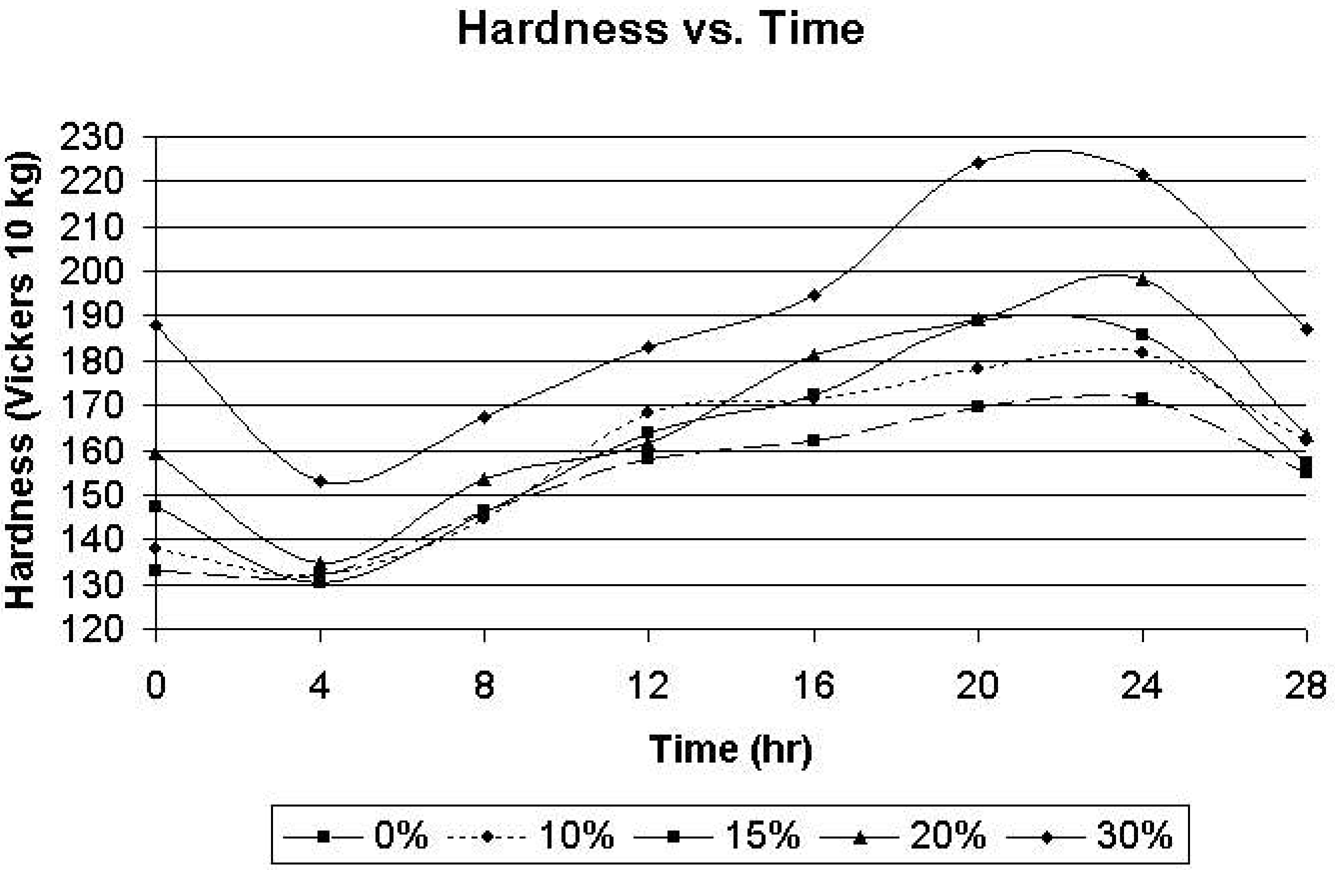

Figure 4.9. Comparison of hardness variation with time.

4.2. Three Point Bending Test Results:

Three point bending tests were performed to observe the fracture behavior of aluminum matrix composite with different percentage additions of silicon carbide. Several three point bending tests are done and their results are listed in Table 4.4. and details are given in Appendix B. Results are given graphically in Figure 4.10. as well.

Table 4.4. Maximum load (kg.) and maximum flexural stress (MPa) values of as-cast aluminum composites.

Alloy	Maximum Load (kg)	Maximum Flexural Strength (MPa)
Al – 0wt%SiC	154	408
Al – 10wt%SiC	170	444
Al – 15wt%SiC	141	375
Al – 20wt%SiC	138	363
Al – 30wt%SiC	124	301

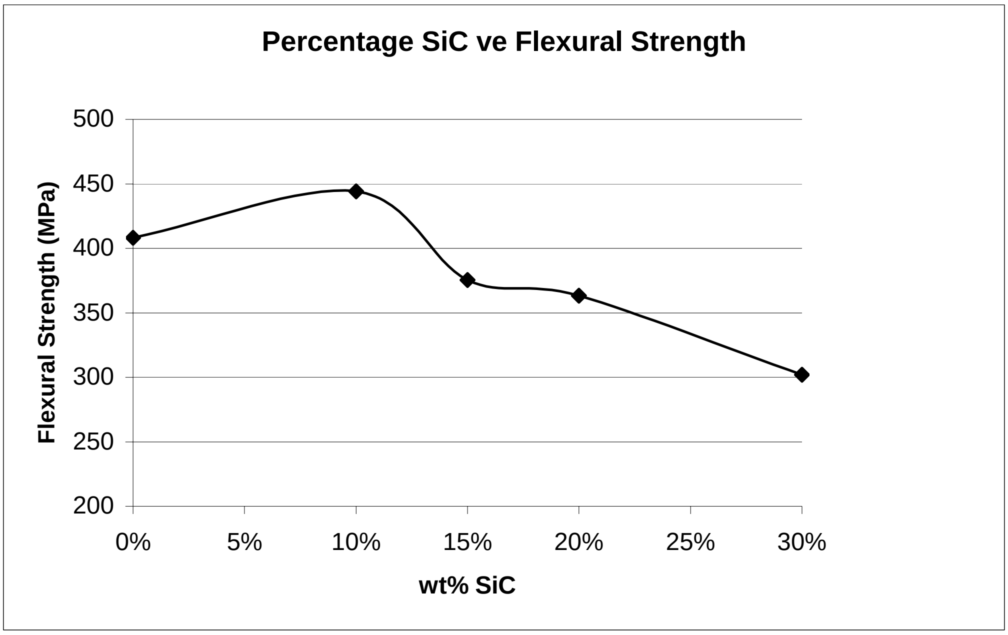

Figure 4.10. Variation of flexural strength of aluminum matrix composite with wt% silicon carbide.

The flexural strength increased with increasing reinforcement content up to 10wt% silicon carbide. Composites show enough internal ductility to attain full strength. After 10 wt% SiC more additions of silicon carbide decreased the strength. In fact the 30wt% silicon carbide aluminum matrix composites' strength fell down to 300 MPa.

Strength began to decrease as content approaches 15wt% silicon carbide. Composites failed at small strain values during the three point bending test for composites reinforced with 30wt% SiC_p. The matrixes probably did not have enough internal ductility and cannot overcome the localized internal stresses. Therefore the composites failed before reaching the fracture strength 10wt% SiC_p composite. All specimens showed brittle fracture at macro scale fracture surface examinations.

The 10wt% SiC reinforced aluminum matrix composites have the maximum strength among the other composites. The optimum conditions were formed and maximum strength increased about 40 MPa. according to aluminum matrix. Silicon carbide particulates having particle size in the range of 10-30 μm form barricades and hinder dislocation motion. This supplies an increase in strain hardening and flexural strength.

Both as-cast composites and T6 heat treated aluminum matrix composites were subjected to three point bending tests. Results are tabulated in Table 4.5 and details are given in Appendix B . Graphical explanations were given in Figure 4.11.

Table 4.5. Maximum load and maximum flexural stress values of heat treated aluminum composites.

Alloy	Maximum Load (kg)	Maximum Flexural Strength (Mpa)
Al – 0wt%SiC	168	446
Al – 10wt%SiC	219	581
Al – 15wt%SiC	172	453
Al – 20wt%SiC	171	438
Al – 30wt%SiC	158	429

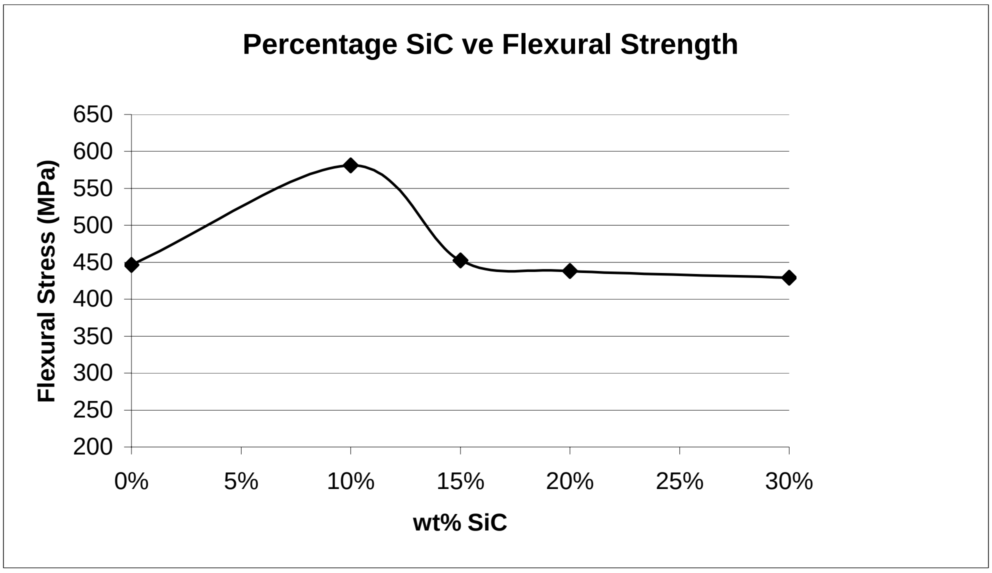

Figure 4.11. Variation of flexural strength of heat treated aluminum matrix composite with wt% silicon carbide.

As in the as-cast composites the 10wt% silicon carbide reinforced aluminum matrix composites have maximum flexural strength. Small $MgZn_2$, $Mg_{32}(Al,Zn)_{49}$ precipitates increased strength after T6 heat treatment. They acted as barriers to dislocation motion. Size of precipitates is very small when compared with SiC particulates. Their size are between 0,5-1,5 µm.

With the effect of precipitates and silicon carbide particulates, the 10%wt SiC reinforced composite reached to 588 MPa of maximum strength. This means a %44 increase compared to as-cast and unreinforced aluminum alloy. Heat treated specimens in all compositions fractured in a brittle manner at macro scale.

Figure 4.12. compares the as-cast and heat treated silicon carbide reinforced aluminum composite.

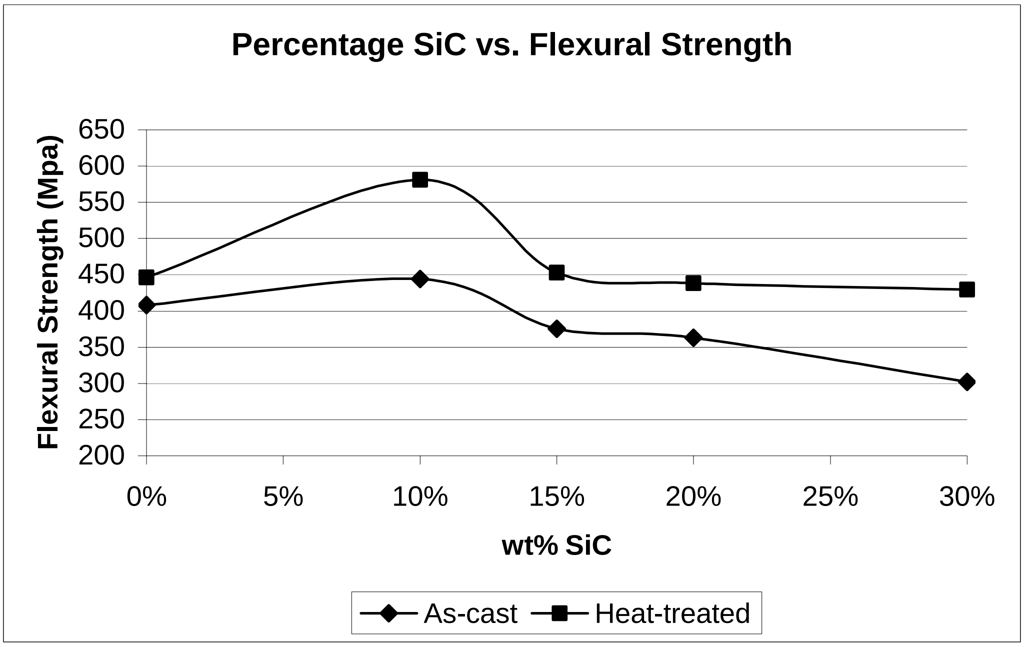

Figure 4.12. Comparison of as-cast and heat treated SiC reinforced aluminum matrix composite.

4.3. Tensile Testing Results

Although tensile testing is not recommended in examining the fracture behavior of SiC reinforced aluminum composite, tensile tests were performed to get stress – strain graphs, to find out Young’s Modulus and ultimate tensile strength values. But unfortunately, specimens fractured in the early stages of tensile tests and lower strength values were obtained. Almost all specimens broken from the curved parts. Agglomeration of silicon carbide particulates was observed in some of the tensile test specimens.

Usually three point bending tests were applied instead of tensile testing in investigating of particulate reinforced metal composites. The main reason is the silicon carbide particulates make notch effect during the testing. Since machining of SiC_p reinforced aluminum matrix composites’ surface is a very delicate and special process, structure may be weakened. Machining requires high speed diamond tools and if it is done by conventional machining, it leaves machining marks on the surfaces.

The results of as-cast and heat treated composites tensile tests are given in Table 4.6 and in Figure 4.13.

Table 4.6. Tensile test results of as-cast and heat treated aluminum composites.

Alloy	As - Cast Ultimate Tensile Strength (MPa)	Heat Treated Ultimate Tensile Strength (MPa)
Al – 0wt%SiC	173,43	206,91
Al – 10wt%SiC	212,15	341,09
Al – 15wt%SiC	200,23	224,93
Al – 20wt%SiC	187,55	202,75
Al – 30wt%SiC	191,11	144,62

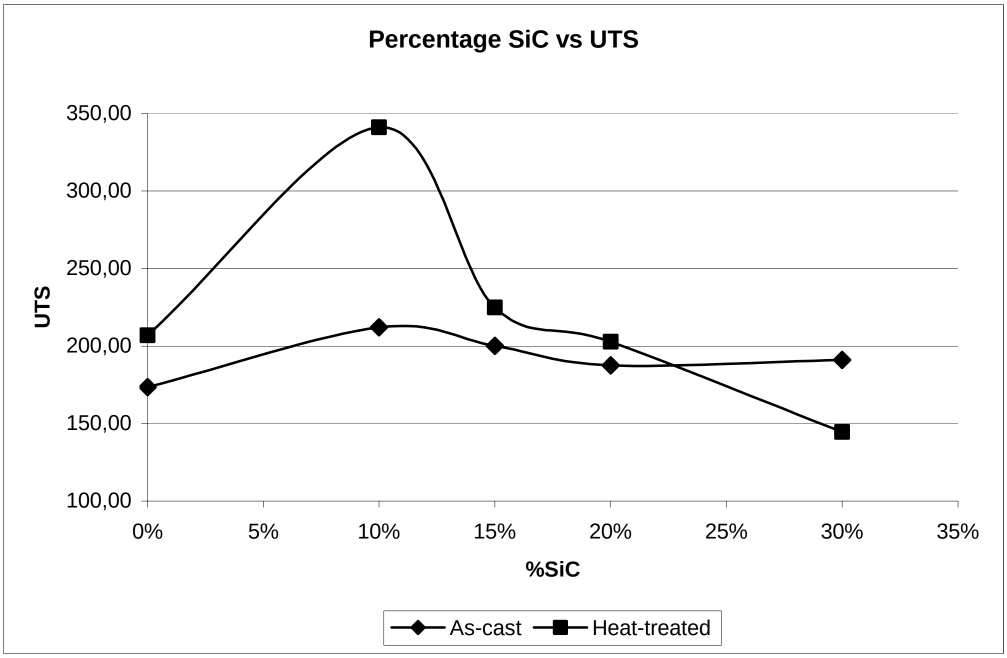

Figure 4.13. Comparison of as-cast and heat treated SiC reinforced aluminum matrix composites tensile test results.

Even tough the ultimate tensile strength values are low, the 10wt% silicon carbide aluminum composite showed the maximum strength. The strength increasing tendency of composites matches in three point bending tests and in tensile testing. Thus reliability of three point bending tests was confirmed in this study.

Elastic modulus values were calculated theoretically with the Rule Of Mixtures formula since proper strength-strain values could not been obtained. According to the formula, range of elastic modulus of composites can be found with the following formula.

For upper limit:

$E_{comp} = (E_p*V_p) + (E_m*V_m)$

For lower bound:

$E_{comp} = E_m*E_p / (E_p*V_m + E_mV_p)$

Where Vp and Vm are volume percentages of silicon carbide particulate and matrix respectively. From the literature, elastic modulus of aluminum 7075 alloy was found between 70-80 GPa and the manufacturer firm states the elastic modulus of SiC as 480 GPa. So, with the calculation according to the rule of mixtures following results obtained and tabulated in Table 4.7.

Table 4.7. Elastic modulus of SiC reinforced aluminum composites

Alloy	**Vol% Matrix**	**$E_{comp.}$ - Lower Bound (GPa)**	**$E_{comp.}$ - Upper Limit (GPa)**
Al – 0wt%SiC_p	100,00%	75,00	75,00
Al – 10wt%SiC_p	80,81%	89,49	152,72
Al – 15wt%SiC_p	72,56%	97,60	186,13
Al – 20wt%SiC_p	64,67%	106,85	218,09
Al – 30wt%SiC_p	52,53%	125,11	267,25

The elastic modulus of the matrix was taken as 75 GPa, which is the average value. Theoretically the elastic modulus increases with increasing vol% of silicon carbide. This increase is valid up to vol% silicon carbide addition where an uniform composite can be produced.

4.4. X-Ray Study Results

X – ray analysis of the heat treated aluminum composites and silicon carbide particulates was done. As it is stated in chapter 3, in x-ray study part, silicon carbide powders have both hexagonal 6H and rhombohedral 15R crystal structure.

Heat treated composites were analyzed to find out the precipitated phases that are formed during T6 heat treatment. Figures 4.14 to 4.17. show the x-ray diffractograms of silicon carbide particulate reinforced aluminum composites.

Specimens, which have showed minimum tensile strength in the three point bending test, were chosen for x-ray analysis. Consequently, samples scanned to reveal any other precipitated phase other than expected precipitate such as Al_4C_3.

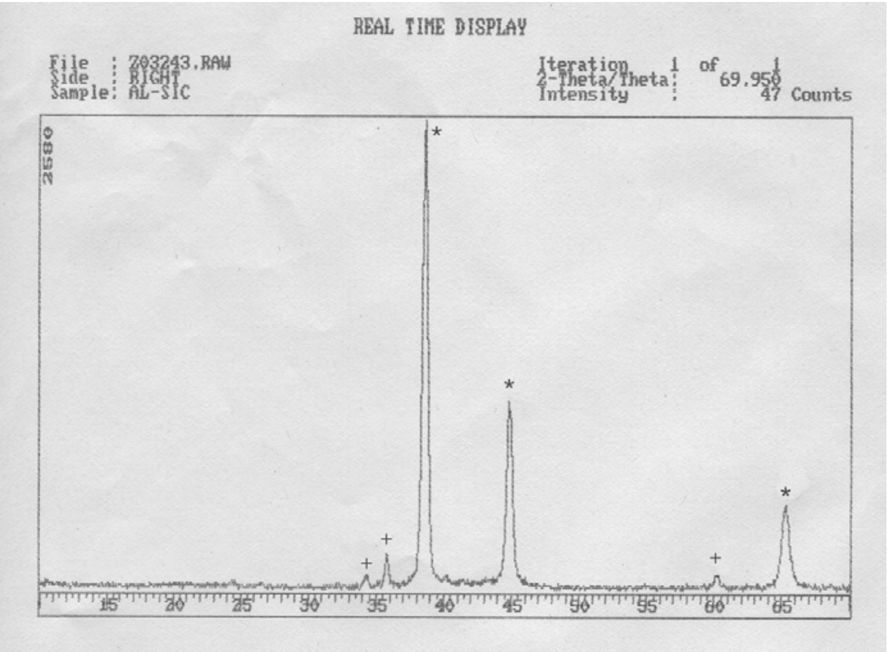

Figure 4.14. X-ray diffractogram of heat treated 10wt%SiC Al composite.

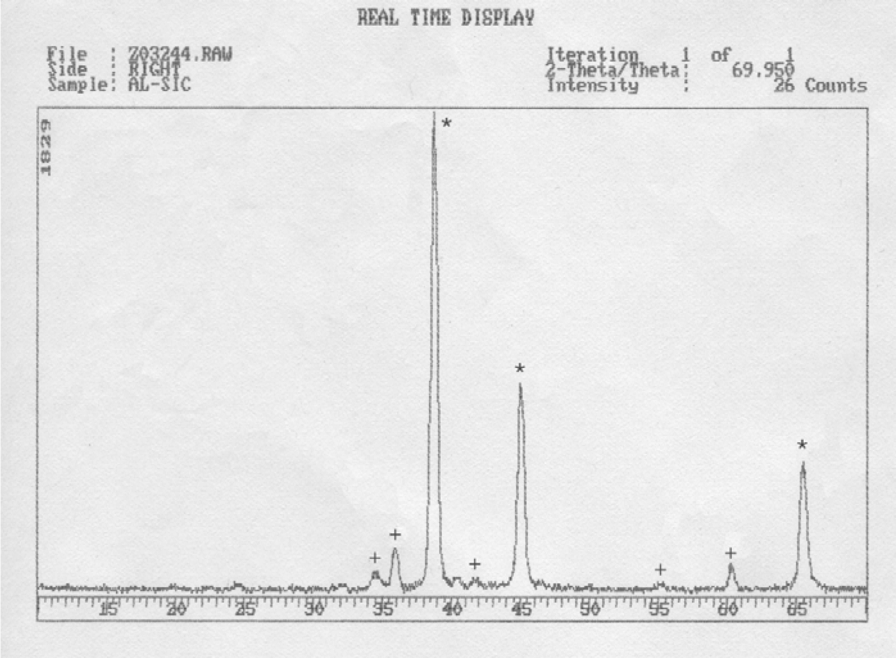

Figure 4.15. X-ray diffractogram of heat treated 15wt%SiC Al composite.

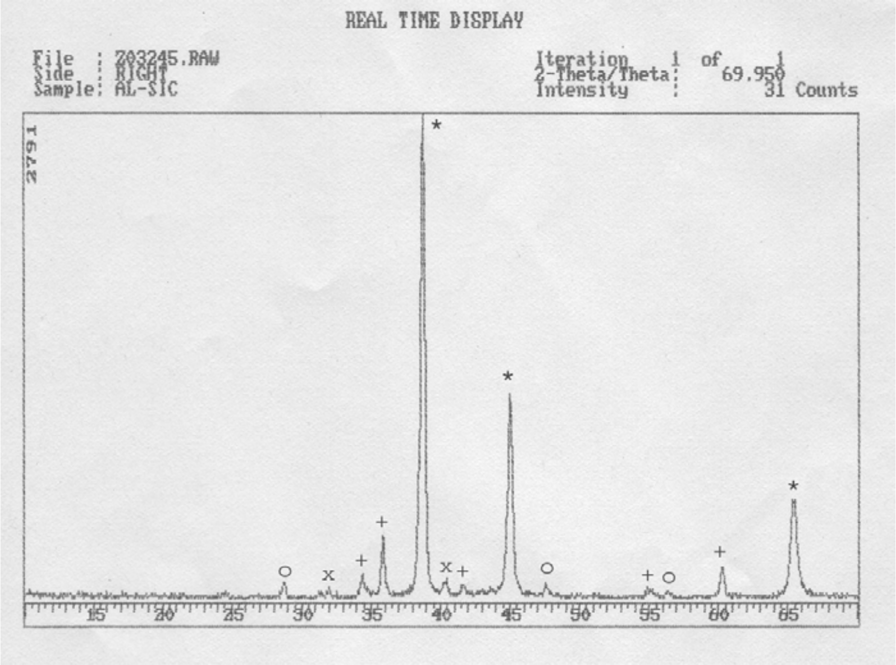

Figure 4.16. X-ray diffractogram of heat treated 20wt%SiC Al composite.

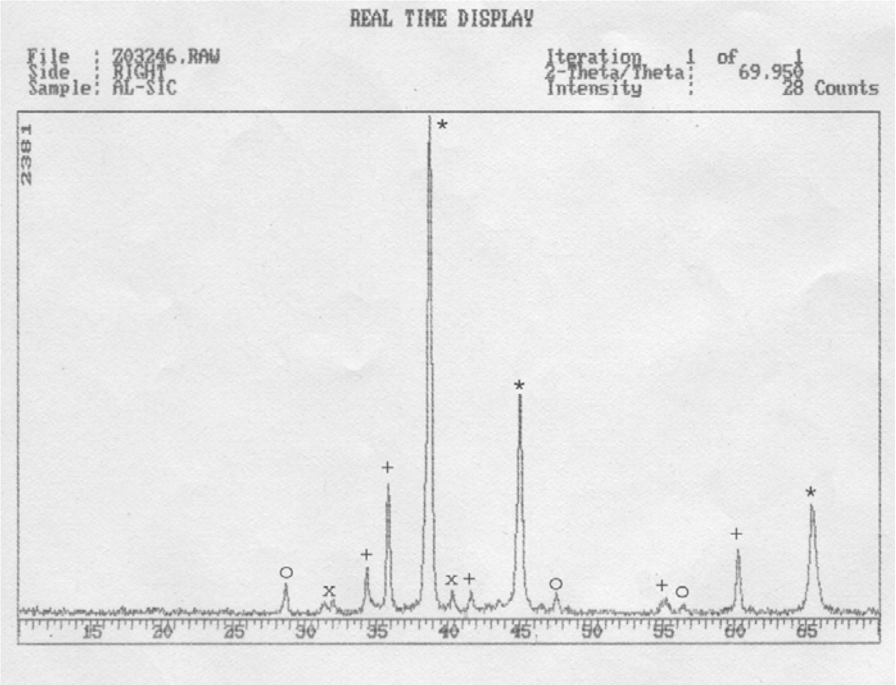

Figure 4.17. X-ray diffractogram of heat treated 30wt%SiC Al composite.

Designations of the phases that are shown in diffractograms given in below:

* = Aluminum
\+ = Silicon Carbide
o = Silicon
x = unknown

In all x-ray diffractograms aluminum and silicon carbide peaks were observed. Aluminum gives 2θ peaks at 37°-39°, 44°-46°, 64.5°-66.5°; silicon carbide give 2θ peaks at 34°-35°, 355°-36.5° and 60°. Silicon peaks were observed in 20wt% and 30wt% silicon carbide aluminum composites. Silicon gives 2θ peaks at 28.5°, 47° and 56°. Also some low intensity peaks were observed in 20wt% and 30wt% silicon carbide aluminum composites. These low intensity peaks rised at 31,5°-32° and at 40°-40,5° 2θ values. Possible phases were searched from x-ray diffractogram database.

During heat treatment of Al-Mg-Zn alloys, η($MgZn_2$) phase may form and at the last state of precipitation heat treatment this phase might turn to $Mg_{32}(Al,Zn)_{49}$ phase. Diffractogram tables of these phases were examined and it was found that the peak values do not match with the unknown "x" phase. Other possible Al-Mg-Zn phases such as Φ-$Al_5Mg_{11}Zn_4$, $Al_{25}Mg_{37,5}Zn_{37,5}$ and $AlMg_2Zn$ were also examined but 2θ peak values did not match again.

In the last two diffractogram silicon 2θ peaks were observed. Therefore carbon was exposed to the structure and reduced by aluminum by the reaction $4Al + 3SiC = Al_4C_3 + 3Si$. Al_4C_3 gives high intensity 2θ peaks at 31.174°-31.801°, 35.920°, 40.176°, and 55.074°-55.183°. 35.920° peak coincides with silicon carbide peak and 55.074°-55.183° peak coincides with silicon peak. The other peaks are very close to the "x" peaks. Therefore most probably the unknown phase is the Al_4C_3 phase.

Detailed diffractograms of searched phases are given in Appendix C.

4.5. Image Analysis Results

Silicon carbide reinforced aluminum composites were examined with Clemex Image Analyzing Program to calculate the volume percentage of silicon carbide addition and compare them with the theoretical volume percentage values. Theoretical volumes of matrix and reinforcement materials were calculated according to amount of addition and density values. Amount of alloying elements that are used in casting processes is given in Table 4.8.

Table 4.8. Amount of alloying elements in each casting process.

ALLOY	0% wt SiC	10% wt SiC	15% wt SiC	20% wt SiC	30% wt SiC
Al	900 gr.	900 gr.	900 gr.	900 gr.	900 gr.
Cu	15 gr.	15 gr.	15 gr.	15 gr.	15 gr.
Mg	28 gr.	28 gr.	28 gr.	28 gr.	28 gr.
Zn	60 gr.	60 gr.	60 gr.	60 gr.	60 gr.
AlTiB	4 gr.	4 gr.	4 gr.	4 gr.	4 gr.
Cr	2,5 gr.	2,5 gr.	2,5 gr.	2,5 gr.	2,5 gr.
SiC	0 gr.	113 gr.	180 gr.	260 gr.	430 gr.
Total Weight	1009,5 gr.	1122,5 gr.	1189,5 gr.	1269,5 gr.	1439,5 gr.
wt% SiC	**0**	**10,07%**	**15,13%**	**20,48%**	**29,87%**

The density of aluminum alloy is 2,80 gr/cm3 and density of silicon carbide is between 1,29 – 1,35 gr/cm3 (1,32 gr/cm3 is taken as average density). In each casting process the amount of matrix is constant and 1009,5 gr. Amount of silicon carbide was changed to adjust the weight percentage of the desired addition in each run. The theoretical volume percentages are calculated according to these data and results are given in table 4.9.

Table 4.9. Volume percentages of silicon carbide in aluminum composites.

Alloy Type	Volume of SiC (cm^3)	Volume of Matrix (cm^3)	Total Volume (cm^3)	Vol% SiC
Al – 0 wt%SiC	0	361	361	0
Al - 10 wt%SiC	86	361	446	19,19%
Al - 15 wt%SiC	136	361	497	27,44%
Al - 20 wt%SiC	197	361	558	35,33%
Al - 30 wt%SiC	326	361	686	47,47%

To use image analyzer program effectively, eight metallographic photographs were taken in the same magnification – 200X. Silicon carbide particulates have different color from matrix. This color difference is used to separate particulate and the matrix. An example for image analyzer study is shown in Figure 4.18.

Total area of silicon carbide and matrix was calculated by the program and converted into volume percentages. Results of image analysis study is given in Table 4.13.

Table 4.13. Results of image analyzer results and comparison with theoretical values.

Alloy	Image Analyzer		Theorical	
	vol% SiC	vol% Al	vol% SiC	vol% Al
Al - 10 wt% SiC	14,49	85,51	19,19	80,81
Al - 15 wt% SiC	21,56	78,44	27,44	72,56
Al - 20 wt% SiC	25,26	74,74	35,33	64,67
Al - 30 wt% SiC	37,60	62,40	47,47	52,53

Image analyzer vol% SiC results are close to the theoretical vol% SiC values. Clemex Image Analyzer program calculated the volume percentage silicon carbide addition. It was calculated from area percentages by this program.

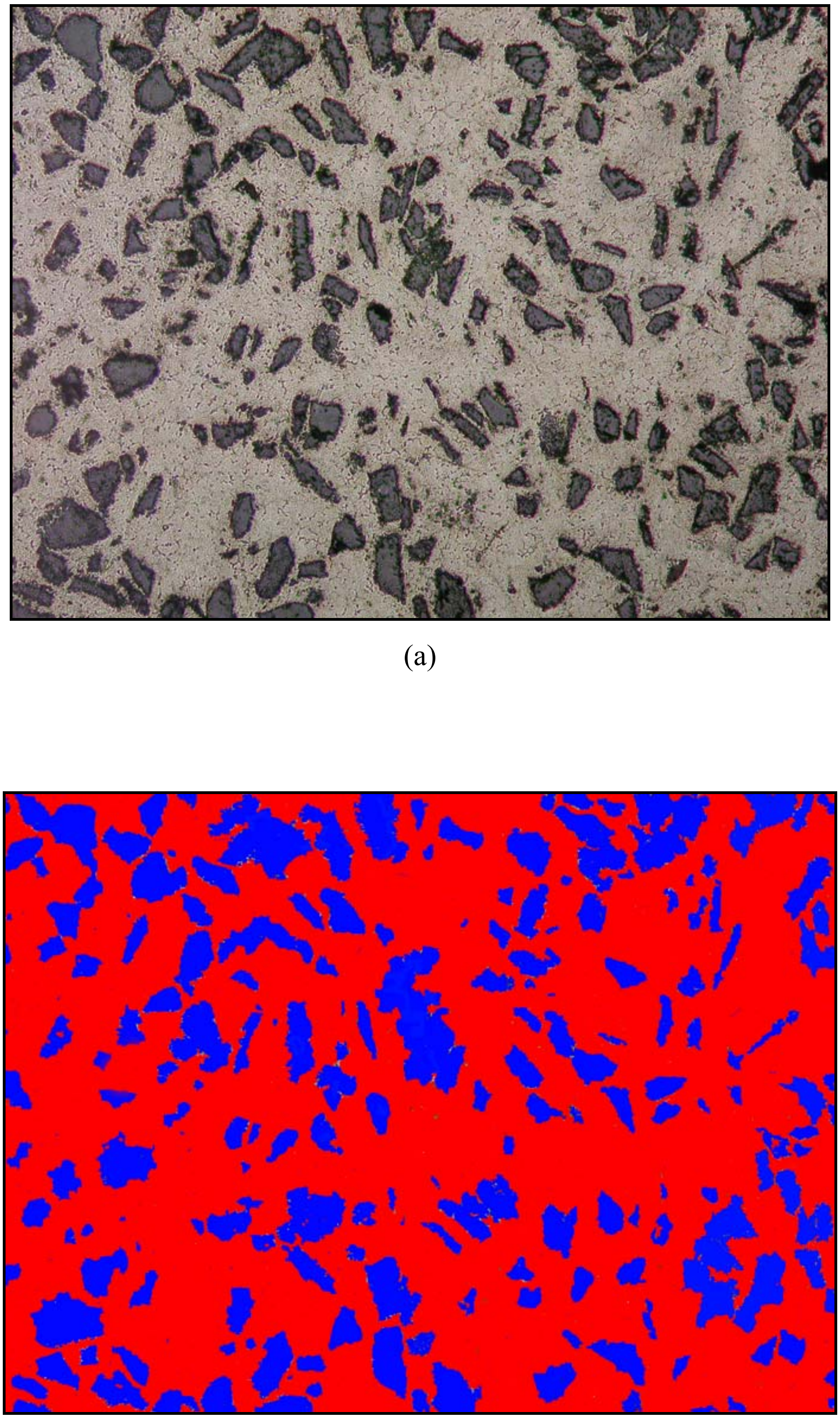

(a)

(b)

Figure 4.18. a) Sample photograph b) Sample photograph after image analyzer program

4.6. Scanning Electron Microscopy (SEM) Results

General elemental analysis of aluminum composites were obtained with scanning electron microscopy and microstructures were investigated at high magnification levels as well. Three specimens from each composition were examined to obtain the elemental analysis. Widest regions were searched to make the analysis as general as possible. Results are given in Table 4.10.

Table 4.10. General analysis results of scanning electron microscopy.

Alloy	Elements	1st Specimen (wt%)	2nd Specimen (wt%)	3rd Specimen (wt%)	Average (wt%)
Al - 0wt% SiC	**Al**	92,22	92,38	92,13	**92,24**
	Zn	4,77	4,55	4,22	**4,51**
	Mg	1,33	0,89	1,14	**1,12**
	Cu	1,68	2,18	2,52	**2,13**
Al - 10wt% SiC	**Al**	77,43	73,00	66,00	**72,14**
	Si	16,87	23,00	29,14	**23,00**
	Zn	4,60	3,25	4,01	**3,95**
	Mg	1,11	0,68	0,84	**0,88**
Al - 15wt% SiC	**Al**	81,87	76,40	85,03	**81,10**
	Si	13,61	19,20	12,40	**15,07**
	Zn	4,52	3,63	2,02	**3,39**
	Mg	0,00	0,78	0,47	**0,42**
Al - 20wt% SiC	**Al**	74,10	65,10	64,88	**68,03**
	Si	21,70	30,36	30,58	**27,55**
	Zn	3,69	3,90	3,87	**3,82**
	Mg	0,51	0,63	0,67	**0,60**
Al - 30wt% SiC	**Al**	62,58	61,33	62,93	**62,28**
	Si	33,46	34,69	33,10	**33,75**
	Zn	3,63	3,32	3,15	**3,37**
	Mg	0,33	0,67	0,77	**0,59**

When these results are compared with theoretical values, following data was obtained and listed in Table 4.11.

Table 4.11. Comparison of theoretical and SEM General Elemental Analysis data.

Elm. (wt%)	0 wt% SiC	0 wt % SEM	10 wt% SiC	10 wt% SEM	15wt % SiC	15 wt% SEM	20 wt% SiC	20 wt% SEM	30 wt% SiC	30 wt% SEM
%Al	89,15	92,24	80,18	80,16	75,66	81,10	70,89	68,03	62,52	62,28
%Cu	1,49	2,13	1,34		1,26		1,82		1,04	
%Mg	2,77	1,12	2,49	1,16	2,35	0,42	2,21	0,60	1,95	0,59
%Zn	5,94		5,35	4,35	5,04	3,39	4,73	3,82	4,17	3,37
%AlTiB	0,40		0,36		0,34		0,32		0,28	
%Cr	0,25		0,22		0,21		0,20		0,17	
%SiC	0,00		10,07		15,14		20,48		29,87	
%Si		0,00		12,35		15,07		27,55		33,75

Not only general elemental analysis performed by scanning electron microscopy, but also microstructure photographs were taken. SEM photographs are important to reveal the precipitates that may form after the heat treatment. Since the precipitates are very small and it is very hard to observe with optical microscopy, the only reliable way to observe them is scanning electron microscopy. Their size can be predicted from SEM photographs and their sizes are between 0,5-1,5 µm. Figure 4.19 to 4.23 show SEM photographs of heat treated silicon carbide reinforced aluminum composites.

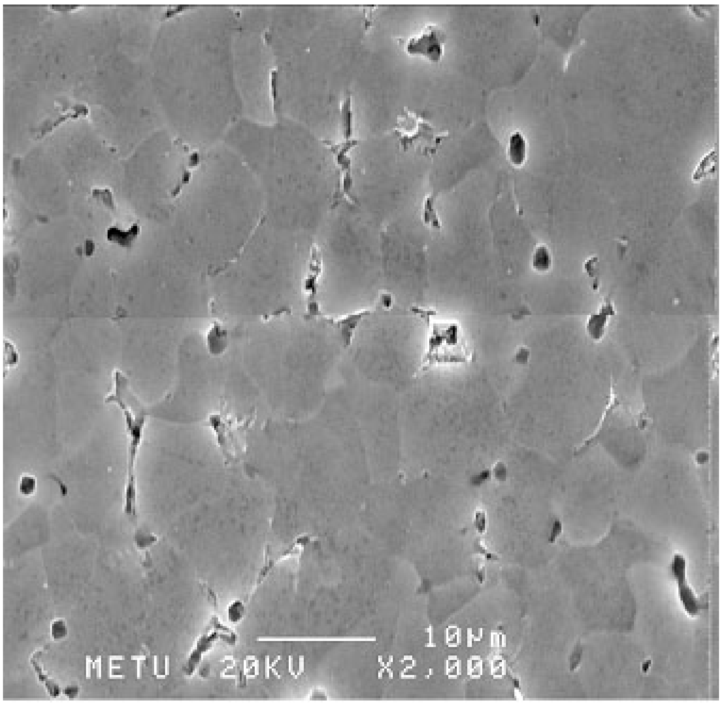

Figure 4.19. SEM photograph of heat treated aluminum matrix in X2000 magnification, showing precipitates.

Grain boundaries and precipitates of heat treated aluminum matrix can be observed in Figure 4.19. Small black points seen in each grain are the precipitates formed during heat treatment.

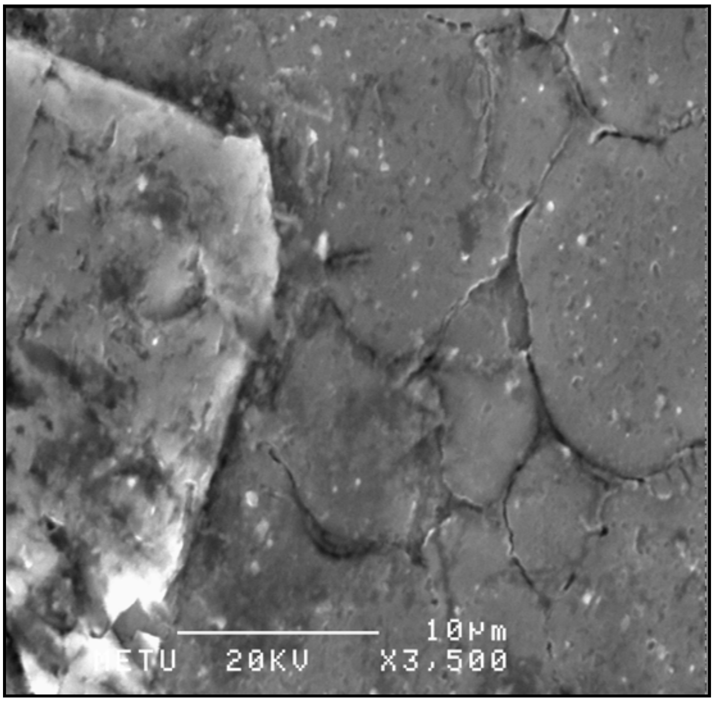

Figure 4.20. SEM photograph of heat treated 10wt% silicon carbide reinforced aluminum composite in X3500 magnification.

Figure 4.20. shows a silicon carbide particulate and the matrix in X3500 magnification. This composite has 10 wt% of silicon carbide. Precipitates formed during heat treatment are also observed within each grain.

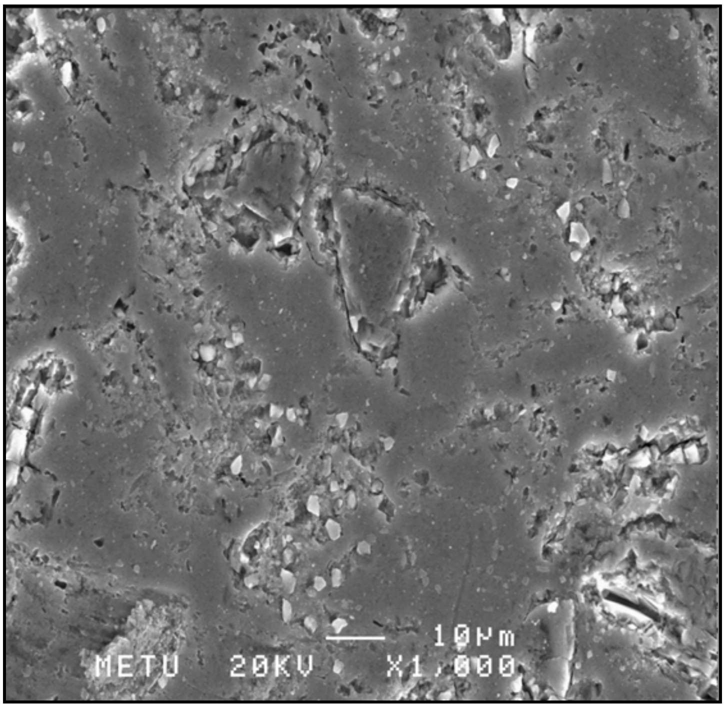

Figure 4.21. SEM photograph of heat treated 15wt% silicon carbide reinforced aluminum composite in X1000 magnification.

Heat treated, 15wt% silicon carbide reinforced aluminum composite's SEM photograph in X1000 magnification is shown in figure 4.21.

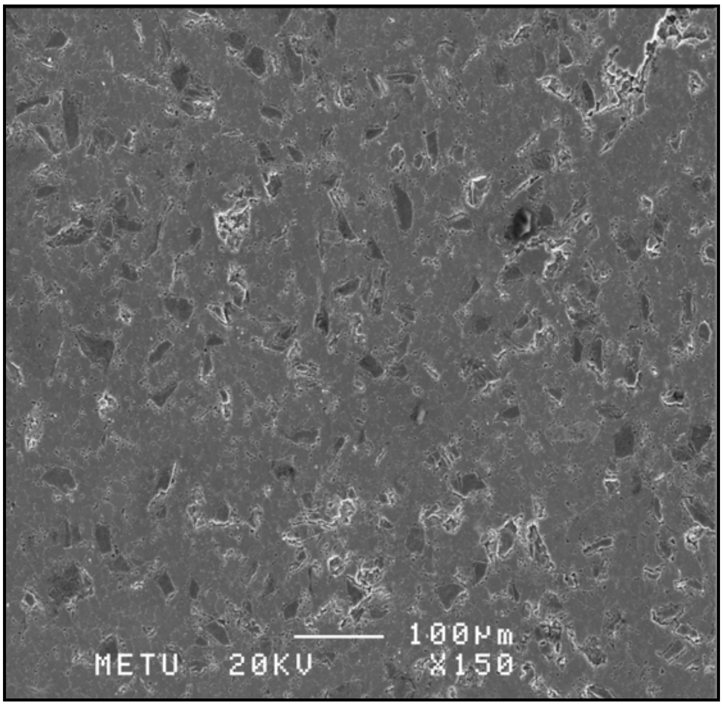

Figure 4.22. SEM photograph of heat treated 20wt% silicon carbide reinforced aluminum composite in X150 magnification.

A X150 magnification SEM photograph of heat treated, 20 wt% silicon carbide reinforced aluminum matrix composite is shown in Figure 4.22. Silicon carbide particulates and precipitates can be observed.

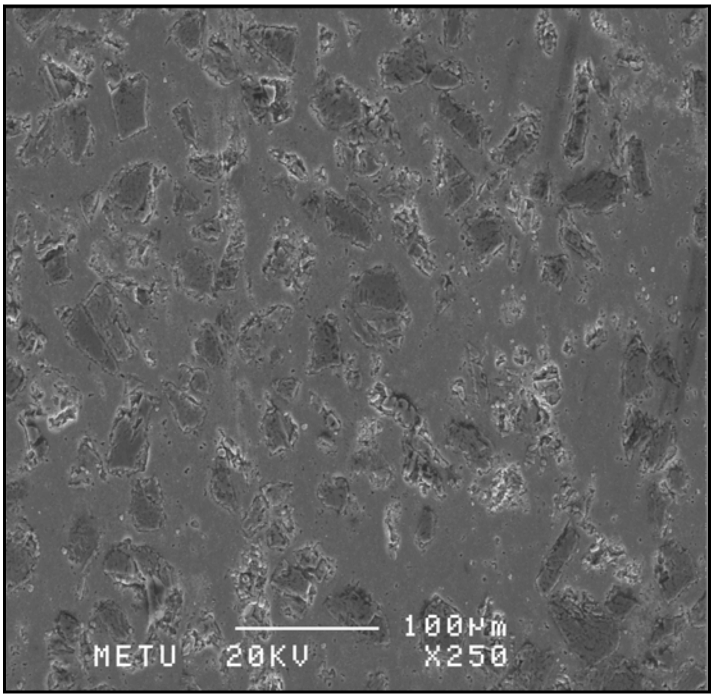

Figure 4.23. SEM photograph of heat treated 30wt% silicon carbide reinforced aluminum composite in X250 magnification.

A X250 magnification SEM photograph of heat treated, 30 wt% silicon carbide reinforced aluminum matrix composite is shown in Figure 4.23. Silicon carbide particulates and precipitates can be observed.

4.7. Metallogaphic Examination Results

Metallographic examinations were carried out to see the distribution of silicon carbide particulates in aluminum matrix and investigate condition of grains. Both as-cast and heat treated aluminum composites were investigated. The precipitates in heat treated composites are difficult to observe since the dimensions of the precipitates are very small. It is more meaningful to investigate the heat treated aluminum composites with SEM instead of optical microscopy. In Figures 4.24 to 4.28, optical microscopy photographs of as-cast aluminum composites are shown.

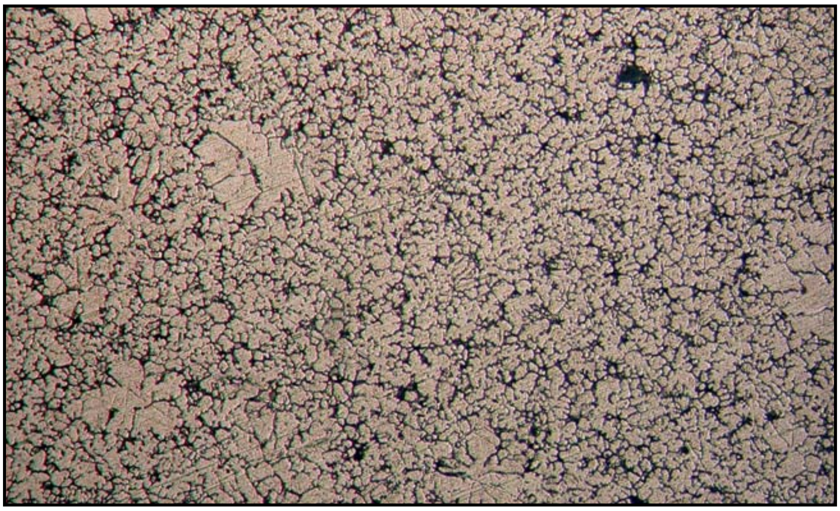

(a)

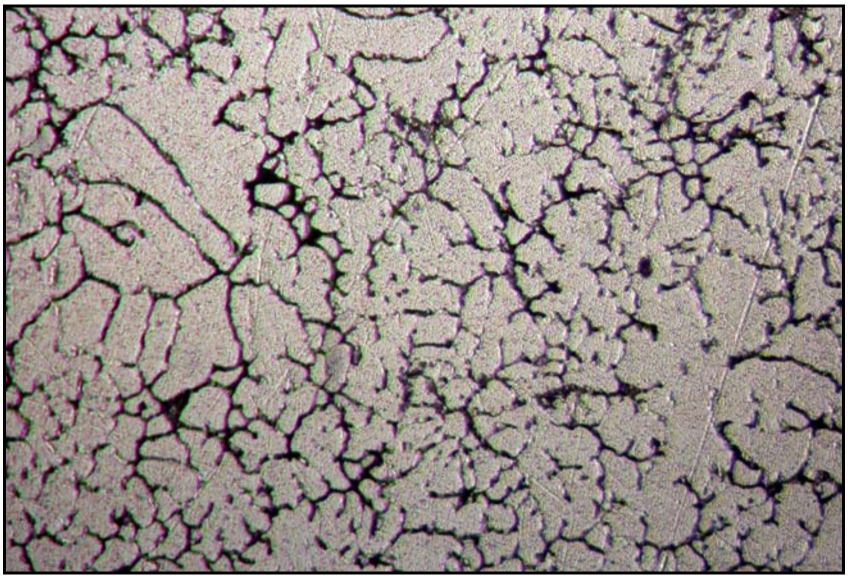

(b)

Figure 4.24. As-cast aluminum matrix photographs a) X200 b) X500 magnification

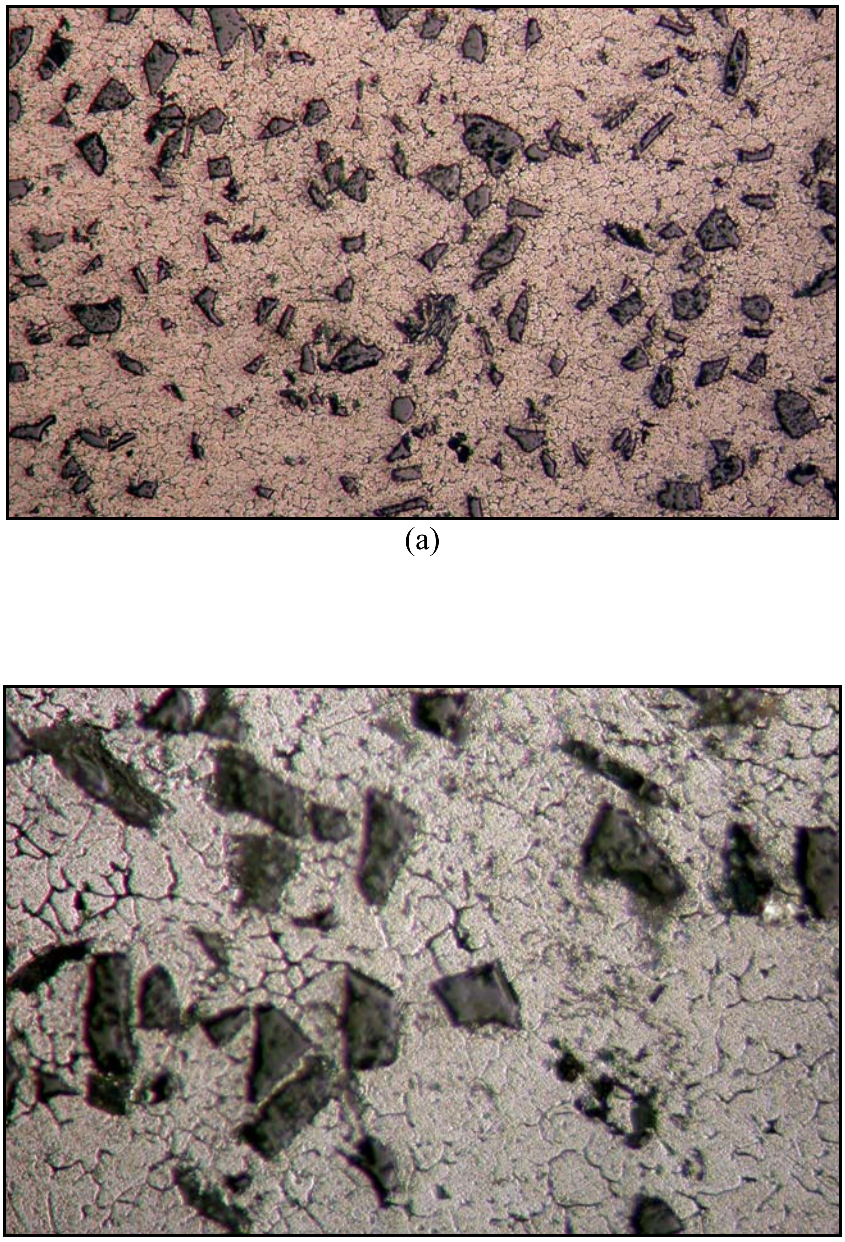

(a)

(b)

Figure 4.25. As-cast 10wt% silicon carbide reinforced aluminum composite photographs a) X200 b) X500 magnification

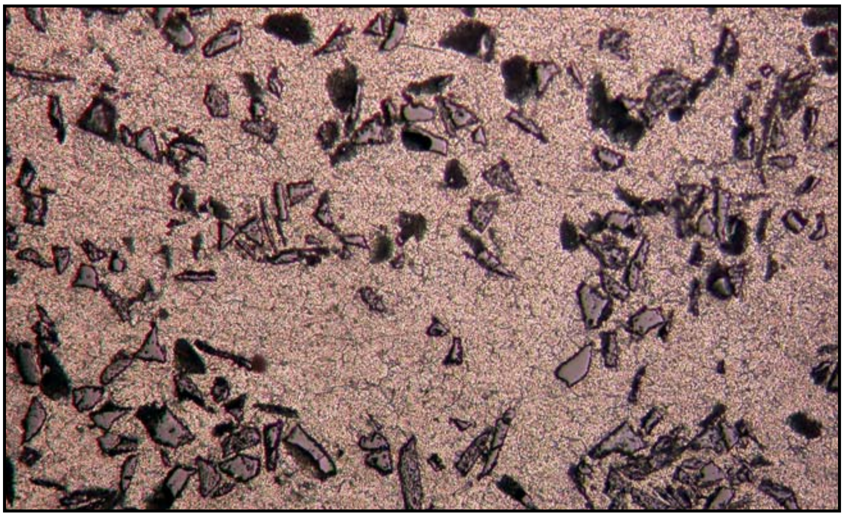

(a)

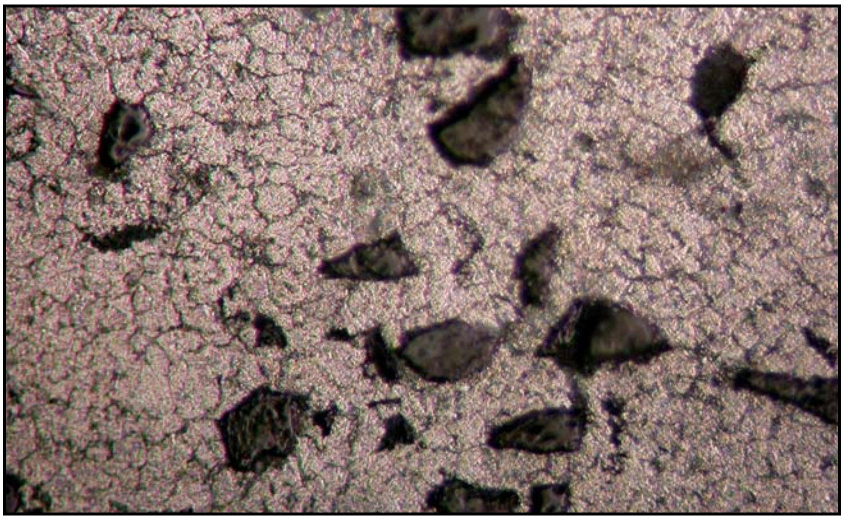

(b)

Figure 4.26. As-cast 15wt% silicon carbide reinforced aluminum composite photographs a) X200 b) X500 magnification

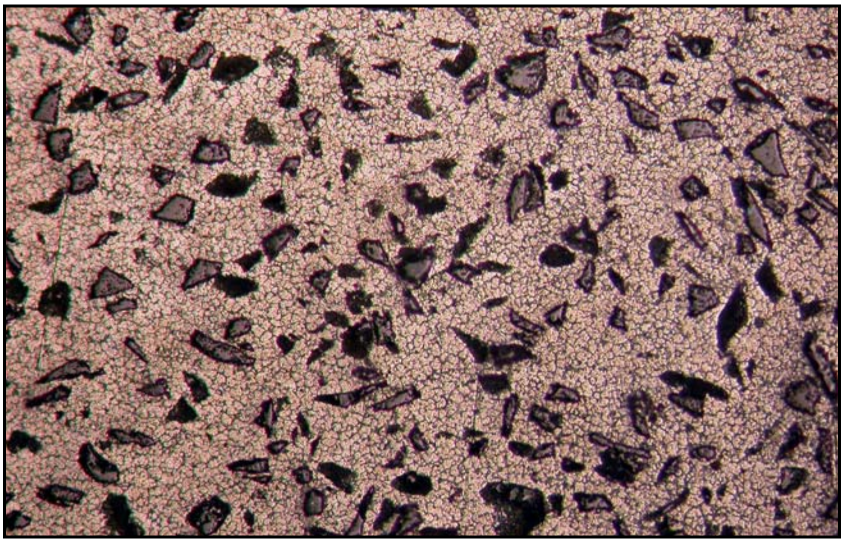

(a)

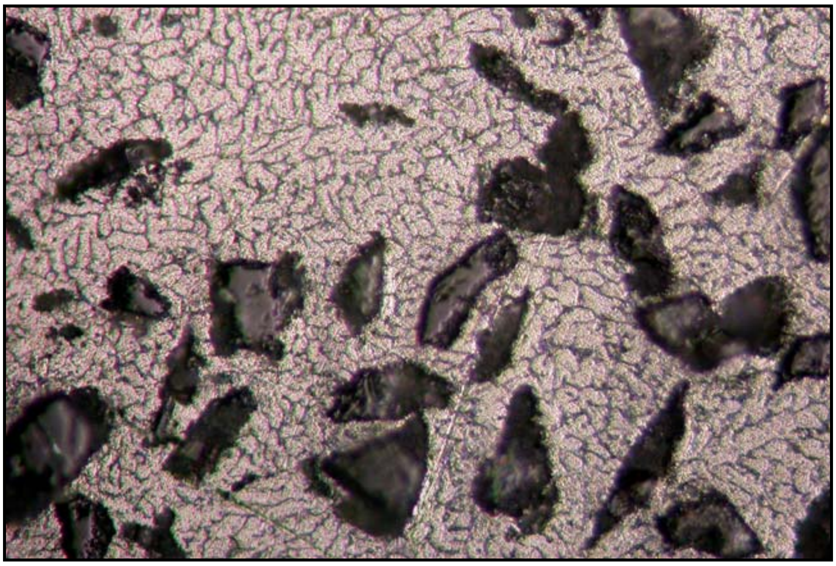

(b)

Figure 4.27. As-cast 20wt% silicon carbide reinforced aluminum composite photographs a) X200 b) X500 magnification

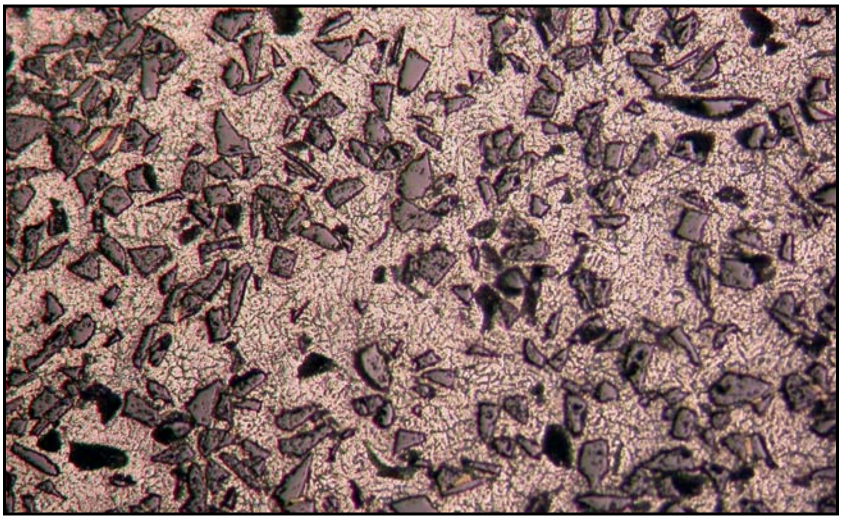

(a)

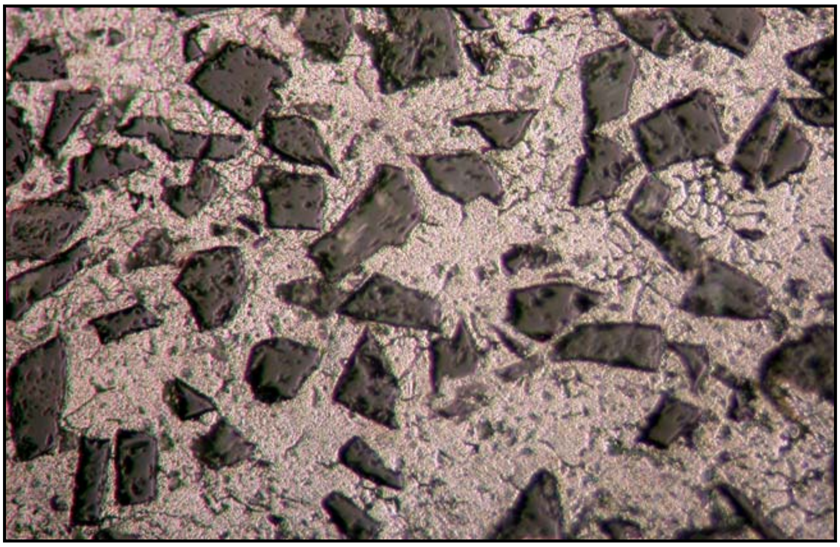

(b)

Figure 4.28. As-cast 30wt% silicon carbide reinforced aluminum composite photographs a) X200 b) X500 magnification

Silicon carbide reinforced aluminum composites have even distribution of reinforcement and this distribution can be seen in X200 magnified optical microscopy photographs. Aluminum matrices have grains with different sizes. This is due to the result of fast cooling during casting process. As it is examined in SEM analysis heat treated aluminum composites generally have equiaxed grains.

CHAPTER 5

CONCLUSIONS

The objective of this study is to investigate the fracture behavior of silicon carbide reinforced aluminum matrix composite. Hardness tests, three point bending tests, tensile testing, x-ray analysis, image analyzing, SEM analysis and metallographic examination were performed to complete the research. The following results were obtained:

1. Hardness values increased with the increase of silicon carbide addition in both as-cast and heat treated composites. The determined hardness values are not different than the matrix alloy up to 10 wt% SiC_p addition. After 10 wt% SiC_p, with addition of SiC_p, an increase was achieved gradually.

2. Peak hardness values were obtained after T6 heat treatment procedure. Composites were solution heat treated at 480 °C for 55-65 minutes and precipitation heat treated at 120 °C for 24 hours. From 4 to 24 hours usually hardness values increased gradually. Peak hardness values are about 20-25% higher than as-cast hardness values.

3. By precipitation heat treatment extra hardening was obtained. Almost 35-40 HV(10kg) were acquired.

4. The flexural strength increased with increasing reinforcement content up to 10wt% silicon carbide in both as-cast and heat treated composites. 10wt% silicon carbide composites showed enough internal ductility to attain full strength.

5. The maximum flexural strength increased about 40 MPa in as-cast, 180 MPa in heat treated composites. This means that a 44% increase in maximum strength was achieved compared to as-cast, unreinforced aluminum alloy.

6. In tensile testing, the composites having 10wt% silicon carbide showed the maximum strength at as-cast and at heat treated states.

7. Tensile strength values of all as-cast and heat treated samples were lower than flexural strength as expected. The difference between maximum tensile strength and flexural strength is 232 MPa in as-cast and 240 MPa in heat treated aluminum composites.

8. Agglomeration of silicon carbide particulates was observed in some of the tensile test specimens.

9. Heat treated composites were examined with x-ray analysis to find precipitated phases. In all x-ray diffractograms aluminum and silicon carbide peaks were observed. Pure silicon peaks were observed in 20wt% and 30wt% silicon carbide aluminum composites. This might be due to reduced SiC_p. As a result of SiC_p reduction the Al_4C_3 phase may form.

10. Image analyzer vol% SiC_p results were found to be close to the theoretical vol% SiC_p values.

11. Silicon carbide particulates usually have even distribution through the as-cast matrix. As-cast aluminum matrices have grains with different sizes as a result of fast cooling during casting and the efficiency of grain refiner addition, Al-Ti-B. Heat treated aluminum composites generally have equiaxed grains as examined with SEM

APPENDICES

A: DETAILED TABULATION OF HARDNESS (VICKERS 10KG) VARIATION WITH PRECIPITATION HEAT TREATMENT TIME

Table A.1. Variation of hardness values (Vickers 10kg) with precipitation heat treatment time. a) Al – 0wt% SiC b) Al – 10wt% SiC c) Al – 15wt% SiC d) Al – 20wt% SiC e) Al – 30wt% SiC

Al - %0 SiC	**As-Cast**							
Time (h)	**0**	**4**	**8**	**12**	**16**	**20**	**24**	**28**
1	131	129	148	158	163	172	173	146
2	131	138	146	157	169	175	172	144
3	131	130	148	153	166	169	178	155
4	136	147	141	139	157	172	171	158
5	136	113	152	161	159	165	166	159
6	132	135	148	167	162	167	171	165
7	135	132	142	171	157	168	168	156
Average	**133**	**132**	**146**	**158**	**162**	**170**	**171**	**155**

(a)

Al - %10 SiC	**As-Cast**							
Time (h)	**0**	**4**	**8**	**12**	**16**	**20**	**24**	**28**
1	139	136	142	163	179	182	182	159
2	138	132	141	167	172	178	180	158
3	138	138	146	169	168	177	184	159
4	138	133	149	169	174	179	178	166
5	136	129	145	172	171	175	183	171
6	138	127	142	173	168	174	183	157
7	137	131	147	165	167	181	181	165
Average	**138**	**132**	**145**	**168**	**171**	**178**	**182**	**162**

(b)

Al - %15 SiC	**As-Cast**						
Time (h)	**0**	**4**	**8**	**12**	**16**	**20**	**24**	**28**
1	134	129	143	166	172	191	185	164
2	138	126	147	162	178	185	189	154
3	153	125	145	167	170	192	186	153
4	154	126	149	162	167	192	183	158
5	153	134	146	155	176	183	189	156
6	154	132	144	167	171	190	184	157
7	146	139	149	167	173	188	185	158
Average	**147**	**130**	**146**	**164**	**172**	**189**	**186**	**157**

(c)

Al - %20 SiC	**As-Cast**							
Time (h)	**0**	**4**	**8**	**12**	**16**	**20**	**24**	**28**
1	155	136	146	159	178	195	201	166
2	163	136	156	163	178	186	202	165
3	166	131	156	160	180	186	192	162
4	155	135	155	159	185	189	199	160
5	160	134	154	163	182	189	192	169
6	157	134	156	163	183	187	201	161
7	160	136	153	164	184	193	200	161
Average	**159**	**135**	**154**	**162**	**181**	**189**	**198**	**163**

(d)

Al - %30 SiC	**As-Cast**							
Time (h)	**0**	**4**	**8**	**12**	**16**	**20**	**24**	**28**
1	172	152	159	184	194	240	221	277
2	205	152	165	180	199	200	222	174
3	175	145	173	184	200	220	232	171
4	185	159	168	184	185	229	229	166
5	182	153	166	186	194	222	218	171
6	192	152	165	180	197	228	202	175
7	206	158	175	183	193	230	226	177
Average	**188**	**153**	**167**	**183**	**195**	**224**	**221**	**187**

(e)

B: DETAILED TABULATION OF THREE POINT BENDING TEST RESULTS OF AS-CAST AND HEAT TREATED ALUMINUM COMPOSITES

Table B.1. Three point bending test results of as-cast aluminum composites; a)Al-0wt% SiC b) Al-10wt% SiC c) Al-15wt% SiC d) Al-20wt% SiC e) Al-30wt% SiC

Al - 0%SiC	**Applied Load "P" (kg)**	**Width "b"(cm)**	**Height "d" (cm)**	**Span Length "L" (cm)**	**3PL**	**$2bd^2$**	**σ (kg/cm^2)**	**σ (MPa)**
1	154	0,98	0,53	5,00	2310	0,55	4196	411,34
2	159	0,98	0,55	5,00	2385	0,59	4023	394,37
3	165	0,98	0,55	5,00	2475	0,59	4174	409,25
4	163	0,99	0,53	5,00	2445	0,56	4396	430,98
5	152	0,99	0,53	5,00	2280	0,56	4099	401,90
6	155	0,98	0,52	5,00	2325	0,53	4387	430,09
7	133	0,99	0,51	5,00	1995	0,51	3874	379,78
						Average=	**4164**	**408,25**

(a)

Al - 10%SiC	**Applied Load "P" (kg)**	**Width "b"(cm)**	**Height "d" (cm)**	**Span Length "L" (cm)**	**3PL**	**$2bd^2$**	**σ (kg/cm^2)**	**σ (MPa)**
1	159	0,99	0,51	5,00	2385	0,51	4631	454,03
2	158	0,99	0,55	5,00	2370	0,60	3957	387,93
3	162	0,99	0,53	5,00	2430	0,56	4369	428,34
4	178	0,99	0,52	5,00	2670	0,54	4987	488,92
5	179	0,99	0,53	5,00	2685	0,56	4828	473,29
6	175	0,99	0,54	5,00	2625	0,58	4546	445,73
7	182	0,99	0,56	5,00	2730	0,62	4397	431,04
						Average=	**4531**	**444,18**

(b)

Al – 15%SiC	**Applied Load "P" (kg)**	**Width "b"(cm)**	**Height "d" (cm)**	**Span Length "L" (cm)**	**3PL**	**$2bd^2$**	**σ (kg/cm^2)**	**σ (MPa)**
1	131	1,00	0,52	5,00	1965	0,54	3634	356,23
2	143	0,99	0,53	5,00	2145	0,56	3857	378,10
3	145	0,99	0,52	5,00	2175	0,54	4062	398,28
4	148	1,00	0,53	5,00	2220	0,56	3952	387,41
5	149	1,00	0,53	5,00	2235	0,56	3978	390,03
6	144	1,00	0,53	5,00	2160	0,56	3845	376,94
7	130	1,00	0,53	5,00	1950	0,56	3471	340,29
						Average=	**3828**	**375,33**

(c)

Al – 20%SiC	**Applied Load "P" (kg)**	**Width "b"(cm)**	**Height "d" (cm)**	**Span Length "L" (cm)**	**3PL**	**$2bd^2$**	**σ (kg/cm^2)**	**σ (MPa)**
1	140	1,01	0,53	5,00	2100	0,57	3701	362,84
2	141	1,01	0,54	5,00	2115	0,59	3591	352,02
3	139	1,00	0,53	5,00	2085	0,56	3711	363,85
4	142	1,00	0,53	5,00	2130	0,56	3791	371,70
5	137	0,99	0,52	5,00	2055	0,54	3838	376,30
6	132	0,99	0,53	5,00	1980	0,56	3560	349,02
7	135	1,00	0,52	5,00	2025	0,54	3744	367,10
						Average=	**3705**	**363,26**

(d)

Al – 30%SiC	**Applied Load "P" (kg)**	**Width "b"(cm)**	**Height "d" (cm)**	**Span Length "L" (cm)**	**3PL**	**$2bd^2$**	**σ (kg/cm^2)**	**σ (MPa)**
1	122	1,00	0,53	5,00	1830	0,56	3257	319,35
2	134	1,02	0,58	5,00	2010	0,69	2929	287,15
3	132	1,00	0,55	5,00	1980	0,61	3273	320,86
4	122	1,00	0,56	5,00	1830	0,63	2918	286,05
5	119	1,00	0,54	5,00	1785	0,58	3061	300,07
6	128	1,00	0,55	5,00	1920	0,61	3174	311,13
7	117	1,02	0,54	5,00	1755	0,59	2950	289,24
						Average=	**3080**	**301,98**

(e)

Table B.2. Three point bending test results of heat treated aluminum matrix composites ; a) Al-0wt% SiC b) Al-10wt% SiC c) Al-15wt% SiC d) Al-20wt% SiC e) Al-30wt% SiC

Al – 0%SiC	**Applied Load "P" (kg)**	**Width "b"(cm)**	**Height "d" (cm)**	**Span Length "L" (cm)**	**3PL**	**2bd^2**	**σ (kg/cm^2)**	**σ (MPa)**
1	164	0,98	0,53	5,00	2460,00	0,55	4468	438,05
2	169	0,98	0,53	5,00	2535,00	0,55	4604	451,41
3	190	0,98	0,52	5,00	2850,00	0,53	5378	527,21
4	173	0,99	0,54	5,00	2595,00	0,58	4495	440,64
5	143	0,99	0,53	5,00	2145,00	0,56	3828	375,27
6	165	0,99	0,53	5,00	2475,00	0,56	4450	436,27
7	172	0,99	0,53	5,00	2580,00	0,56	4639	454,78
						Average=	**4552**	**446,23**

(a)

Al – 10%SiC	**Applied Load "P" (kg)**	**Width "b"(cm)**	**Height "d" (cm)**	**Span Length "L" (cm)**	**3PL**	**2bd^2**	**σ (kg/cm^2)**	**σ (MPa)**
1	237	0,99	0,52	5,00	3555	0,54	6601	647,18
2	205	1,00	0,53	5,00	3075	0,56	5473	536,62
3	194	1,00	0,52	5,00	2910	0,54	5381	527,54
4	235	1,00	0,54	5,00	3525	0,58	6044	592,57
5	189	0,99	0,53	5,00	2835	0,56	5059	495,98
6	239	1,00	0,53	5,00	3585	0,56	6381	625,62
7	234	0,99	0,52	5,00	3510	0,54	6556	642,74
						Average=	**5928**	**581,18**

(b)

Al – 15%SiC	**Applied Load "P" (kg)**	**Width "b"(cm)**	**Height "d" (cm)**	**Span Length "L" (cm)**	**3PL**	**2bd^2**	**σ (kg/cm^2)**	**σ (MPa)**
1	181	0,99	0,52	5,00	2715	0,54	5041	494,26
2	163	1,00	0,54	5,00	2445	0,58	4192	411,02
3	178	0,99	0,53	5,00	2670	0,56	4765	467,11
4	184	1,00	0,54	5,00	2760	0,58	4721	462,87
5	151	0,99	0,52	5,00	2265	0,54	4206	412,34
6	169	1,00	0,53	5,00	2535	0,56	4512	442,38
7	176	1,00	0,52	5,00	2640	0,54	4882	478,59
						Average=	**4617**	**452,65**

(c)

Al – 20%SiC	**Applied Load "P" (kg)**	**Width "b"(cm)**	**Height "d" (cm)**	**Span Length "L" (cm)**	**3PL**	**$2bd^2$**	**σ (kg/cm^2)**	**σ (MPa)**
1	169	0,99	0,55	5,00	2535	0,59	4290	420,62
2	158	1,00	0,54	5,00	2370	0,59	4034	395,48
3	177	1,00	0,55	5,00	2655	0,61	4341	425,58
4	151	1,00	0,54	5,00	2265	0,57	3957	387,91
5	157	1,00	0,56	5,00	2355	0,61	3834	375,91
6	223	0,99	0,52	5,00	3345	0,54	6248	612,53
7	165	1,00	0,52	5,00	2475	0,54	4577	448,68
						Average=	**4469**	**438,10**

(d)

Al – 30%SiC	**Applied Load "P" (kg)**	**Width "b"(cm)**	**Height "d" (cm)**	**Span Length "L" (cm)**	**3PL**	**$2bd^2$**	**σ (kg/cm^2)**	**σ (MPa)**
1	156	1,00	0,53	5,00	2340	0,56	4157	407,54
2	159	1,00	0,54	5,00	2385	0,57	4151	406,94
3	147	1,00	0,53	5,00	2205	0,56	3930	385,27
4	147	1,00	0,53	5,00	2205	0,57	3886	380,95
5	163	0,99	0,58	5,00	2445	0,66	3692	362,01
6	177	1,00	0,51	5,00	2655	0,52	5104	500,37
7	157	0,93	0,47	5,00	2355	0,41	5732	561,93
						Average=	**4379**	**429,29**

(e)

C: X-RAY DETAILS OF SEARCHED PHASES

Table C.1. X-Ray Analysis Details of Φ-$Al_5Mg_{11}Zn_4$

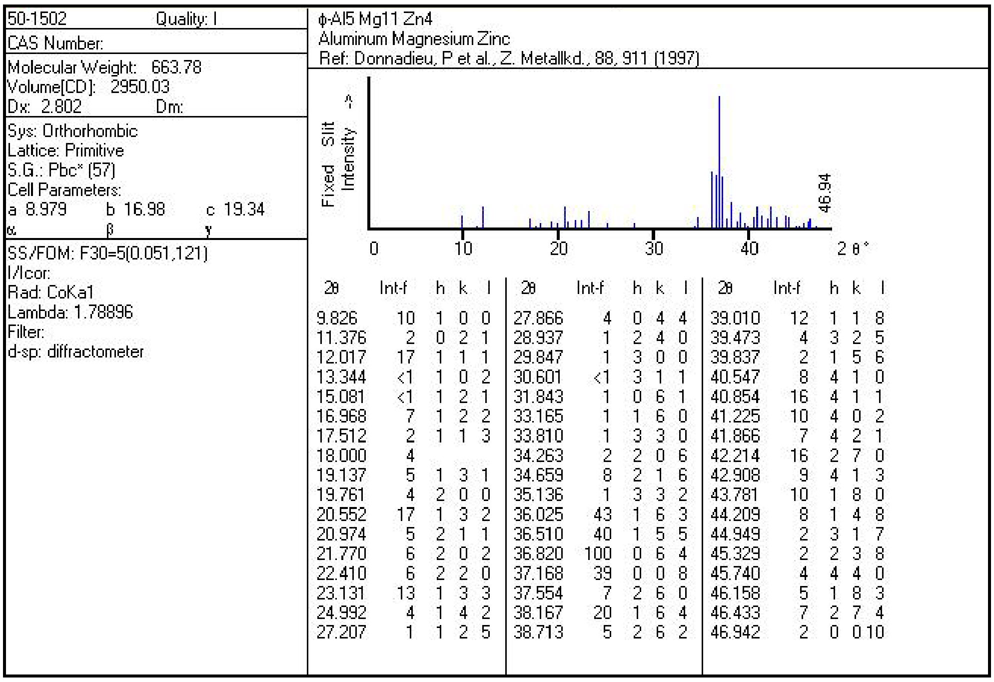

50-1502 Quality: I
CAS Number:
Molecular Weight: 663.78
Volume[CD]: 2950.03
Dx: 2.802 Dm:
Sys: Orthorhombic
Lattice: Primitive
S.G.: Pbc* (57)
Cell Parameters:
a 8.979 b 16.98 c 19.34
α β γ
SS/FOM: F30=5(0.051,121)
I/Icor:
Rad: CoKa1
Lambda: 1.78896
Filter:
d-sp: diffractometer

ϕ-Al5 Mg11 Zn4
Aluminum Magnesium Zinc
Ref: Donnadieu, P et al., Z. Metallkd., 88, 911 (1997)

2θ	Int-f	h	k	l
9.826	10	1	0	0
11.376	2	0	2	1
12.017	17	1	1	1
13.344	<1	1	0	2
15.081	<1	1	2	1
16.968	7	1	2	2
17.512	2	1	1	3
18.000	4			
19.137	5	1	3	1
19.761	4	2	0	0
20.552	17	1	3	2
20.974	5	2	1	1
21.770	6	2	0	2
22.410	6	2	2	0
23.131	13	1	3	3
24.992	4	1	4	2
27.207	1	1	2	5
27.866	4	0	4	4
28.937	1	2	4	0
29.847	1	3	0	0
30.601	<1	3	1	1
31.843	1	0	6	1
33.165	1	1	6	0
33.810	1	3	3	0
34.263	2	2	0	6
34.659	8	2	1	6
35.136	1	3	3	2
36.025	43	1	6	3
36.510	40	1	5	5
36.820	100	0	6	4
37.168	39	0	0	8
37.554	7	2	6	0
38.167	20	1	6	4
38.713	5	2	6	2
39.010	12	1	1	8
39.473	4	3	2	5
39.837	2	1	5	6
40.547	8	4	1	0
40.854	16	4	1	1
41.225	10	4	0	2
41.866	7	4	2	1
42.214	16	2	7	0
42.908	9	4	1	3
43.781	10	1	8	0
44.209	8	1	4	8
44.949	2	3	1	7
45.329	2	2	3	8
45.740	4	4	4	0
46.158	5	1	8	3
46.433	7	2	7	4
46.942	2	0	0	10

Table C.2. X-Ray Analysis Details of $Al2_5Mg_{37.5}Zn_{37.5}$

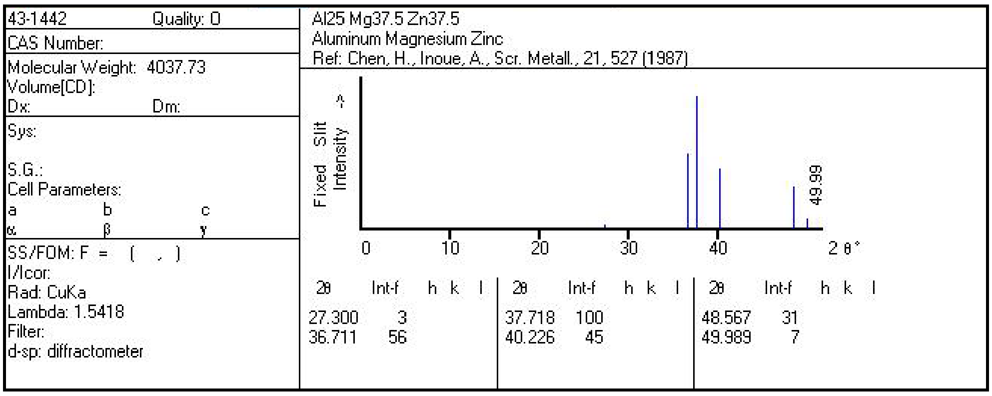

43-1442 Quality: O
CAS Number:
Molecular Weight: 4037.73
Volume[CD]:
Dx: Dm:
Sys:
S.G.:
Cell Parameters:
a b c
α β γ
SS/FOM: F = (,)
I/Icor:
Rad: CuKa
Lambda: 1.5418
Filter:
d-sp: diffractometer

Al25 Mg37.5 Zn37.5
Aluminum Magnesium Zinc
Ref: Chen, H., Inoue, A., Scr. Metall., 21, 527 (1987)

2θ	Int-f	h	k	l
27.300	3			
36.711	56			
37.718	100			
40.226	45			
48.567	31			
49.989	7			

Table C.3. X-Ray Analysis Details of $Mg_{32}(Al,Zn)_{49}$

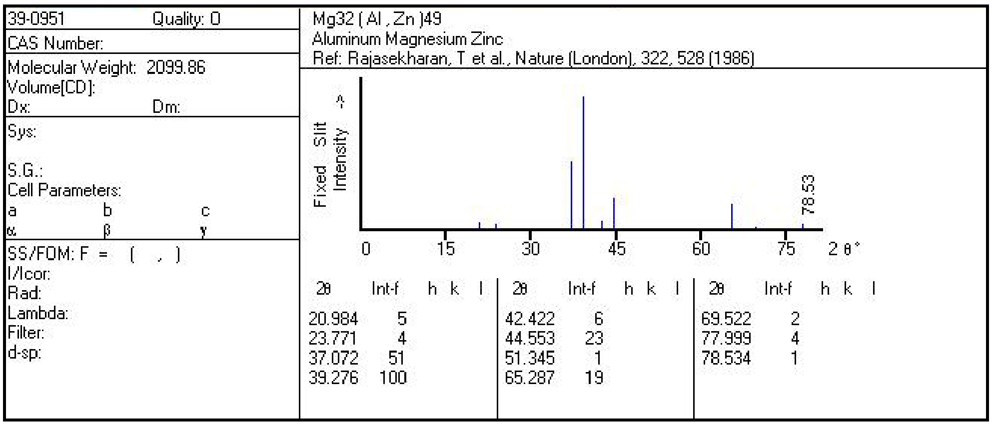

39-0951 Quality: O
CAS Number:
Molecular Weight: 2099.86
Volume[CD]:
Dx: Dm:
Sys:
S.G.:
Cell Parameters:
a b c
α β γ
SS/FOM: F = (,)
I/Icor:
Rad:
Lambda:
Filter:
d-sp:

Mg32 (Al , Zn)49
Aluminum Magnesium Zinc
Ref: Rajasekharan, T et al., Nature (London), 322, 528 (1986)

2θ	Int-f	h	k	l	2θ	Int-f	h	k	l	2θ	Int-f	h	k	l
20.984	5				42.422	6				69.522	2			
23.771	4				44.553	23				77.999	4			
37.072	51				51.345	1				78.534	1			
39.276	100				65.287	19								

Table C.4. X-Ray Analysis Details of AlMg$_4$Zn11

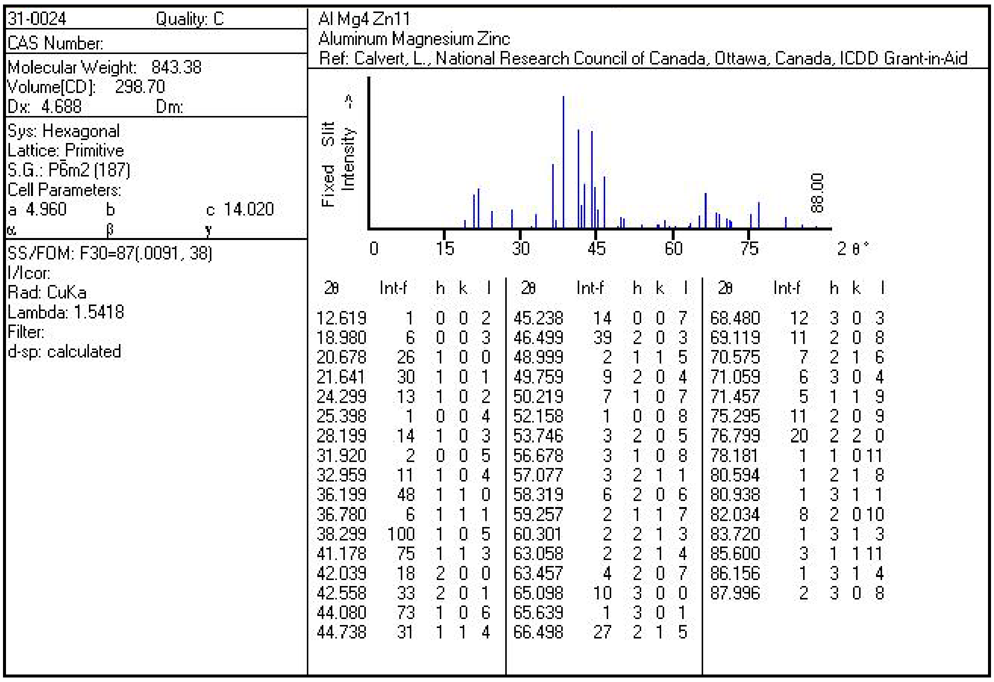

31-0024 Quality: C
CAS Number:
Molecular Weight: 843.38
Volume[CD]: 298.70
Dx: 4.688 Dm:
Sys: Hexagonal
Lattice: Primitive
S.G.: $P\bar{6}m2$ (187)
Cell Parameters:
a 4.960 b c 14.020
α β γ
SS/FOM: F30=87(.0091, 38)
I/Icor:
Rad: CuKa
Lambda: 1.5418
Filter:
d-sp: calculated

Al Mg4 Zn11
Aluminum Magnesium Zinc
Ref: Calvert, L., National Research Council of Canada, Ottawa, Canada, ICDD Grant-in-Aid

2θ	Int-f	h	k	l	2θ	Int-f	h	k	l	2θ	Int-f	h	k	l
12.619	1	0	0	2	45.238	14	0	0	7	68.480	12	3	0	3
18.980	6	0	0	3	46.499	39	2	0	3	69.119	11	2	0	8
20.678	26	1	0	0	48.999	2	1	1	5	70.575	7	2	1	6
21.641	30	1	0	1	49.759	9	2	0	4	71.059	6	3	0	4
24.299	13	1	0	2	50.219	7	1	0	7	71.457	5	1	1	9
25.398	1	0	0	4	52.158	1	0	0	8	75.295	11	2	0	9
28.199	14	1	0	3	53.746	3	2	0	5	76.799	20	2	2	0
31.920	2	0	0	5	56.678	3	1	0	8	78.181	1	1	0	11
32.959	11	1	0	4	57.077	3	2	1	1	80.594	1	2	1	8
36.199	48	1	1	0	58.319	6	2	0	6	80.938	1	3	1	1
36.780	6	1	1	1	59.257	2	1	1	7	82.034	8	2	0	10
38.299	100	1	0	5	60.301	2	2	1	3	83.720	1	3	1	3
41.178	75	1	1	3	63.058	2	2	1	4	85.600	3	1	1	11
42.039	18	2	0	0	63.457	4	2	0	7	86.156	1	3	1	4
42.558	33	2	0	1	65.098	10	3	0	0	87.996	2	3	0	8
44.080	73	1	0	6	65.639	1	3	0	1					
44.738	31	1	1	4	66.498	27	2	1	5					

Table C.5. X-Ray Analysis Details of $Mg_{32}(Al,Zn)_{49}$

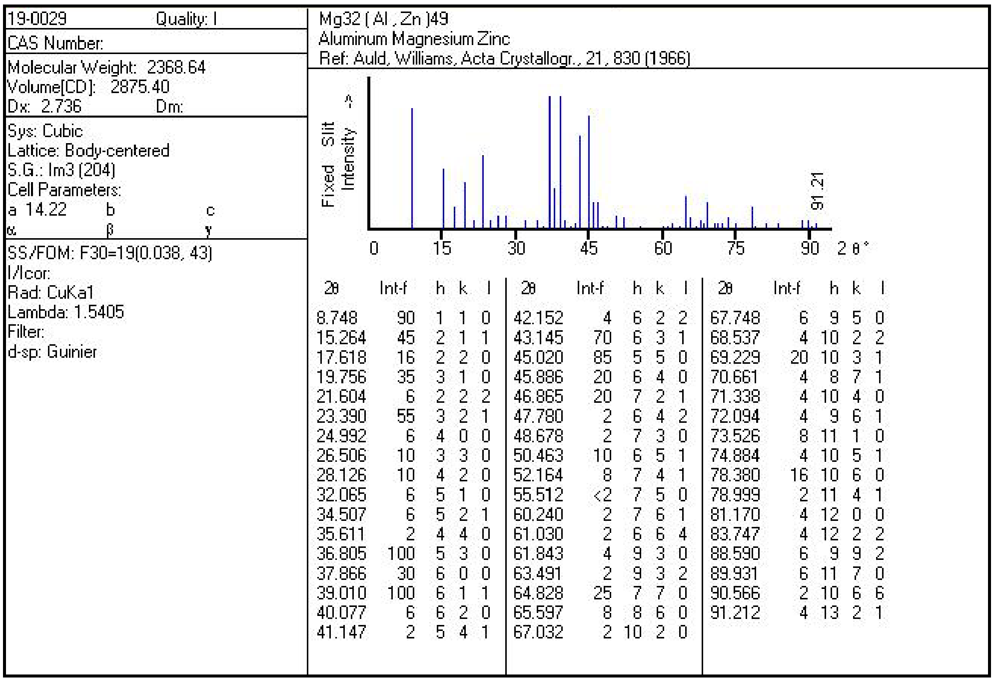

19-0029 Quality: I

CAS Number:

Molecular Weight: 2368.64
Volume[CD]: 2875.40
Dx: 2.736 Dm:

Sys: Cubic
Lattice: Body-centered
S.G.: Im3 (204)
Cell Parameters:
a 14.22 b c
α β γ

SS/FOM: F30=19(0.038, 43)
I/Icor:
Rad: CuKa1
Lambda: 1.5405
Filter:
d-sp: Guinier

Mg32 (Al , Zn)49
Aluminum Magnesium Zinc
Ref: Auld, Williams, Acta Crystallogr., 21, 830 (1966)

2θ	Int-f	h	k	l
8.748	90	1	1	0
15.264	45	2	1	1
17.618	16	2	2	0
19.756	35	3	1	0
21.604	6	2	2	2
23.390	55	3	2	1
24.992	6	4	0	0
26.506	10	3	3	0
28.126	10	4	2	0
32.065	6	5	1	0
34.507	6	5	2	1
35.611	2	4	4	0
36.805	100	5	3	0
37.866	30	6	0	0
39.010	100	6	1	1
40.077	6	6	2	0
41.147	2	5	4	1
42.152	4	6	2	2
43.145	70	6	3	1
45.020	85	5	5	0
45.886	20	6	4	0
46.865	20	7	2	1
47.780	2	6	4	2
48.678	2	7	3	0
50.463	10	6	5	1
52.164	8	7	4	1
55.512	<2	7	5	0
60.240	2	7	6	1
61.030	2	6	6	4
61.843	4	9	3	0
63.491	2	9	3	2
64.828	25	7	7	0
65.597	8	8	6	0
67.032	2	10	2	0
67.748	6	9	5	0
68.537	4	10	2	2
69.229	20	10	3	1
70.661	4	8	7	1
71.338	4	10	4	0
72.094	4	9	6	1
73.526	8	11	1	0
74.884	4	10	5	1
78.380	16	10	6	0
78.999	2	11	4	1
81.170	4	12	0	0
83.747	4	12	2	2
88.590	6	9	9	2
89.931	6	11	7	0
90.566	2	10	6	6
91.212	4	13	2	1

Table C.6. X-Ray Analysis Details of $AlMg_2Zn$

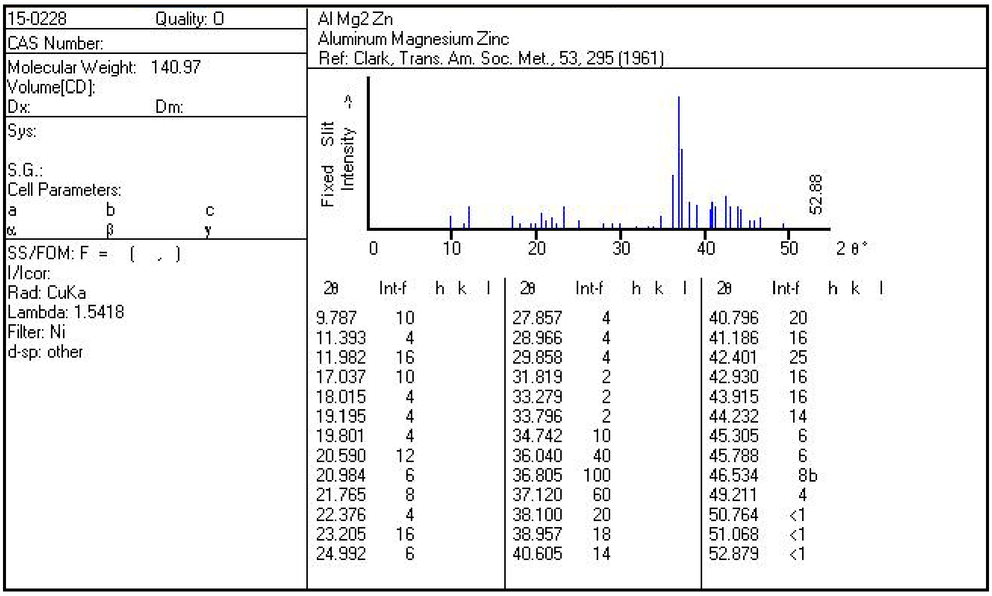

15-0228 Quality: O

CAS Number:

Molecular Weight: 140.97
Volume[CD]:
Dx: Dm:

Sys:

S.G.:
Cell Parameters:
a b c
α β γ

SS/FOM: F = (,)
I/Icor:
Rad: CuKa
Lambda: 1.5418
Filter: Ni
d-sp: other

Al Mg2 Zn
Aluminum Magnesium Zinc
Ref: Clark, Trans. Am. Soc. Met., 53, 295 (1961)

2θ	Int-f	h	k	l
9.787	10			
11.393	4			
11.982	16			
17.037	10			
18.015	4			
19.195	4			
19.801	4			
20.590	12			
20.984	6			
21.765	8			
22.376	4			
23.205	16			
24.992	6			
27.857	4			
28.966	4			
29.858	4			
31.819	2			
33.279	2			
33.796	2			
34.742	10			
36.040	40			
36.805	100			
37.120	60			
38.100	20			
38.957	18			
40.605	14			
40.796	20			
41.186	16			
42.401	25			
42.930	16			
43.915	16			
44.232	14			
45.305	6			
45.788	6			
46.534	8b			
49.211	4			
50.764	<1			
51.068	<1			
52.879	<1			

Table C.7. X-Ray Analysis Details of SiC

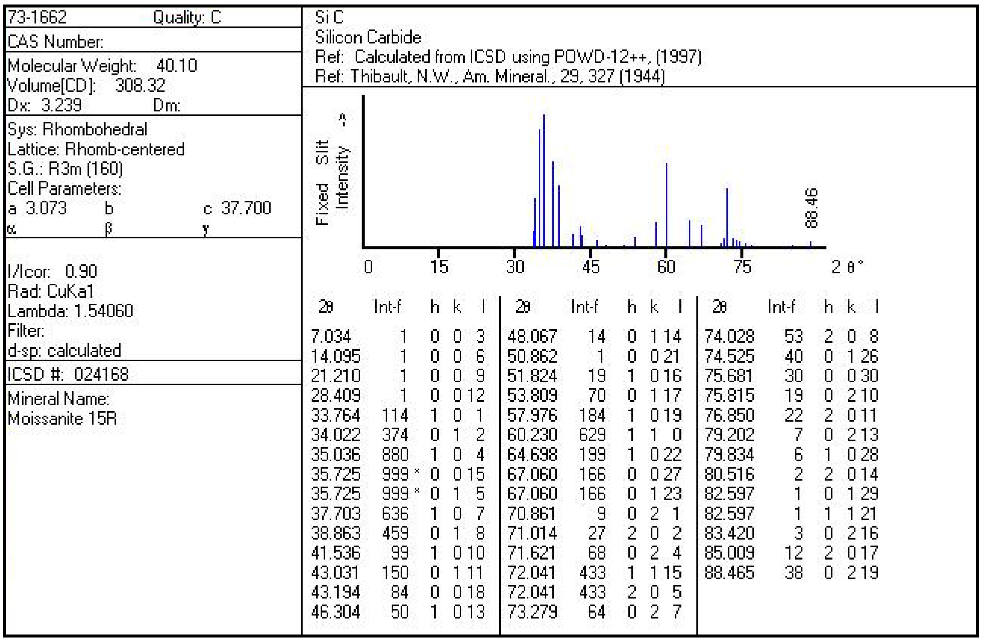

73-1662 Quality: C
CAS Number:
Molecular Weight: 40.10
Volume[CD]: 308.32
Dx: 3.239 Dm:
Sys: Rhombohedral
Lattice: Rhomb-centered
S.G.: R3m (160)
Cell Parameters:
a 3.073 b c 37.700
α β γ

I/Icor: 0.90
Rad: CuKa1
Lambda: 1.54060
Filter:
d-sp: calculated
ICSD #: 024168
Mineral Name:
Moissanite 15R

Si C
Silicon Carbide
Ref: Calculated from ICSD using POWD-12++, (1997)
Ref: Thibault, N.W., Am. Mineral., 29, 327 (1944)

2θ	Int-f	h	k	l
7.034	1	0	0	3
14.095	1	0	0	6
21.210	1	0	0	9
28.409	1	0	0	12
33.764	114	1	0	1
34.022	374	0	1	2
35.036	880	1	0	4
35.725	999 *	0	0	15
35.725	999 *	0	1	5
37.703	636	1	0	7
38.863	459	0	1	8
41.536	99	1	0	10
43.031	150	0	1	11
43.194	84	0	0	18
46.304	50	1	0	13
48.067	14	0	1	14
50.862	1	0	0	21
51.824	19	1	0	16
53.809	70	0	1	17
57.976	184	1	0	19
60.230	629	1	1	0
64.698	199	1	0	22
67.060	166	0	0	27
67.060	166	0	1	23
70.861	9	0	2	1
71.014	27	2	0	2
71.621	68	0	2	4
72.041	433	1	1	15
72.041	433	2	0	5
73.279	64	0	2	7
74.028	53	2	0	8
74.525	40	0	1	26
75.681	30	0	0	30
75.815	19	0	2	10
76.850	22	2	0	11
79.202	7	0	2	13
79.834	6	1	0	28
80.516	2	2	0	14
82.597	1	0	1	29
82.597	1	1	1	21
83.420	3	0	2	16
85.009	12	2	0	17
88.465	38	0	2	19

Table C.8. X-Ray Analysis Details of Al_4C_3

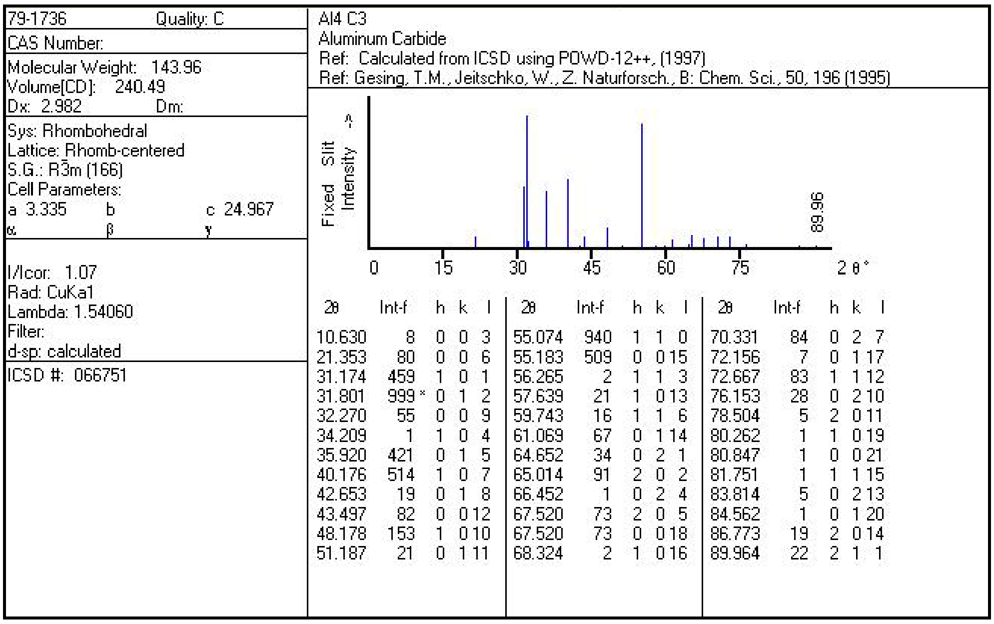

79-1736 Quality: C
CAS Number:
Molecular Weight: 143.96
Volume[CD]: 240.49
Dx: 2.982 Dm:
Sys: Rhombohedral
Lattice: Rhomb-centered
S.G.: R$\bar{3}$m (166)
Cell Parameters:
a 3.335 b c 24.967
α β γ

I/Icor: 1.07
Rad: CuKa1
Lambda: 1.54060
Filter:
d-sp: calculated
ICSD #: 066751

Al4 C3
Aluminum Carbide
Ref: Calculated from ICSD using POWD-12++, (1997)
Ref: Gesing, T.M., Jeitschko, W., Z. Naturforsch., B: Chem. Sci., 50, 196 (1995)

2θ	Int-f	h	k	l
10.630	8	0	0	3
21.353	80	0	0	6
31.174	459	1	0	1
31.801	999 *	0	1	2
32.270	55	0	0	9
34.209	1	1	0	4
35.920	421	0	1	5
40.176	514	1	0	7
42.653	19	0	1	8
43.497	82	0	0	12
48.178	153	1	0	10
51.187	21	0	1	11
55.074	940	1	1	0
55.183	509	0	0	15
56.265	2	1	1	3
57.639	21	1	0	13
59.743	16	1	1	6
61.069	67	0	1	14
64.652	34	0	2	1
65.014	91	2	0	2
66.452	1	0	2	4
67.520	73	2	0	5
67.520	73	0	0	18
68.324	2	1	0	16
70.331	84	0	2	7
72.156	7	0	1	17
72.667	83	1	1	12
76.153	28	0	2	10
78.504	5	2	0	11
80.262	1	1	0	19
80.847	1	0	0	21
81.751	1	1	1	15
83.814	5	0	2	13
84.562	1	0	1	20
86.773	19	2	0	14
89.964	22	2	1	1

Table C.9. X-Ray Analysis Details of Al_4C_3

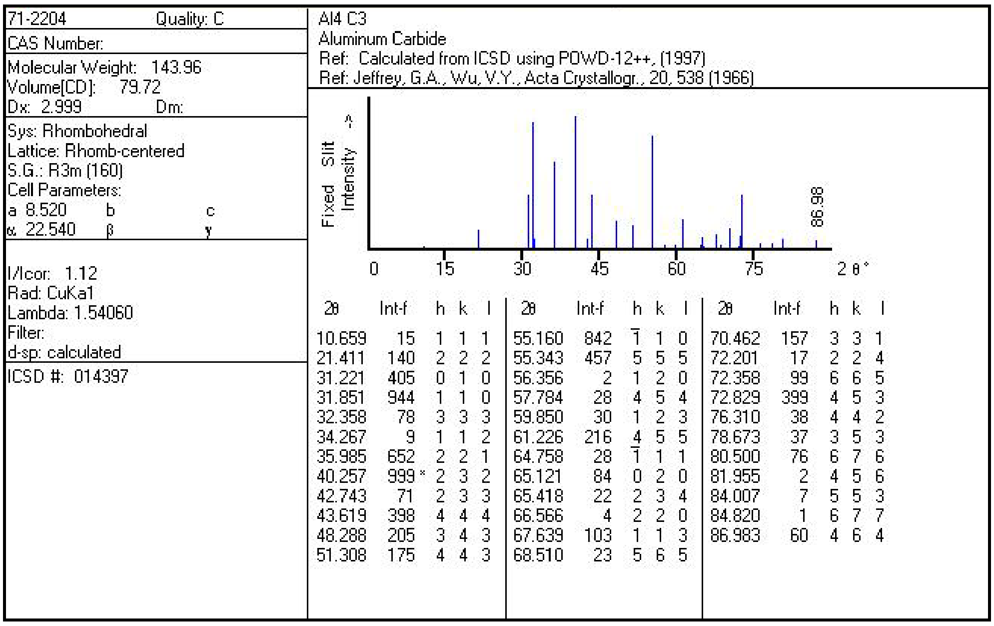

71-2204 Quality: C
CAS Number:
Molecular Weight: 143.96
Volume[CD]: 79.72
Dx: 2.999 Dm:
Sys: Rhombohedral
Lattice: Rhomb-centered
S.G.: R3m (160)
Cell Parameters:
a 8.520 b c
α 22.540 β γ
I/Icor: 1.12
Rad: CuKa1
Lambda: 1.54060
Filter:
d-sp: calculated
ICSD #: 014397

Al4 C3
Aluminum Carbide
Ref: Calculated from ICSD using POWD-12++, (1997)
Ref: Jeffrey, G.A., Wu, V.Y., Acta Crystallogr., 20, 538 (1966)

2θ	Int-f	h	k	l
10.659	15	1	1	1
21.411	140	2	2	2
31.221	405	0	1	0
31.851	944	1	1	0
32.358	78	3	3	3
34.267	9	1	1	2
35.985	652	2	2	1
40.257	999*	2	3	2
42.743	71	2	3	3
43.619	398	4	4	4
48.288	205	3	4	3
51.308	175	4	4	3
55.160	842	$\bar{1}$	1	0
55.343	457	5	5	5
56.356	2	1	2	0
57.784	28	4	5	4
59.850	30	1	2	3
61.226	216	4	5	5
64.758	28	$\bar{1}$	1	1
65.121	84	0	2	0
65.418	22	2	3	4
66.566	4	2	2	0
67.639	103	1	1	3
68.510	23	5	6	5
70.462	157	3	3	1
72.201	17	2	2	4
72.358	99	6	6	5
72.829	399	4	5	3
76.310	38	4	4	2
78.673	37	3	5	3
80.500	76	6	7	6
81.955	2	4	5	6
84.007	7	5	5	3
84.820	1	6	7	7
86.983	60	4	6	4

Table C.10. X-Ray Analysis Details of δ-Al_4C_3

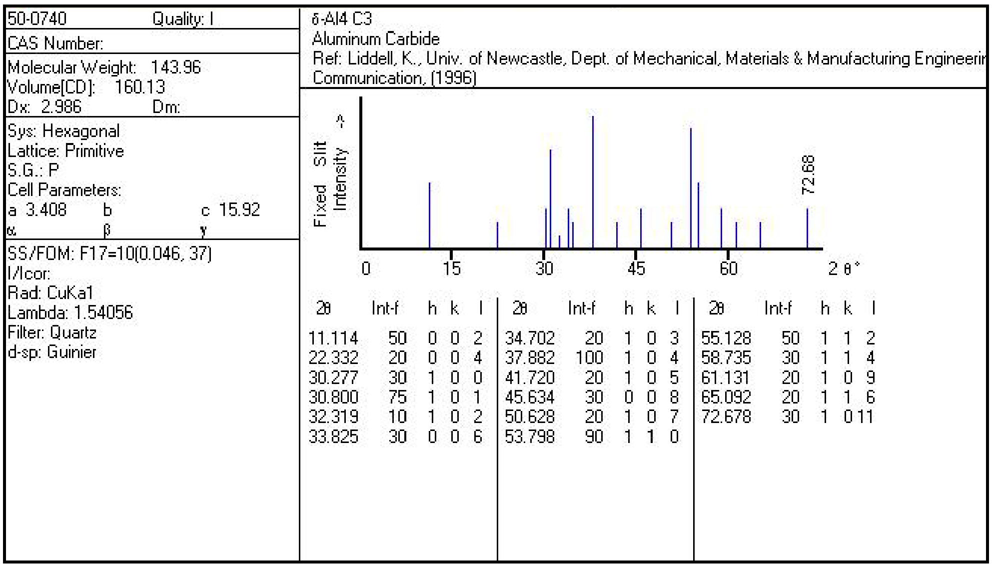

50-0740 Quality: I
CAS Number:
Molecular Weight: 143.96
Volume[CD]: 160.13
Dx: 2.986 Dm:
Sys: Hexagonal
Lattice: Primitive
S.G.: P
Cell Parameters:
a 3.408 b c 15.92
α β γ
SS/FOM: F17=10(0.046, 37)
I/Icor:
Rad: CuKa1
Lambda: 1.54056
Filter: Quartz
d-sp: Guinier

δ-Al4 C3
Aluminum Carbide
Ref: Liddell, K., Univ. of Newcastle, Dept. of Mechanical, Materials & Manufacturing Engineeri
Communication, (1996)

2θ	Int-f	h	k	l
11.114	50	0	0	2
22.332	20	0	0	4
30.277	30	1	0	0
30.800	75	1	0	1
32.319	10	1	0	2
33.825	30	0	0	6
34.702	20	1	0	3
37.882	100	1	0	4
41.720	20	1	0	5
45.634	30	0	0	8
50.628	20	1	0	7
53.798	90	1	1	0
55.128	50	1	1	2
58.735	30	1	1	4
61.131	20	1	0	9
65.092	20	1	1	6
72.678	30	1	0	11

Table C.11. X-Ray Analysis Details of Al_4Si

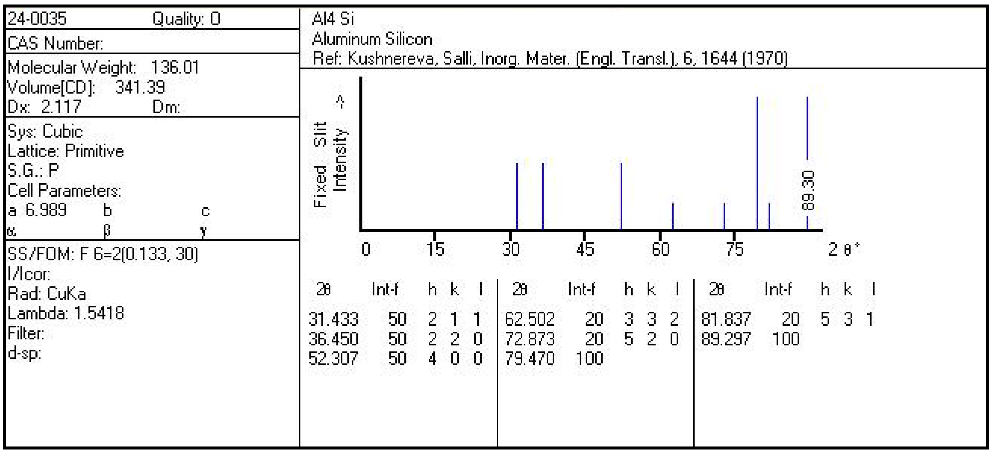

24-0035 Quality: 0
CAS Number:
Molecular Weight: 136.01
Volume[CD]: 341.39
Dx: 2.117 Dm:
Sys: Cubic
Lattice: Primitive
S.G.: P
Cell Parameters:
a 6.989 b c
α β γ
SS/FOM: F 6=2(0.133, 30)
I/Icor:
Rad: CuKa
Lambda: 1.5418
Filter:
d-sp:

Al4 Si
Aluminum Silicon
Ref: Kushnereva, Salli, Inorg. Mater. (Engl. Transl.), 6, 1644 (1970)

2θ	Int-f	h	k	l	2θ	Int-f	h	k	l	2θ	Int-f	h	k	l
31.433	50	2	1	1	62.502	20	3	3	2	81.837	20	5	3	1
36.450	50	2	2	0	72.873	20	5	2	0	89.297	100			
52.307	50	4	0	0	79.470	100								

Table C.12. X-Ray Analysis Details of Aluminum

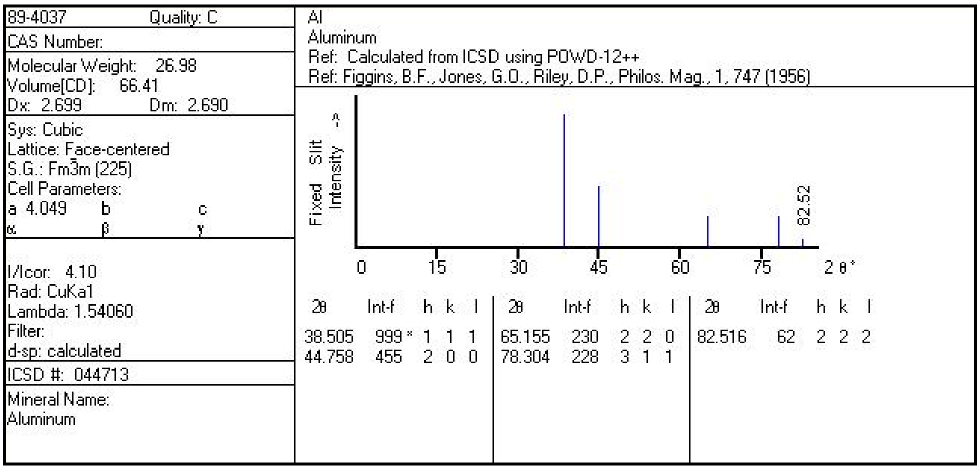

89-4037 Quality: C
CAS Number:
Molecular Weight: 26.98
Volume[CD]: 66.41
Dx: 2.699 Dm: 2.690
Sys: Cubic
Lattice: Face-centered
S.G.: Fm$\bar{3}$m (225)
Cell Parameters:
a 4.049 b c
α β γ
I/Icor: 4.10
Rad: CuKa1
Lambda: 1.54060
Filter:
d-sp: calculated
ICSD #: 044713
Mineral Name:
Aluminum

Al
Aluminum
Ref: Calculated from ICSD using POWD-12++
Ref: Figgins, B.F., Jones, G.O., Riley, D.P., Philos. Mag., 1, 747 (1956)

2θ	Int-f	h	k	l	2θ	Int-f	h	k	l	2θ	Int-f	h	k	l
38.505	999 *	1	1	1	65.155	230	2	2	0	82.516	62	2	2	2
44.758	455	2	0	0	78.304	228	3	1	1					

Table C.13. X-Ray Analysis Details of Aluminum

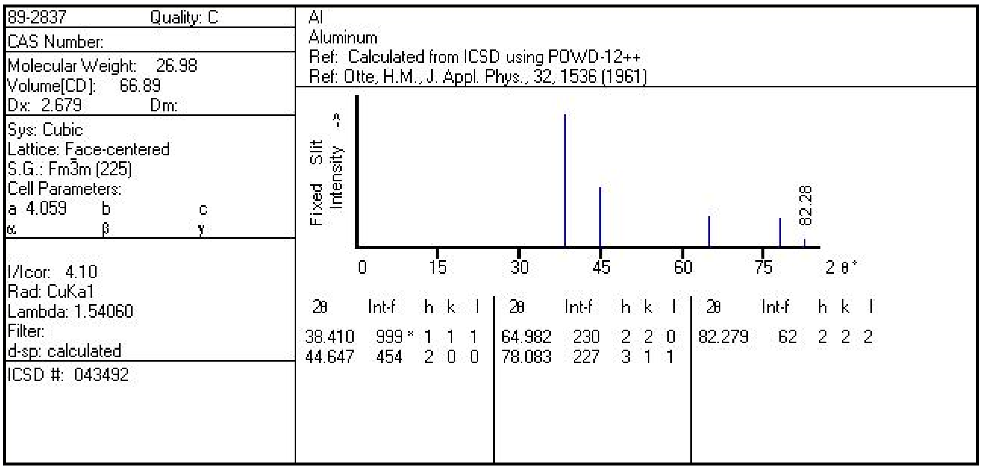

89-2837 Quality: C
CAS Number:
Molecular Weight: 26.98
Volume[CD]: 66.89
Dx: 2.679 Dm:
Sys: Cubic
Lattice: Face-centered
S.G.: Fm$\bar{3}$m (225)
Cell Parameters:
a 4.059 b c
α β γ
I/Icor: 4.10
Rad: CuKa1
Lambda: 1.54060
Filter:
d-sp: calculated
ICSD #: 043492

Al
Aluminum
Ref: Calculated from ICSD using POWD-12++
Ref: Otte, H.M., J. Appl. Phys., 32, 1536 (1961)

2θ	Int-f	h	k	l
38.410	999 *	1	1	1
44.647	454	2	0	0
64.982	230	2	2	0
78.083	227	3	1	1
82.279	62	2	2	2

Table C.14. X-Ray Analysis Details of Al_2O_3

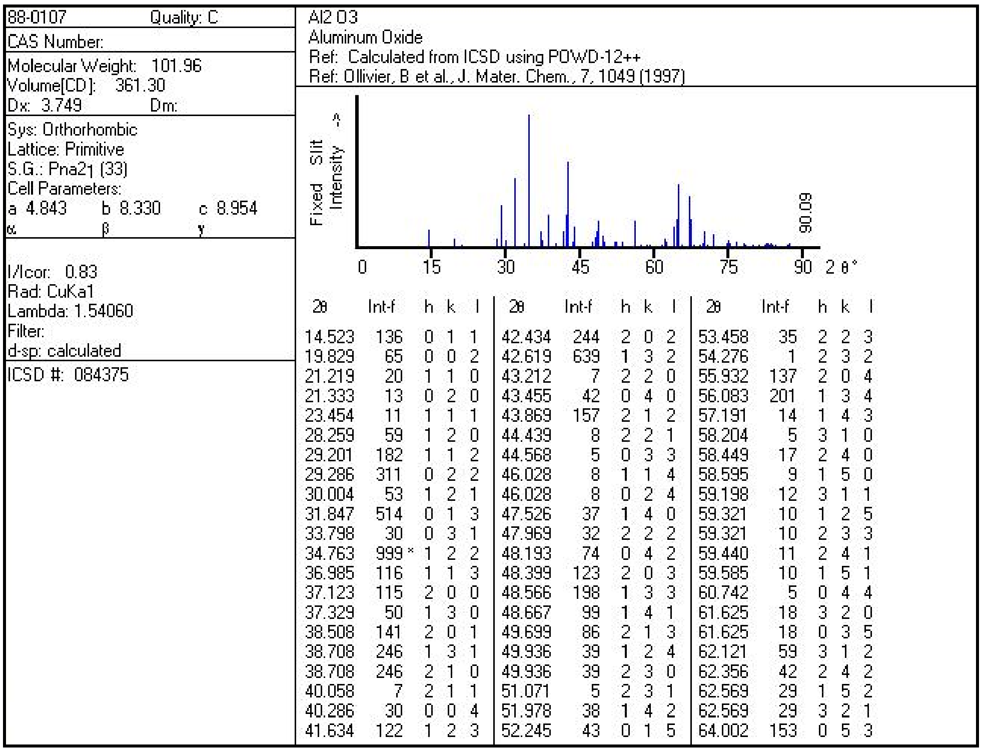

88-0107 Quality: C
CAS Number:
Molecular Weight: 101.96
Volume[CD]: 361.30
Dx: 3.749 Dm:
Sys: Orthorhombic
Lattice: Primitive
S.G.: Pna2_1 (33)
Cell Parameters:
a 4.843 b 8.330 c 8.954
α β γ
I/Icor: 0.83
Rad: CuKa1
Lambda: 1.54060
Filter:
d-sp: calculated
ICSD #: 084375

Al2 O3
Aluminum Oxide
Ref: Calculated from ICSD using POWD-12++
Ref: Ollivier, B et al., J. Mater. Chem., 7, 1049 (1997)

2θ	Int-f	h	k	l
14.523	136	0	1	1
19.829	65	0	0	2
21.219	20	1	1	0
21.333	13	0	2	0
23.454	11	1	1	1
28.259	59	1	2	0
29.201	182	1	1	2
29.286	311	0	2	2
30.004	53	1	2	1
31.847	514	0	1	3
33.798	30	0	3	1
34.763	999 *	1	2	2
36.985	116	1	1	3
37.123	115	2	0	0
37.329	50	1	3	0
38.508	141	2	0	1
38.708	246	1	3	1
38.708	246	2	1	0
40.058	7	2	1	1
40.286	30	0	0	4
41.634	122	1	2	3
42.434	244	2	0	2
42.619	639	1	3	2
43.212	7	2	2	0
43.455	42	0	4	0
43.869	157	2	1	2
44.439	8	2	2	1
44.568	5	0	3	3
46.028	8	1	1	4
46.028	8	0	2	4
47.526	37	1	4	0
47.969	32	2	2	2
48.193	74	0	4	2
48.399	123	2	0	3
48.566	198	1	3	3
48.667	99	1	4	1
49.699	86	2	1	3
49.936	39	1	2	4
49.936	39	2	3	0
51.071	5	2	3	1
51.978	38	1	4	2
52.245	43	0	1	5
53.458	35	2	2	3
54.276	1	2	3	2
55.932	137	2	0	4
56.083	201	1	3	4
57.191	14	1	4	3
58.204	5	3	1	0
58.449	17	2	4	0
58.595	9	1	5	0
59.198	12	3	1	1
59.321	10	1	2	5
59.321	10	2	3	3
59.440	11	2	4	1
59.585	10	1	5	1
60.742	5	0	4	4
61.625	18	3	2	0
61.625	18	0	3	5
62.121	59	3	1	2
62.356	42	2	4	2
62.569	29	1	5	2
62.569	29	3	2	1
64.002	153	0	5	3

Table C.15. X-Ray Analysis Details of Al_2O_3

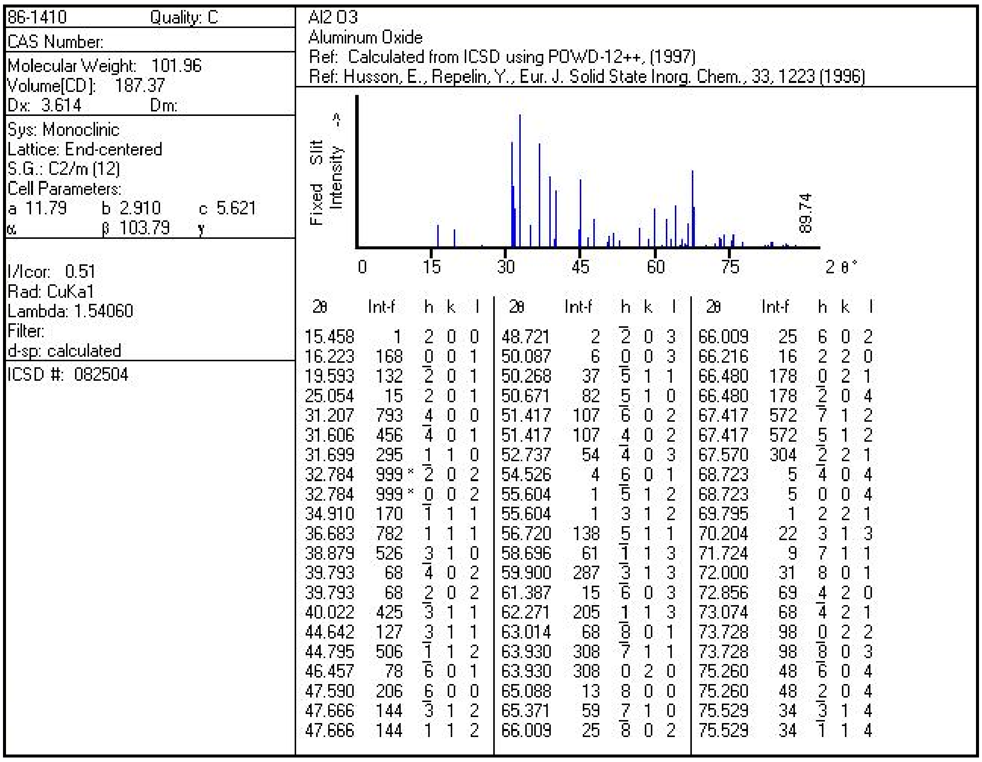

86-1410 Quality: C
CAS Number:
Molecular Weight: 101.96
Volume[CD]: 187.37
Dx: 3.614 Dm:
Sys: Monoclinic
Lattice: End-centered
S.G.: C2/m (12)
Cell Parameters:
a 11.79 b 2.910 c 5.621
α β 103.79 γ
I/Icor: 0.51
Rad: CuKa1
Lambda: 1.54060
Filter:
d-sp: calculated
ICSD #: 082504

Al2 O3
Aluminum Oxide
Ref: Calculated from ICSD using POWD-12++, (1997)
Ref: Husson, E., Repelin, Y., Eur. J. Solid State Inorg. Chem., 33, 1223 (1996)

2θ	Int-f	h	k	l
15.458	1	2	0	0
16.223	168	0	0	1
19.593	132	$\bar{2}$	0	1
25.054	15	2	0	1
31.207	793	4	0	0
31.606	456	$\bar{4}$	0	1
31.699	295	1	1	0
32.784	999 *	$\bar{2}$	0	2
32.784	999 *	0	0	2
34.910	170	$\bar{1}$	1	1
36.683	782	1	1	1
38.879	526	3	1	0
39.793	68	$\bar{4}$	0	2
39.793	68	2	0	2
40.022	425	$\bar{3}$	1	1
44.642	127	3	1	1
44.795	506	$\bar{1}$	1	2
46.457	78	$\bar{6}$	0	1
47.590	206	6	0	0
47.666	144	$\bar{3}$	1	2
47.666	144	1	1	2
48.721	2	$\bar{2}$	0	3
50.087	6	0	0	3
50.268	37	$\bar{5}$	1	1
50.671	82	5	1	0
51.417	107	$\bar{6}$	0	2
51.417	107	4	0	2
52.737	54	$\bar{4}$	0	3
54.526	4	6	0	1
55.604	1	$\bar{5}$	1	2
55.604	1	3	1	2
56.720	138	5	1	1
58.696	61	$\bar{1}$	1	3
59.900	287	$\bar{3}$	1	3
61.387	15	$\bar{6}$	0	3
62.271	205	1	1	3
63.014	68	$\bar{8}$	0	1
63.930	308	$\bar{7}$	1	1
63.930	308	0	2	0
65.088	13	8	0	0
65.371	59	7	1	0
66.009	25	$\bar{8}$	0	2
66.009	25	6	0	2
66.216	16	2	2	0
66.480	178	0	2	1
66.480	178	$\bar{2}$	0	4
67.417	572	$\bar{7}$	1	2
67.417	572	5	1	2
67.570	304	$\bar{2}$	2	1
68.723	5	$\bar{4}$	0	4
68.723	5	0	0	4
69.795	1	2	2	1
70.204	22	3	1	3
71.724	9	7	1	1
72.000	31	8	0	1
72.856	69	4	2	0
73.074	68	$\bar{4}$	2	1
73.728	98	0	2	2
73.728	98	$\bar{8}$	0	3
75.260	48	$\bar{6}$	0	4
75.260	48	2	0	4
75.529	34	$\bar{3}$	1	4
75.529	34	$\bar{1}$	1	4

Table C.16. X-Ray Analysis Details of $Al_{2.427}O_{3.64}$

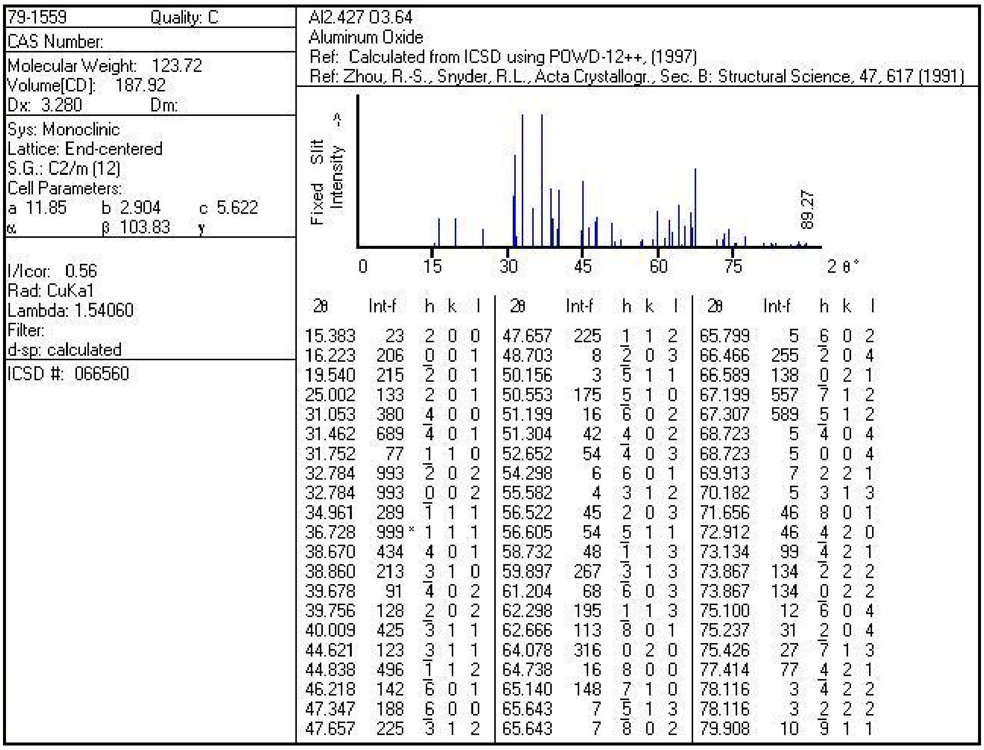

79-1559 Quality: C
CAS Number:
Molecular Weight: 123.72
Volume[CD]: 187.92
Dx: 3.280 Dm:
Sys: Monoclinic
Lattice: End-centered
S.G.: C2/m (12)
Cell Parameters:
a 11.85 b 2.904 c 5.622
α β 103.83 γ
I/Icor: 0.56
Rad: CuKa1
Lambda: 1.54060
Filter:
d-sp: calculated
ICSD #: 066560

Al2.427 O3.64
Aluminum Oxide
Ref: Calculated from ICSD using POWD-12++, (1997)
Ref: Zhou, R.-S., Snyder, R.L., Acta Crystallogr., Sec. B: Structural Science, 47, 617 (1991)

2θ	Int-f	h	k	l
15.383	23	2	0	0
16.223	206	0	0	1
19.540	215	$\bar{2}$	0	1
25.002	133	2	0	1
31.053	380	4	0	0
31.462	689	$\bar{4}$	0	1
31.752	77	1	1	0
32.784	993	$\bar{2}$	0	2
32.784	993	0	0	2
34.961	289	$\bar{1}$	1	1
36.728	999 *	1	1	1
38.670	434	4	0	1
38.860	213	3	1	0
39.678	91	$\bar{4}$	0	2
39.756	128	2	0	2
40.009	425	$\bar{3}$	1	1
44.621	123	3	1	1
44.838	496	$\bar{1}$	1	2
46.218	142	$\bar{6}$	0	1
47.347	188	6	0	0
47.657	225	$\bar{3}$	1	2
47.657	225	1	1	2
48.703	8	$\bar{2}$	0	3
50.156	3	$\bar{5}$	1	1
50.553	175	5	1	0
51.199	16	$\bar{6}$	0	2
51.304	42	4	0	2
52.652	54	$\bar{4}$	0	3
54.298	6	6	0	1
55.582	4	3	1	2
56.522	45	2	0	3
56.605	54	5	1	1
58.732	48	$\bar{1}$	1	3
59.897	267	$\bar{3}$	1	3
61.204	68	$\bar{6}$	0	3
62.298	195	1	1	3
62.666	113	$\bar{8}$	0	1
64.078	316	0	2	0
64.738	16	8	0	0
65.140	148	7	1	0
65.643	7	$\bar{5}$	1	3
65.643	7	$\bar{8}$	0	2
65.799	5	6	0	2
66.466	255	$\bar{2}$	0	4
66.589	138	0	2	1
67.199	557	$\bar{7}$	1	2
67.307	589	5	1	2
68.723	5	$\bar{4}$	0	4
68.723	5	0	0	4
69.913	7	2	2	1
70.182	5	3	1	3
71.656	46	8	0	1
72.912	46	4	2	0
73.134	99	$\bar{4}$	2	1
73.867	134	$\bar{2}$	2	2
73.867	134	0	2	2
75.100	12	$\bar{6}$	0	4
75.237	31	2	0	4
75.426	27	$\bar{7}$	1	3
77.414	77	4	2	1
78.116	3	$\bar{4}$	2	2
78.116	3	2	2	2
79.908	10	$\bar{9}$	1	1

Table C.17. X-Ray Analysis Details of $MgZn_2$

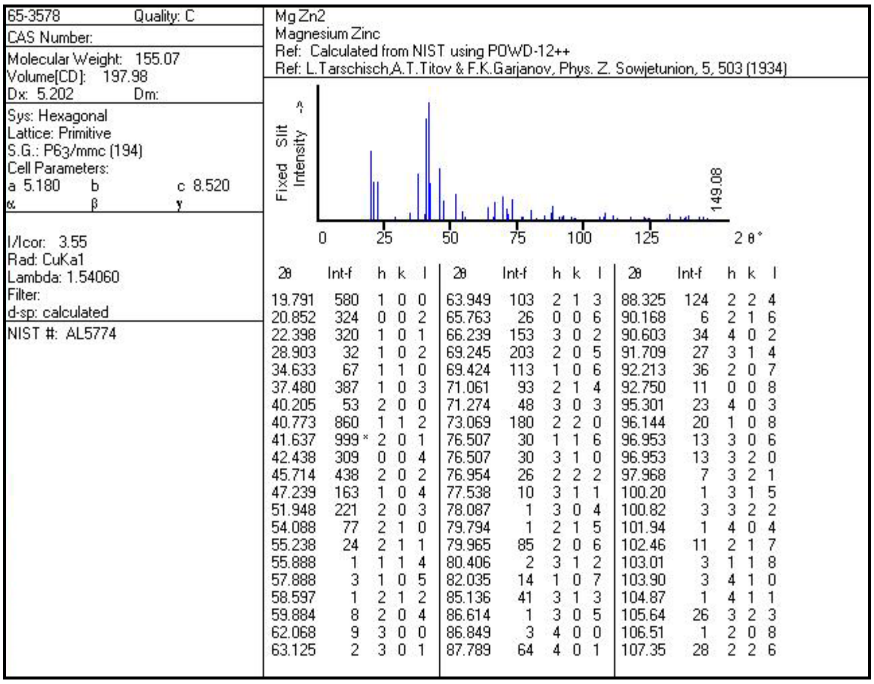

65-3578 Quality: C
CAS Number:
Molecular Weight: 155.07
Volume[CD]: 197.98
Dx: 5.202 Dm:
Sys: Hexagonal
Lattice: Primitive
S.G.: $P6_3/mmc$ (194)
Cell Parameters:
a 5.180 b c 8.520
α β γ
I/Icor: 3.55
Rad: CuKa1
Lambda: 1.54060
Filter:
d-sp: calculated
NIST #: AL5774

Mg Zn2
Magnesium Zinc
Ref: Calculated from NIST using POWD-12++
Ref: L.Tarschisch,A.T.Titov & F.K.Garjanov, Phys. Z. Sowjetunion, 5, 503 (1934)

2θ	Int-f	h	k	l	2θ	Int-f	h	k	l	2θ	Int-f	h	k	l
19.791	580	1	0	0	63.949	103	2	1	3	88.325	124	2	2	4
20.852	324	0	0	2	65.763	26	0	0	6	90.168	6	2	1	6
22.398	320	1	0	1	66.239	153	3	0	2	90.603	34	4	0	2
28.903	32	1	0	2	69.245	203	2	0	5	91.709	27	3	1	4
34.633	67	1	1	0	69.424	113	1	0	6	92.213	36	2	0	7
37.480	387	1	0	3	71.061	93	2	1	4	92.750	11	0	0	8
40.205	53	2	0	0	71.274	48	3	0	3	95.301	23	4	0	3
40.773	860	1	1	2	73.069	180	2	2	0	96.144	20	1	0	8
41.637	999 *	2	0	1	76.507	30	1	1	6	96.953	13	3	0	6
42.438	309	0	0	4	76.507	30	3	1	0	96.953	13	3	2	0
45.714	438	2	0	2	76.954	26	2	2	2	97.968	7	3	2	1
47.239	163	1	0	4	77.538	10	3	1	1	100.20	1	3	1	5
51.948	221	2	0	3	78.087	1	3	0	4	100.82	3	3	2	2
54.088	77	2	1	0	79.794	1	2	1	5	101.94	1	4	0	4
55.238	24	2	1	1	79.965	85	2	0	6	102.46	11	2	1	7
55.888	1	1	1	4	80.406	2	3	1	2	103.01	3	1	1	8
57.888	3	1	0	5	82.035	14	1	0	7	103.90	3	4	1	0
58.597	1	2	1	2	85.136	41	3	1	3	104.87	1	4	1	1
59.884	8	2	0	4	86.614	1	3	0	5	105.64	26	3	2	3
62.068	9	3	0	0	86.849	3	4	0	0	106.51	1	2	0	8
63.125	2	3	0	1	87.789	64	4	0	1	107.35	28	2	2	6

Table C.18. X-Ray Analysis Details of $MgZn_2$

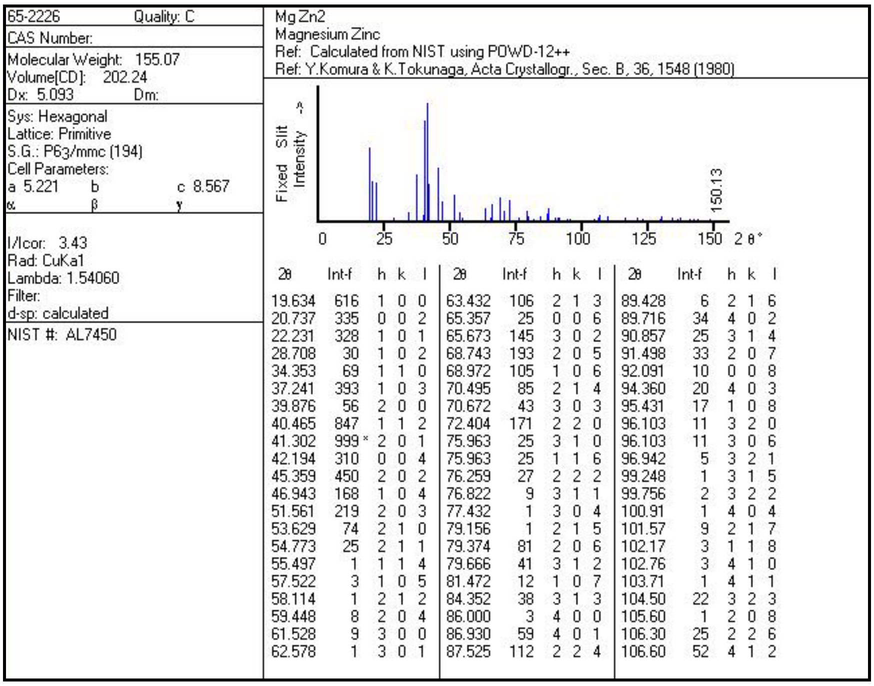

65-2226 Quality: C
CAS Number:
Molecular Weight: 155.07
Volume[CD]: 202.24
Dx: 5.093 Dm:
Sys: Hexagonal
Lattice: Primitive
S.G.: $P6_3/mmc$ (194)
Cell Parameters:
a 5.221 b c 8.567
α β γ
I/Icor: 3.43
Rad: CuKa1
Lambda: 1.54060
Filter:
d-sp: calculated
NIST #: AL7450

Mg Zn2
Magnesium Zinc
Ref: Calculated from NIST using POWD-12++
Ref: Y.Komura & K.Tokunaga, Acta Crystallogr., Sec. B, 36, 1548 (1980)

2θ	Int-f	h	k	l	2θ	Int-f	h	k	l	2θ	Int-f	h	k	l
19.634	616	1	0	0	63.432	106	2	1	3	89.428	6	2	1	6
20.737	335	0	0	2	65.357	25	0	0	6	89.716	34	4	0	2
22.231	328	1	0	1	65.673	145	3	0	2	90.857	25	3	1	4
28.708	30	1	0	2	68.743	193	2	0	5	91.498	33	2	0	7
34.353	69	1	1	0	68.972	105	1	0	6	92.091	10	0	0	8
37.241	393	1	0	3	70.495	85	2	1	4	94.360	20	4	0	3
39.876	56	2	0	0	70.672	43	3	0	3	95.431	17	1	0	8
40.465	847	1	1	2	72.404	171	2	2	0	96.103	11	3	2	0
41.302	999 *	2	0	1	75.963	25	3	1	0	96.103	11	3	0	6
42.194	310	0	0	4	75.963	25	1	1	6	96.942	5	3	2	1
45.359	450	2	0	2	76.259	27	2	2	2	99.248	1	3	1	5
46.943	168	1	0	4	76.822	9	3	1	1	99.756	2	3	2	2
51.561	219	2	0	3	77.432	1	3	0	4	100.91	1	4	0	4
53.629	74	2	1	0	79.156	1	2	1	5	101.57	9	2	1	7
54.773	25	2	1	1	79.374	81	2	0	6	102.17	3	1	1	8
55.497	1	1	1	4	79.666	41	3	1	2	102.76	3	4	1	0
57.522	3	1	0	5	81.472	12	1	0	7	103.71	1	4	1	1
58.114	1	2	1	2	84.352	38	3	1	3	104.50	22	3	2	3
59.448	8	2	0	4	86.000	3	4	0	0	105.60	1	2	0	8
61.528	9	3	0	0	86.930	59	4	0	1	106.30	25	2	2	6
62.578	1	3	0	1	87.525	112	2	2	4	106.60	52	4	1	2

REFERENCES

[1] “Cast metal matrix composites”, S.J. HARRIS, Materials Science and Technology, 1988, vol. 4, pp 231-239

[2] “Fracture Mechanisms of a 2124 Aluminum Matrix Composite Reinforced with SiC Whiskers”, Young-Hwan KIm, Sunghak Lee and Nack J. Kım, Metallurgical and Materials Transactions A 1991, Vol23A, 2589-2596

[3] “Influence of microstructure of fiber/matrix interface on mechanical properties of Al/SiC composites”, B.R.Henriksen, T.E. Johnsen, Materials Science and Technology, 1990, vol. 6, pp 857-863

[4] “Fabrication and Mechanical Properties of Aluminum Matrix Composite Materials”, Y.H. KIm, C.S.Lee and K.S. Han; Journal of Composite Materials 1992, Vol.26, pp 1062-1086

[5] “Processing techniques for particulate-reinforced metal aluminum matrix composites”, T.S. Srivatsan, I.A. Ibrahim, F.A.Mohamed, E.J.Lavernia, Journal of Materials Science, 1991, vol. 26, pp 5965-5978

[6] “Characterization of reinforcement distribution in cast Al-alloy/SiC_p composites”, P.A. Karnezis, G.Durrant and B.Cantor, Materials Characterization, 1998, vol 40, pp 97-109

[7] “Strength of Al-Zn-Mg-Cu Matrix Composite Reinforced with SiC Partiles”, Kon Bae Lee and Hoon Kwon, Metallurgical and Materials Transactions A Vol. 33A, Feburary 2002 pp 455-465

[8] “Fracture Behavior of Particle Reinforced Metal Matrix Composites”, X.Xia, H.J. McQueen, H.Zhu, Applied Composite Materials, 2002, pp.17-31

[9] “Structural indices in design optimization with metal-matrix composites”, J.E. Schoutens and D.A. Zarate, Composites, 1986, vol17, pp 188-204

[10] “SiC Particulate-reinforced, Aluminum-Matrix Composite Rods and Wires Produced by a New Continious Casting Route”, A. Mclean, H.Soda, Q.XIa, A.K. ParamanIck, A. Ohno, T.ShImIzu, S.A.Gedeon and T.North; Composites Part A 1996, Vol. 28, pp. 153-162

[11] “SiC-Al interface bonding mechanism in a squeeze casting SiC_w/Al composite” L.Geng, C.K.Yao, Journal of Materials Science Letters, 1995, vol. 14, pp 606-608

[12] “Optimum Parameters for Wetting Silicon Carbide by Aluminum Alloys”, M.I. Pech-Canul, R.N. Katz, M.M. Makhlouf, Metallurgical and Materials Transactions A, vol. 31 A, Feburary 2000, pp. 565-573

[13] “SiC Particle Cracking in Powder Metallurgy Processed Aluminum Matrix Composite Materials”, B. Wang, G.M.JanowskI and B.R.Patterson, Metallurgical and Materials Transactions A 1995, vol.26(9), pp 2457-2467

[14] “Microstructure and tensile properties of squeeze cast SiC particulate reinforced Al-7Si alloy”, P.A.Karnezis, G. Durrant, B. Cantor, Materials Science and Technology, 1998, vol. 14, pp 97-107

[15] “Effect of applied pressure on the microstructure and mechanical properties of squeeze-cast aluminum AA6061 alloy”, S. Skolianos, Griourtsidis, Thomas, Xatzifotiou, Materials Science and Engineering, 1997, vol231A, pp 17-24

[16] “The Wettability of Silicon Carbide by Liquid Aluminium: The Effect of Free Silicon in the Carbide and of Magnesium, Silicon and Copper Alloy Additions to the Aluminum”, Do-Suck Han, H.Jones, H.V. Atkinson, Journal of Materials Science, 1993, pp.2654-2658.

[17] “Wetting Kinetics and Bonding of Al and Al Alloys on α - SiC”, V.Laurent, C.Rado, N. Eustathopoulos, Materials Science and engineering, A205, 1996, pp.1-8

[18] “Wetting of Ceramic Particulates with Liquid Aluminum Alloys”, S.-Y. OH, J.A.Cornie, K.C. Russell, Metallurgical Transactions A, vol 20A, March 1989, pp. 527-541.

[19] “The Wettability and the Reaction for SiC particle/Al Alloy System”, M.Kobashi, T.Choh, Journal of Materials Science, 1993, pp. 684-690

[20] “Wettability of SiC to aluminum and aluminum alloys”, T.Choh, T.Oki, Materials Science and Technology, 1987, vol 3 pp 378-385

[21] “Casting of SiC Reinforced Metal Matrix Composites”, W. Zhou, Z. M. Xu,, Journal of Materials Processing Technology, vol. 63, 1997, 358-363

[22] “Tensile Properties of Particulate-Reinforced Metal Matrix Composites”, T.J.A. Doel, P.Bowen, Composites Part A, vol. 27A, 1996, pp.655-665

[23] “Analysis of stress-strain, fracture and ductility behavior of aluminum matrix composites containing discontinuous silicon carbide reinforcement” David L. McDanels, Metallurgical and Materials Transactions A, 1985, vol. 16A, pp 1105-1115

[24] "Fluidity of Aluminum Alloy AlSi7Mg-SiC Particulate Composite Melts", A.Kolsgaard, S. Brusethaug, Materials Science and Technology, Vol.10, June 1994, pp.545-551

[25] "Cast Metal Matrix Composites Proceedings of the 2nd International Conference on Cast Metal Matrix Composites", University of Alabama Tuscaloosa.Al, October 4-6 1993, pp.263-269

[26] "Deformation and Fracture Behavior of Cast and extruded 7075Al-SiCp Composites at Room and Elevated Temperatures, M.D. Kulkarni", P.S. Robi, R.C. Prasad, P.Ramakrishnan, Materials Transactions, JIM, Vol37, No.3, 1996, pp.223-229

[27] "Heat Treating of Aluminum Alloys", ASM Committee on Heat Treating of Aluminum Alloys, pp. 675-718

[28] Strengthening Mechanism of Aluminum Alloys, Aluminum Matter Organization, U.K. (www.aluminum.matter.org.uk, 2004)